KAISO OVEREXPRESSION IN THE MOUSE INTESTINES

A TRANSGENIC MODEL OF CONSTITUTIVE KAISO OVEREXPRESSION IN THE MOUSE INTESTINES

By

KYSTER K. NANAN, B.Sc.

A Thesis

Submitted to the School of Graduate Studies

in Partial Fulfillment of the Requirements

for the Degree

Master of Science

McMaster University

MASTER OF SCIENCE (2009) McMaster University

(Biology) Hamilton, Ontario

TITLE: A Transgenic Model of Constitutive Kaiso Overexpression in the Mouse Intestines

AUTHOR: Kyster K. Nanan, B.Sc. (McMaster University)

SUPERVISOR: Dr. Juliet M. Daniel

NUMBER OF PAGES: xii, 97

Abstract

Kaiso is a member of the BTB/POZ-ZF (hereafter POZ-ZF) family of transcription factors that was initially identified as a p120 interaction partner. Like typical POZ-ZF transcription factors, Kaiso has an N-terminal POZ domain that facilitates protein-protein interactions and a DNA-binding zinc finger region at the C-terminus. Kaiso is implicated in the Wnt signaling pathway and has important roles in both normal development and in disease pathogenesis. In the *Xenopus* model system, Kaiso depletion results in gastrulation defects during embryogenesis. However, Kaiso expression rescues the axis-duplication phenotype resulting from β-catenin overexpression in *Xenopus* tadpoles. Additionally, Kaiso has been shown to bind the *xWnt11* promoter directly and downregulate expression of this non-canonical Wnt ligand involved in directing cell movement, adhesion, and polarity. Taken together these two findings confirm Kaiso's role as a negative regulator of Wnt signaling in *Xenopus*. In the mouse model system, however, it was found that Kaiso was dispensable throughout embryogenesis and adulthood. In the $Apc^{Min/+}$ model of intestinal cancer, constitutive Wnt signaling induces polyp formation in the small intestines of affected mice and this closely mimics the human disease familial adenomatous polyposis (FAP). Kaiso null mice actually display a resistance to intestinal tumorigenesis; they exhibit a delay in tumor formation and a reduction in tumor size and number. Hence, in contract to the *Xenopus* system, data from the mouse model hints at Kaiso's role as a positive regulator of Wnt signaling. To resolve this discrepancy, we engineered an intestinal-specific Kaiso overexpression mouse model and observed the phenotype in a wildtype and $Apc^{Min/+}$ background.

Kaiso overexpression mice were created by pronuclear injection of Kaiso cDNA under control of the intestinal-specific *villin* promoter. Four founder animals were initially identified but only three of these founders, A, B, and, C, produced viable and fertile Kaiso transgenic offspring. Western blot analysis of A, B, and C mouse

intestinal tissue showed that Kaiso is efficiently overexpressed in the intestines at high, moderate, and low levels, respectively. RT-PCR analysis showed that Kaiso overexpression is limited to villin positive tissues, including the kidney, small intestine, and large intestine. Immunohistochemical analysis showed that Kaiso overexpression had no overt effect on normal intestinal development. When crossed with $Apc^{Min/+}$ mice, high levels of Kaiso overexpression correlated with increased intestinal tumorigenesis. This implicated Kaiso as a positive regulator of Wnt signaling in the mammalian mouse model and supports previous independent studies. Future experiments should include the analysis of Kaiso's effect on cell proliferation along the crypt-villus axis in the intestines of Kaiso overexpression mice. Further investigation of Kaiso's role in intestinal development and tumorigenesis could be achieved through crosses with p120 intestinal-specific misexpression mice in wildtype and $Apc^{Min/+}$ backgrounds.

Acknowledgements

Even though this thesis was an individual work, it would not have been possible without the insight, advice, and support of several people. First, I would like to thank my supervisor, Dr. Juliet M. Daniel for allowing me to perform my thesis under her expert guidance. I will forever be grateful to Dr. Daniel for recognizing and nurturing my interest in science at such an early stage of my academic career. I appreciate the support, encouragement, and friendship that she has provided throughout my graduate studies at McMaster University. I would also like to thank the other members of my supervisory committee, Dr. J. Roger Jacobs and Dr. Jonathan Bramson, for sharing their wisdom and scientific prowess. They were particularly helpful during committee meetings and contributed significant insight into the overall direction of my thesis.

I would especially like to acknowledge all of the members of the Daniel Lab, past and present, for the good times that we have shared. Special thanks go out to friends outside the confines of the lab including, Ryan Jugdeo, Amit Mistry, Kevin Kelly, Henry Haiser, and Jon Midwood. I have enjoyed a rare contrast of extremely intelligent and ridiculously unintelligible conversation with each of these individuals. I must also acknowledge members of my family who have supported and entertained me in various ways during my time at McMaster.

Finally, I have to thank Christina Liak for her continuous love, encouragement, support, and understanding and for being there from the very beginning.

Contributions by Others

The intestinal specific villin promoter was a gift from Dr. Silvie Robine (Institute Curie, Paris, France). Transgenesis via pronuclear DNA injection was performed by Dr. Siu-Pok Yee of the London Regional Cancer Center. Paraffin embedding and sectioning of mouse tissue was performed by Mary Jo Smith and Mary Bruni of the McMaster University Centre for Gene Therapeutics Central Histology Facility. All other experiments were performed by Kyster K. Nanan.

Table of Contents

Abstract.....iii

Acknowledgements.....v

Contributions by Others.....vi

List of Figures and Tables.....x

Abbreviations.....xii

1. **Introduction**
    - 1.1. Cancer and Tumor Cell Metastasis.....1
    - 1.2. The Adherens Junction Component E-Cadherin.....2
    - 1.3. The Cadherin-Catenin Adhesion System.....4
    - 1.4. The Wnt Signaling Pathway.....5
    - 1.5. Wnt Signaling in Development and Disease.....8
    - 1.6. Wnt Signaling in the Intestines.....10
    - 1.7. Intestinal Cancer and the $Apc^{Min/+}$ Mouse.....14
    - 1.8. Multistep Carcinogenesis in the $Apc^{Min/+}$ Mouse.....16
    - 1.9. The Role of BTB/POZ-ZF Transcription Factors in Development and Disease.....17
    - 1.10. The BTB/POZ-ZF Transcription Factor Kaiso.....20
    - 1.11. Rationale for Experiments and Hypothesis.....23

2. **Materials and Methods**
    - 2.1. Plasmid and Expression Vector Constructs.....24
    - 2.2. Cell Culture.....25
    - 2.3. Transient Transfections and IP-Western Blot.....25
    - 2.4. Transgenesis and Mouse Strains.....26

2.5. Preparation of Mouse Genomic DNA and PCR Genotyping.....27
2.6. PCR Standards and Transgene Copy Number Determination.....27
2.7. Mouse Tissue Protein Harvest.....28
2.8. Mouse Tissue RNA Purification.....29
2.9. Semi-quantitative RT-PCR.....29
2.10. Immunohistochemistry.....30

3. **Results**

3.1. Cloning and Transgenesis.....32
3.2. Transgene Copy Number.....34
3.3. Kaiso Overexpression in Transgenic Mice.....36
3.4. Kaiso Overexpression in the Mouse Intestines.....43
3.5. Kaiso Localization in $Apc^{Min/+}$ Mouse Intestines.....54
3.6. Effects of Kaiso on Polyp Formation in $Apc^{Min/+}$ Mouse.....65
3.7. Kaiso expression in $Apc^{Min/+}$;Kaiso-Tg Tumors.....67

4. Discussion

4.1. A Mouse Model for Intestinal-Specific Kaiso Overexpression.....71
4.2. Effects of Kaiso Overexpression on Normal Intestinal Development.....74
4.3. Kaiso Expression and Localization in the $Apc^{Min/+}$ Intestines.....76
4.4. Kaiso Overexpression in the $Apc^{Min/+}$ Background.....77
4.5. Conclusions and Significance.....79

Appendix A: Control Experiments

Materials and Methods

A.1.1. Cell Culture and Transient Transfection.....82

A.1.2. Immunoprecipitation and Western Blot.....82

Results and Discussion

A.2. The Villin-Kaiso-MT Vector Lacks Functionality in Tissue Culture Cells.....84

References.....90

List of Figures and Tables

Figure 1:	The Canonical Wnt Signaling Pathway	7
Figure 2:	The Mammalian GI Tract	11
Figure 3:	Intestinal crypts and villi	13
Figure 4:	POZ-ZF Proteins and their Interactions	18
Figure 5:	Kaiso and p120 are interaction partners	21
Figure 6:	The villin-Kaiso transgene	33
Figure 7:	Kaiso-Tg mice breeding colony	35
Figure 8:	Villin-Kaiso Transgene copy number	37
Figure 9:	Kaiso overexpression in the large intestines	38
Figure 10:	Tissue RT-PCR from "A" Line Kaiso-Tg and nontransgenic mice	39
Figure 11:	Tissue RT-PCR from "B" Line Kaiso-Tg and non-transgenic mice	40
Figure 12:	Tissue RT-PCR from "C" Line Kaiso-Tg and non-transgenic mice	41
Figure 13:	Kaiso Localization in the Small Intestines ("A" Line mice)	44
Figure 14:	Kaiso Localization in the Small Intestines ("B" Line mice)	45
Figure 15:	Kaiso Localization in the Small Intestines ("C" Line mice)	46
Figure 16:	Kaiso Localization in the Large Intestine ("A" Line mice)	47
Figure 17:	Kaiso Localization in the Large Intestine ("B" Line mice)	48
Figure 18:	Kaiso Localization in the Large Intestine ("C" Line mice)	49
Table I:	Mouse Vital Statistics	50
Figure 19:	Kaiso Transgenic and Non-transgenic Litermate ("A" Line)	51
Figure 20:	Kaiso Transgenic and Non-transgenic Litermate ("B" Line)	52
Figure 21:	Kaiso Transgenic and Non-transgenic Litermate ("C" Line)	53
Figure 22:	Effect of Kaiso Overexpression on the Small Intestines ("A" Line)	55
Figure 23:	Effect of Kaiso Overexpression on the Small Intestines ("B" Line)	56
Figure 24:	Effect of Kaiso Overexpression on the Small Intestines ("C" Line)	57
Figure 25:	Effect of Kaiso Overexpression on the Large Intestines ("A" Line)	58
Figure 26:	Effect of Kaiso Overexpression on the Large Intestines ("B" Line)	59
Figure 27:	Effect of Kaiso Overexpression on the Large Intestines ("C" Line)	60
Figure 28:	Kaiso Localization in the $Apc^{Min/+}$ Small Intestine	61
Figure 29:	Kaiso Localization in the $Apc^{Min/+}$ Large Intestine	62
Figure 30:	Kaiso localization in $Apc^{Min/+}$ Tumors (Tumor 1)	63
Figure 31:	Kaiso localization in $Apc^{Min/+}$ Tumors (Tumor 2)	64
Table II:	Average size of intestinal tumors	66
Figure 32:	Kaiso Localization in $Apc^{Min/+}$;Kaiso	68
Figure 33:	Kaiso Localization in $Apc^{Min/+}$;Kaiso	69

Figure 34: Comparison of Kaiso Localization in $Apc^{Min/+}$ and $Apc^{Min/+}$;Kaiso 70
Figure A-1 Villin-Kaiso Overexpression in IEC-6 Cells 86
Figure A-2 Villin-Kaiso Overexpression in CaCO2 Cells 87
Figure A-3 Villin-Kaiso Overexpression in LLC-PK1 Cells 88
Table A-1 Mouse Identification and Information 89

Abbreviations

AJ	**a**dherens **j**unction
APC	**a**denomatosis **p**olyposis **c**oli
BCL6	**B**-**c**ell **l**ymphoma
BTB	**B**ric-a-brac, **T**ramtrak, and **B**road complex
ChIP	**ch**romatin **i**mmuno**p**recipitation
CKI	**c**asein **k**inase **I**
CRC	**c**olo**r**ectal **c**ancer
Dkk	**D**i**kk**opf
DNA	**d**eoxyribo**n**uclic **a**cid
EC	**e**xtra**c**ellular (domain)
EMSA	**e**lectrophoretic **m**obility **s**hift **a**ssay
EMT	**e**pithelial-to-**m**esenchymal **t**ransition
ENU	**e**thyl**n**itroso**u**rea
FAP	**f**amilial **a**denomatous **p**olyposis
Fz	**f**ri**z**zled receptor
GSK3	**g**lycogen **s**ynthase **k**inase 3
H&E	**h**ematoxylin and **e**osin
HDAC	**h**istone **de**a**c**etylase
IHC	**i**mmuno**h**isto**c**hemistry
IP	**i**mmuno**p**recipitation
JNK	C-**J**un **N**-terminal **k**inase
KD	**k**nock**d**own
KO	**k**nock**o**ut
LRP5/6	**l**ow-density lipoprotein receptor-**r**elated **p**rotein **5/6**
MMP-7	**m**atrix **m**etallo**p**roteinase-**7** (matrilysin)
mSin3	**m**ammalian homologue of yeast **Sin3**
NCoR	**n**uclear **co**-**r**epressor
NT	**n**on-**t**ransgenic
PCP	**p**lanar **c**ell **p**olarity
PLZF	**p**romyelocytic **l**eukemia **z**inc **f**inger
POZ-ZF	**po**xvirus and **z**inc finger
RT-PCR	**r**everse **t**ranscriptase-**p**olymerase **c**hain **r**eaction
SMRT	**s**ilencing **m**ediator of **r**etinoid and **t**hyroid receptors
TCF/LEF	**T**-**c**ell **l**ymphoma/**l**ymphoma-**e**nhancing **f**actor
TFIID	**t**ranscription **f**actor **IID**
Tg	**t**rans**g**enic
Wnt	**W**ingless/MMTV i**nt** site family member
ZBTB4/38	**z**inc-finger and **BTB** domain-containing protein **4/38**

Introduction

1.1. Cancer and Tumor Cell Metastasis

Cancer is a disease resulting from uncontrolled cell proliferation and is responsible for one in four deaths in the United States(37). In 2008, it was predicted that 1.4 million new cancer cases and over half a million cancer deaths would be observed in the United States that year(37). Although available data indicate that cancer incidence has been steadily increasing since 1975, the resulting mortality has been on a decline due to new technological advances that aid in the detection and treatment of the disease(37). The most common incidences of cancer are diagnosed in the breast, prostate, lung, and colon but cancer can affect any organ or tissue of the body including the blood(37). Often times, tumor cell metastasis and the colonization of vital organs is the primary cause of death in cancer patients (Reviewed by Steeg, 2006)(83).

One of the first steps in tumor cell metastasis is the loss of the cell adhesion molecule E-cadherin from the cell surface(3). E-cadherin loss can occur via a number of means: (1) mutation in the E-cadherin gene or promoter, (2) epigenetic silencing through DNA methylation, (3) endocytosis away from the cell membrane, and (4) expression of other non-epithelial cadherins like N-cadherin(90). This loss of E-cadherin is commonly regarded as the start of the multistep process known as epithelial to mesenchymal transition (EMT)(3). EMT is important in both normal embryonic development and disease(99). It is an organized process that involves a highly conserved series of cellular changes that allow normally stationary epithelial cells to become motile mesenchymal cells(99). For example, one of the first incidences of EMT during normal vertebrate development is gastrulation, which marks the beginning of mesoderm formation(99).

During gastrulation, a subpopulation of polarized epithelial cells in the primitive streak undergo an EMT that involves a dramatic change in gene

expression, cell morphology, and motility(99). Migrating cells undergo a downregulation of epithelial markers like E-cadherin and an upregulation of mesenchymal markers including N-cadherin, vimentin, and α-smooth-muscle actin(3, 59). Expression of Rho GTP-ase family members leads to a rearrangement of the actin cytoskeleton resulting in a swap of the apical-basal polarity of epithelial cells for the anterior-posterior polarity of motile cells(3, 59). As cells become more motile, they lose the strong adhesions normally shared between neighbouring epithelial cells and retain contact only at focal adhesions(99). For gastrulation to occur successfully, migrating cells must also degrade and invade the underlying basement membrane, which is accomplished through the secretion of proteolytic enzymes including matrix metalloproteinases(59, 99). The changes in gene expression necessary to orchestrate the multi-step EMT are controlled by a number of well-conserved pathways including the Notch, TGF-B, BMP, and Wnt signaling pathways(3, 99). Not only is EMT fundamental to proper embryonic development but EMT signaling is also exploited by tumor cells during metastasis(86). Tumor cell metastasis occurs when cells of the primary tumor lose adhesion with their neighbours, infiltrate surrounding blood vessels, and are carried to other parts of the body where they form a secondary tumor(86). One of the main molecular features that facilitate cell-cell adhesion is the adherens junction (AJ) and the key AJ component is E-cadherin.

1.2. The Adherens Junction Component E-cadherin

Adherens junctions (AJ) are found in almost all types of tissue and facilitate homotypic cell adhesion(76). The AJ is responsible for maintaining tissue architecture in both the developing and adult organism(76, 86). In many malignant tumors, AJ components are downregulated and this leads to a loss of cell-cell adhesion and increased cell motility(76, 86). Components of the AJ include the

transmembrane cadherins, and the intracellular catenins that link the cadherins to the cytoskeleton or regulate cadherin stability and turnover(76). Epithelial cadherin (E-cadherin) is the prototypical member of a large family of cell adhesion proteins that include the "classical cadherins" N-cadherin (neuronal), P-cadherin (placental), and VE-cadherin (vascular endothelial)(1). E-cadherin and the other classical cadherins are modular glycoproteins that mediate calcium-dependent cell-cell adhesion through their extracellular domains (EC), EC1-EC5 (reviewed by Angst *et al.*, 2001)(1). These transmembrane glycoprotein components of the AJ participate in strong calcium-dependent homophilic interactions between adjacent cells. Originally recognized simply as the "molecular glue" that holds cells together in a multicellular organism, recent findings have revealed important roles for E-cadherin during signal transduction, embryonic development, and tissue differentiation (reviewed by van Roy and Berx, 2008)(90). It was first observed by Gabbert *et al.*, 1985 that undifferentiated carcinomas were far more invasive than their well-differentiated counterpart. The main histological difference between differentiated and undifferentiated tumors was the presence or absence of strong cell-cell contact at their borders(25). Future production of E-cadherin specific antibodies and the cloning of the E-cadherin *CDH1* cDNA made it possible to directly study the effects of cell adhesion on tumor cell growth and metastasis. Using epithelial and fibroblast carcinoma cell lines from the bladder, breast, lung, and pancreas, Frixen *et al.*, 1991 determined that overexpression of E-cadherin in fibroblast cell lines significantly reduced their metastatic ability during collagen invasion assay(23). Furthermore, the addition of anti-E-cadherin monoclonal antibodies to the culture media decreased the formation of cell-cell junctions and increased invasiveness of epithelial carcinoma cell lines(23). Collectively, these studies highlight the importance of E-cadherin in cell-cell adhesion and it is evident that deregulation of this adhesion system can lead to tumor cell invasion and metastasis.

1.3. The Cadherin-Catenin Adhesion System

The transmembrane E-cadherin molecule is stabilized primarily by interactions with its cytosolic binding partners, the catenins, which also help to transmit extracellular signals from E-cadherin to the nucleus. Members of the catenin family of cell adhesion cofactors include α-, β-, and p120-catenin, which either link the AJ to the actin cytoskeleton (α - and β -catenin) or stabilize the complex (p120-catenin)(7, 16, 76). Their defining structure is the presence of the Armadillo (Arm) repeat domain, which was first identified in *Drosophila* and facilitates protein-protein interactions(32). Unlike α -catenin, both β- and p120-catenin have roles not just at the cell membrane but also in the nucleus (Reviewed in 16, 57, 91). This was first revealed for β-catenin when it was discovered that it translocated to the nucleus and acted as a downstream effector of Wnt signaling(4). In the canonical Wnt signaling pathway, signal transduction from the cell membrane to the nucleus occurs through β-catenin. At the cell membrane, β-catenin physically links E-cadherin to α-catenin, thus bridging the adherens junction and the actin cytoskeleton(14, 26, 60). When phosphorylated on serine/threonine residues, β-catenin is stabilized in complex with E-cadherin near the cell membrane(60). Tyrosine phosphorylation of β-catenin by Src or EGFR, however, destabilizes the complex, resulting in downregulation of cadherin-mediated cell-cell adhesion and the release of β-catenin into the cytoplasm(60). Once in the cytoplasm, β-catenin is rapidly phosphorylated by glycogen synthase kinase 3β (GSK-3β) and subsequently undergoes ubiquitin-mediated degradation. In certain developmental contexts and disease states, cytoplasmic β-catenin is not phosphorylated; β-catenin thus escapes degradation and accumulates in the cytoplasm. Cytoplasmic accumulation of β-catenin is followed by its translocation to the nucleus where it also functions as a transcriptional activator with members of the TCF/LEF family(7, 8, 14). Nuclear targets of β-catenin are genes that have been implicated in cell growth and tumor progression; some gene targets include *c-myc*, *cyclin D1*, *fibronectin*, and *MMP7*(10).

Like β-catenin, recent evidence indicates that p120 also translocates to the nucleus to regulate gene expression(16, 40, 75, 91). Unlike β-catenin, however, p120 binds to the novel POZ-ZF transcription factor Kaiso and it remains to be determined whether signaling from E-cadherin affects p120-Kaiso-mediated gene regulation (Reviewed in 16, 17).

1.4. The Wnt Signaling Pathway

Wnts are involved in two major pathways that are important during early development and disease pathogenesis. The major Wnt pathways are the canonical Wnt signaling pathway and the non-canonical Wnt-signaling pathway, also known as the planar cell polarity (PCP) pathway(38). Both the canonical Wnt pathway and the PCP pathway were first discovered in *Drosophila*; the canonical Wnt pathway has been well characterized while the PCP pathway remains to be fully understood (38, 93). Much of the current experimental evidence regarding the PCP pathway has been acquired using *Drosophila* but emerging research is focused on identifying the vertebrate components of the PCP pathway (38, 93, 100). Examples of invertebrate and vertebrate PCP include the uniform alignment of bristles on the apical surface of wing cells in *Drosophila* and the process of convergent extension in mammals, respectively(38). The basis of the PCP pathway is the asymmetrical localization of core PCP pathway components within the cell(100). Core components of PCP signaling include the transmembrane Frizzled (Fz) receptor and the intracellular Dishevelled (Dsh)(38, 93, 100). The role of Wnt ligands in PCP signaling is still unknown but evidence indicates that Wnt5a, Wnt7a, and Wnt11 may bind Fz and initiate the signaling cascade (38, 100). Upon activation of PCP signaling through Fz, recruitment of Dsh to the cell membrane activates Rho GTPase family members and the C-Jun N-terminal kinase (JNK) pathway(38, 100). The Rho GTPase pathway is responsible for actin cytoskeletal rearrangements that facilitate cellular movements

and activation of the JNK pathway upregulates target genes, including Wnt5a, necessary to achieve successful cellular movements (93, 98).

The canonical Wnt signaling pathway, also known as the β-catenin-dependent Wnt signaling pathway, is associated with a different subset of Wnt ligands, transmembrane receptors, cellular complexes, and nuclear components(93). Canonical Wnt signaling is mediated mainly by β-catenin whose stabililty is dependent on the presence or absence of an extracellular Wnt ligand(4, 26). In the absence of a Wnt signal, the cytoplasmic destruction complex is responsible for the phosphorylation and degradation of β-catenin(4, 26). The complex consists of the Axin scaffold protein, the adenomatous polyposis coli (APC) tumor suppressor, and the kinases glycogen synthase kinase 3 (GSK3) and casein kinase I (CKI). This complex binds and phosphorylates β-catenin and labels it for proteasomal degradation. When β-catenin is degraded, it cannot enter the nucleus to transcribe any Wnt target genes. During active Wnt signaling, however, β-catenin accumulates in the cytoplasm, translocates to the nucleus and interacts with the TCF/LEF family of transcription factors to activate Wnt target gene transcription(4, 26).

The Wnt signaling pathway is activated once extracellular Wnt ligands are recognized by the transmembrane Fz receptor on the target cell (Figure 1)(19, 50). Wnts bind directly to the extracellular cysteine-rich domain of Fz(5, 19, 50). In addition to Fz binding, interaction with LRP coreceptors is necessary to activate the Wnt pathway in the target cell(14, 50, 92). The active signaling complex consists of the Wnt ligand, Fz, and LRP coreceptor(11, 50, 96). Upon receiving a Wnt signal, Axin is recruited to the cell membrane via its interaction with Dsh, which also interacts with the LRP5/6 coreceptor(6, 27, 50). Since the Axin scaffold is necessary for destruction complex formation, its sequestration at the cell membrane prevents

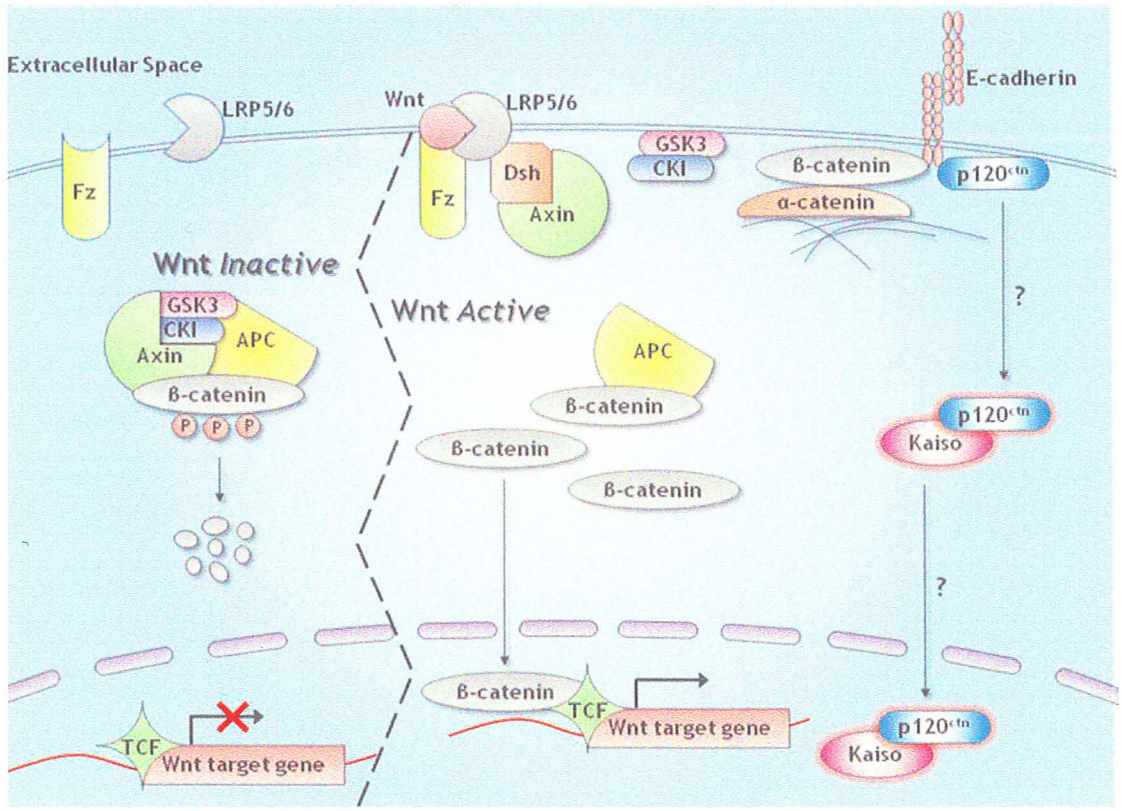

Figure 1- The Canonical Wnt Signaling Pathway. In the absence of a Wnt ligand, β-catenin is labeled for degradation by a "destruction complex" consisting of Axin, APC, GSK3, and CKI. Upon stimulation of the Fz and LRP5/6 coreceptor with an extracellular Wnt ligand, β-catenin is stabilized in the cytoplasm. Once stabilized, β-catenin translocates to the nucleus to activate transcription of Wnt target genes.

destruction complex formation. β-catenin thus escapes phosphorylation by the kinases of the destruction complex and accumulates in the cytoplasm(8, 46, 50). Cytoplasmic accumulation leads to nuclear translocation where β-catenin interacts with the TCF/LEF family of transcription factors to activate transcription of Wnt target genes(4, 54, 57). Targets of the Wnt signaling pathway include genes such as *mmp-7, c-myc,* and *cyclin D1,* each with important roles in developmental and disease pathways(4, 54, 88).

1.5. Wnt Signaling in Development and Disease

During the early development of multicellular organisms, a small subset of cells secrete various evolutionarily conserved signaling molecules (e.g. Wnts, BMPs, and Hedgehogs) that direct the proliferation, differentiation, and migration of neighbouring cells in a concentration-dependent manner(14, 50, 94). These same signals are responsible for controlling renewal of organs like the skin and intestines in the adult organism(13, 14, 26, 28, 67, 68). However, aberrant regulation of these signals can lead to malformation of bones, teeth, and internal organs as well as diseases such as cancer(27-29, 50). The canonical Wnt/β-catenin signaling pathway is well characterized and its role in the developing embryo and during disease pathogenesis has been clearly defined (Reviewed by 26)(8, 26, 48). The first Wnt to be studied by gene knockout (KO) in the mouse was the CNS- and testis-specific Wnt-1(53, 87). These studies showed that Wnt-1 was essential for the development of the mouse brain; homozygous Wnt-1 knockout mice lacked a large portion of the midbrain and cerebellum(53, 87). Further work using Wnt-3 KO mice confirmed the importance of the Wnt signaling pathway during normal development(48).

In 1999, Liu and colleagues were the first to demonstrate that a Wnt ligand was essential for primary axis formation in the mouse embryo(48). Wnt-3, normally expressed in the murine epiblast as early as embryonic day 6.25, is

localized mainly to the primitive streak as development proceeds. The primitive streak is an embryonic feature shared between mammals and birds and its location marks the site of gastrulation(12). The primitive streak is a furrow that forms at the future caudal portionof the embryo and acts as a reference point for axis formation and future body patterning during development(12). At embryonic day 8.5, Wnt-3 is no longer detectable in the primitive streak suggesting that its main role is in the formation or maintenance of this early embryonic feature(48). Targeted KO of Wnt-3 showed that Wnt-$3^{+/-}$ mice were viable and fertile whereas Wnt-$3^{-/-}$ homozygous KO mice died during embryogenesis(48). Wnt-$3^{-/-}$ embryo morphology was comparable to wildtype and heterozygous mice and revealed no abnormalities before gastrulation(48). Wildtype and heterozygous Wnt-3 mice underwent gastrulation and proceeded with normal embryonic development while Wnt-$3^{-/-}$ embryos continued to grow as egg cylinders(48). Histological analysis showed that Wnt-3 KO mice failed to form a mesoderm layer and displayed irregularities in the extra-embryonic tissue, the combined effect of which caused Wnt-$3^{-/-}$ mice to die *in utero(48, 95)*.

Not only do Wnts play a role in the developing organism but abnormal Wnt signaling in adults is responsible for a number of diseases. In one example, a single amino acid substitution in the Wnt component LRP5 renders the Wnt pathway insensitive to inhibition by Dikkopf (Dkk)(6). This mutation results in increased Wnt signaling in the bone, leading to an increase in bone density(6). In another analysis of LRP5, frame-shift and mis-sense mutations produced a loss-of-function mutation in LRP5 that led to a *decrease* in bone mass(27). The data from the aforementioned studies demonstrate the necessity of LRP5 and Wnt signaling in maintaining bone density in adult humans.

Aberrant Wnt signaling has become a hallmark of many cancers(46, 49, 67, 80). For example, patients with mutations in Axin2 are predisposed to the development of colon cancer(46, 49). Axin2 mutations commonly stabilize β-

catenin, which then activates TCF/LEF target genes, resulting in overproliferation of certain cell types(46, 49). Perhaps the most well-known component of the Wnt pathway that is dysfunctional in human cancers is the adenomatosis polyposis coli (APC) tumor suppressor. APC was one of the first tumor suppressors to be cloned and it is responsible for the hereditable condition termed familiar adenomatous polyposis (FAP)(14, 43, 50, 61). FAP patients develop hundreds to thousands of polyps in the large intestine during early adulthood and, as the disease advances, these adenomas progress to adenocarcinomas(30, 43). The increased cell proliferation that causes FAP is due to constitutive Wnt signaling, caused most frequently by truncations in the APC tumor suppressor(43, 61). As a result of this truncated APC, the destruction complex is not formed and β-catenin is stabilized even in the absence of a Wnt ligand, leading to constitutive activation of Wnt target genes(7, 14, 67). Wnt signaling has important roles in disease and development but is also necessary in the healthy adult organism for maintaining homeostasis in tissues that undergo constant renewal like the skin and the intestinal epithelium.

1.6. Wnt Signaling in the Intestines

There is a well-established necessity for active and carefully regulated Wnt signaling not only during embryogenesis and early development, but also in the adult organism(14, 28, 67, 68). Tissues such as the skin and the gut epithelium constantly undergo regeneration; in mice, the epithelium turnover occurs in 3 days whereas humans require 5 days for complete turnover(14). The gut has two functionally distinct segments; the small intestine (divided into duodenum, jejunum, and ileum), and the large intestine (colon) (Figure 2). On the luminal surface of the small intestine, the epithelium has two distinct features: the finger-like projections

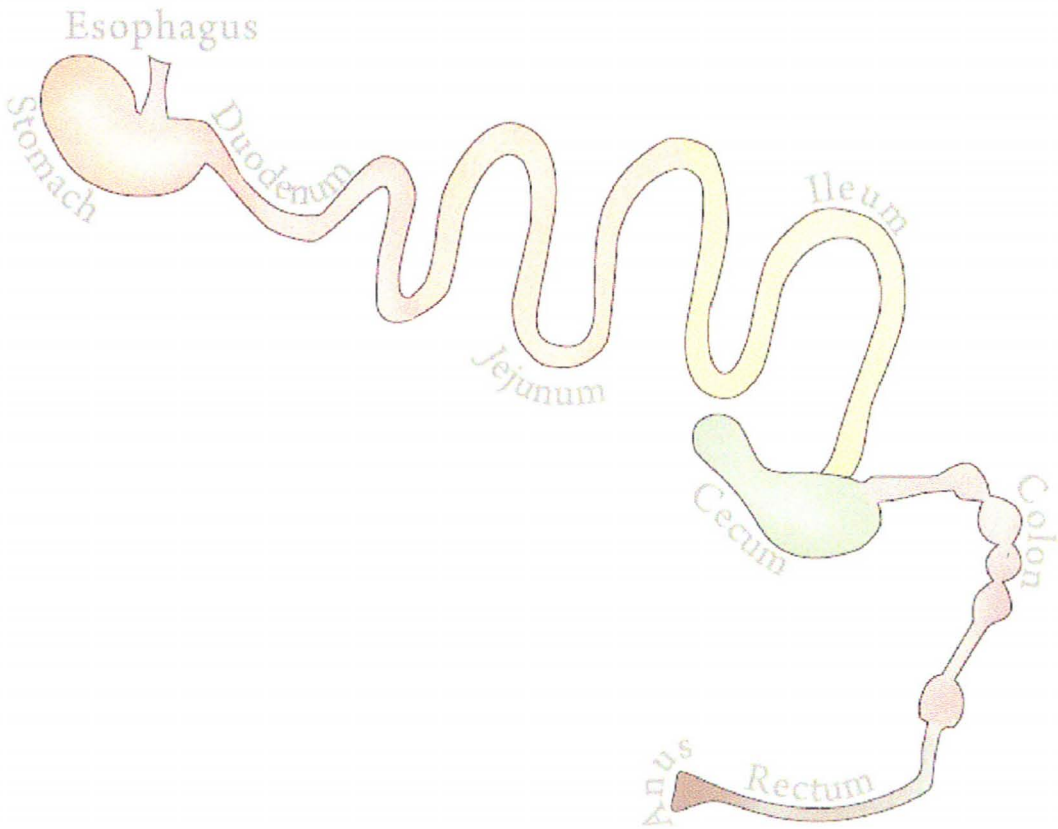

Figure 2 - The Mammalian Gastrointestinal (GI) Tract. The mammalian GI tract begins with the mouth at the anterior end, leading to the stomach via the esophagus. The stomach empties into the first segment of the small intestine called the duodenum. The duodenum is followed by the jejunum and ileum, which empties into the cecum. The cecum connects to the colon, which directs waste to the rectum and finally out the anus at the posterior end of the organism (Adapted from *The Virtual Mouse Necropsy* and Hägebarth, 2005)(31).

known as villi and the opening to deep invaginations known as crypts of Lieberkühn (Figure 3)(14, 28). In contrast to the small intestine, the epithelial layer of the colon possesses deeper crypts and lack villi(14, 28). The villi of the small intestine act to greatly increase its surface area, allowing for efficient absorption of nutrients. The epithelial layer of both the small and large intestine undergo constant renewal as epithelial cells regularly undergo apoptosis and slough off into the lumen of the intestines. The renewal of all cells along the crypt-villus axis is ensured by stem cells that reside near the base of the crypts in both the small and large intestines(14, 28).

The crypt contains approximately 250 cells belonging to four major cell types; absorptive enterocytes, mucus-secreting goblet cells, Paneth cells that secrete antimicrobial agents, and enteroendocrine cells that release hormones into the lumen(67, 71). There are two populations of crypt cells; the larger population contains 120-130 proliferative cells that divide about twice per day in order to replenish cells that are sloughed off at the villus tip(67, 71). The second population doubles once every 24 hours and clonogenic analysis revealed that these are, in fact, the actual stem cells of the crypt(70, 71). These stem cells give rise to all cell types in the intestines and are also able to replenish themselves via self-renewal (14, 67, 71). These intestinal stem cells divide asymmetrically and produce one daughter stem cell and one committed daughter cell, the latter being able to differentiate into one of the four major types of epithelial cells found in the intestine (31, 67). It is now understood that the self-renewal, differentiation, and migration capabilities of these intestinal stem cells are due largely to continued activation of the Wnt signaling pathway(52, 67).

The importance of active Wnt/β-catening signaling in the formation of the gut was first demonstrated in ascidian (sea squirt) embyos and later in mice (34, 47). In both ascidians and mice, it was shown that β-catenin is essential for endoderm formation but its exact role in this process remains unclear(34, 47).

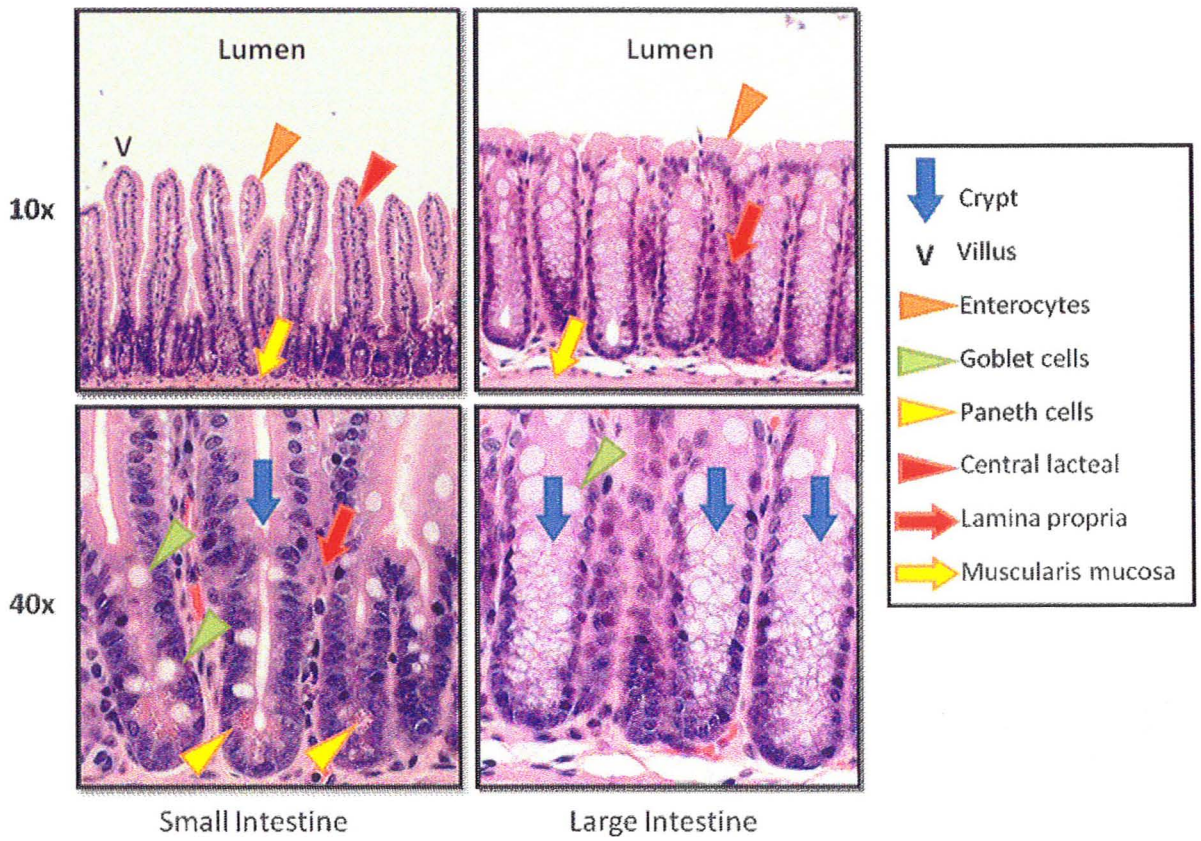

Figure 3 - The crypt-villus axis of the small (left) and large (right) intestine. The small and large intestine both contain crypts of Lieberkühn but only the small intestines have villi that project into the lumen. Another difference between small and large intestine crypts is that the former contains Paneth cells while the latter does not. Paneth cells secrete lysozyme and defensin that help to protect the host organism from harmful bacteria. The various cell types found along the crypt-villus axis include the mucus-secreting goblet cells, and the absortive enterocytes that line the villi of the small intestine and the luminal surface of the large intestine. Enterocytes are simple columnar epithelial cells with a brush border composed of densely packed microvilli which aid in nutrient absorption. Intestinal stem cells lie near the base of the crypts and give rise to each cell type present along the crypt-villus axis. Cells migrate from the base of the crypt to the luminal surface to replace cells that have become damaged and apoptotic (Adapted from Hägebarth, 2005)(31).

Wnt components Tcf4 and Tcf1 were detected in the developing hindgut by *in situ* hybridization and it was found that their disruption led to severe deformation of the hindgut and a loss of endodermal markers(29). Another Wnt component, APC, was found to be necessary in foregut development; hypomorphic APC mutant mice showed defects in foregut involution(36). It was postulated that these defects result from upregulated β-catenin/Tcf transcription in the gut precursor endodermal cells(36). Indeed, Wnt signaling is one of the important factors controlling early cell fate and directing intestinal development but it is also important in maintaining intestinal homeostasis. *In vivo* evidence from several studies showed that proliferation of transit-amplifying cells in both the fetal and adult intestine is dependent mainly on stimulation of the Wnt pathway since ablation of Tcf4 or β-catenin activity severely reduced their proliferative abilities(35, 45, 68). In addition, nuclear β-catenin is found in cells at the bottom of the crypt, indicating that this accumulation is in response to active Wnt signling(28, 89). Finally, while knockdown of β-catenin or expression of dominant negative Tcf4 induces cell cycle arrest in intestinal cancer cell lines, mutations in the APC tumor suppressor or overexpression of oncogenic β-catenin causes hyperproilferation of these cells(58, 63, 77). The normal and pathological proliferation observed in the intestines is due mainly to active Wnt/β-catenin signaling and the above studies demonstrate that misregulation of components of the pathway can have dramatic effects on intestinal tumorigenesis.

1.7. Intestinal Cancer and the *Apc*$^{Min/+}$ Mouse

It is estimated that sporadic and hereditary colorectal cancer (CRC) account for 8-9% of cancer-related deaths in males and females in North America(37). Recent advances in molecular biology have made it possible to identify genes responsible for this disorder. Aberrations in mismatch-repair genes like *MLH1*,

MSH2, and *MSH6* are frequently observed in colonic lesions as well as mutations in the *Apc* tumor suppressor (Reviewed in Castells *et al.*, 2009)(9). Germline mutations in *Apc* have been implicated in familial adenomatous polyposis (FAP) but somatic mutations are found in sporadic colon tumors, indicating that *Apc* mutation is an important early step in intestinal tumorigenesis(51, 72, 97).

FAP is a hereditable autosomal dominant disorder characterized by early onset of intestinal polyps(26, 43, 61). FAP patients develop hundreds to thousands of initially benign adenomas in the large intestine. These polyps eventually progress to malignant carcinomas in the absence of therapeutic intervention. Utilizing samples collected from 61 unrelated FAP patients, the human adenomatous polyposis coli (APC) gene was identified, cloned, and characterized in 1991(30). A year prior to this, however, a mouse mutant was unknowingly created that became the first and most widely used model for studying the genetics and biochemistry of colon cancer: the $Apc^{Min/+}$ mouse model(14, 56, 67, 78). The *Min* mouse was derived from the offspring of a mouse treated with the mutagen ethylnitrosourea (ENU) in the laboratory of Dr. William Dove(56). Progeny of this mouse displayed circling behavior and adult-onset anemia; the former trait was eliminated through multiple backcrosses but the offspring that maintained the anemic phenotype were used for further study(56). In these anemic offspring, there were numerous visible tumors in the small and large intestines of the anemic animals whereas non-anemic littermates had no intestinal tumors(56). Intestines of the affected mice were populated with 19-39 tumors at the time of death and these tumors ranged in size from 1-8 mm. It was determined that the primary phenotype of these mice was the propensity to develop multiple intestinal tumors and anemia was presumed to be secondary; as a result, the mutant gene was named multiple intestinal neoplasia (*Min*)(56).

Due to the similar features of *Min* and FAP conditions, it was thought that the *Min* phenotype resulted from a mutation in the previously described APC gene(30,

84). In 1992, Su and colleagues used human APC probes to screen a wildtype mouse brain cDNA library and identified a single clone that corresponded to nucleotides 135 to 1412 of the human APC sequence(84). Reverse transcriptase PCR followed by Sanger sequencing was used with the goal of identifying the nucleotide sequence. The murine APC transcript was 8.5 kb in length and was predicted to encode a protein containing 2845 amino acids(84). Further analysis indicated that the human and murine coding sequences were 90% identical at the amino acid and 86% identical at the nucleotide level(84). In the *Min* mice, but not in any of the normal control mice, a T to A transversion was found at nucleotide 2549 and this introduced a premature stop codon at leucine 850, resulting in a truncated APC protein(84). Since these mice shared a similar mutation to human FAP patients, they have been widely used as a model for understanding human colorectal cancer (Reviewed in Shoemaker *et al.*, 1997 and Clarke, 2007)(13, 78).

1.8. Multistep Carcinogenesis in the $Apc^{Min/+}$ Mouse

Knudson's two-hit model of cancer progression was the first to demonstrate with statistical data the importance of accumulated mutations resulting in carcinogenesis(44). The availability of molecular tools has allowed for the identification of genetic aberrations responsible for tumorigenesis. Based on observations of numerous adenomas and invasive carcinomas, Fearon and Vogelstein proposed a mulstistep model of colorectal carcinogenesis which starts with an *Apc* mutation(22). Numerous studies provide support for this as *Apc* mutations are commonly observed in human colorectal tumors and colon cancer cell lines(33, 72). In the model by Fearon and Vogelstein, this loss of *Apc* functionality results in hyperproliferation in the intestinal epithelium(22). DNA hypomethylation is often observed in very small adenomas, indicating that it is also an early event in tumorigenesis and could lead to aneuploidy and a loss of tumor suppressor

genes(22). *K-ras* mutation occurs in one cell of the adenoma and clonal expansion creates a larger dysplastic tumor(22). Accumulated loss of tumor suppressor genes, including p53, result in a progression to a carcinoma *in situ* and further accumulation of mutations results in the formation of an invasive carcinoma(22).

1.9. The Role of BTB/POZ-ZF Transcription Factors in Development and Disease

Members of the BTB/POZ-ZF family possess an N-terminal BTB/POZ (Bric-a-brac, Tramtrak, and Broad complex/Pox virus and zinc finger) domain and a C-terminal zinc finger domain (Figure 4)(17, 65). The BTB/POZ domain, or simply "POZ domain," is a protein-protein interaction motif present in over 350 human gene products, and facilitates dimerization or oligomerization with itself or other proteins(17, 65). The POZ domain is present in all eukaryotic organisms ranging from fungi and plants to metazoans(65). X-ray crystallography was used to solve the structure of different transcription factor POZ domains, including that of the transcription factors ElonginC, PLZF, and BCL6. Interestingly, despite their low degree of primary sequence similarity, the secondary and tertiary structure of the examined POZ domains were strikingly similar(65). The POZ domains of each of these transcription factors contained five alpha-helices capped at one end with a beta-sheet and they each displayed a similar compact, globular shape (Reviewed by 65).

In addition to the protein-protein interaction POZ domain, POZ-ZF proteins possess zinc finger motifs, present predominantly at the C-terminus, which allow for DNA-binding(65). The combination of these two domains is found in approximately 80 POZ-ZF proteins in the human genome; all are postulated to function as transcription factors(65). The POZ domain of POZ-ZF proteins allows for diverse protein-protein interactions that can alter the affinity or specificity of a protein

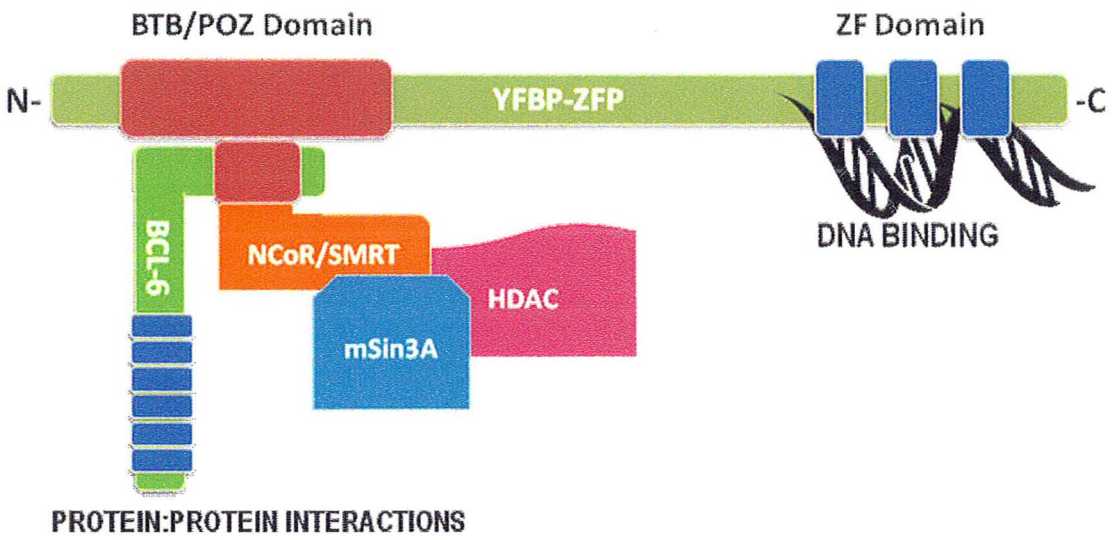

Figure 4 – POZ-ZF Proteins and their Interactions. POZ-ZF proteins typically possess an N-terminal POZ protein-protein interaction domain and a DNA-binding zinc finger region at the C-terminus. The POZ domain facilitates interaction with other POZ domain-containing proteins as well as components of chromatin remodeling complexes. It is hypothesized that POZ-ZF transcription factors achieve gene regulation by altering chromosome state. Histone deacetylase-containing proteins (HDACs) will cause the chromatin to condense and become inaccessible to transcription machinery while histone actyl transferases (HATs) will cause the chromatin to become more relaxed and facilitate gene transcription.

complex toward DNA(65). For example, the POZ domain of POZ-ZF transcription factors recruits transcriptional cofactors like mammalian Sin3 (mSin3), silencing mediator for retinoid and thyroid hormone receptor (SMRT), and nuclear co-repressor (NCoR) which, in turn, recruit corepressors like histone deacetylase complexes (HDACs) (Reviewed in Kelly and Daniel, 2006)(39). As a result, POZ-ZF transcription factors can function as genetic switches by altering chromatin configuration to produce a transcriptionally active "open state" or an inactive "closed state"(15, 65). Because of the key role they play in regulating gene expression, POZ-ZF transcription factors play important roles in development and disease.

For example, promyelocytic leukemia zinc finger (PLZF) is a POZ-ZF transcription factor that was first identified as a fusion protein with retinoic acid receptor-α in patients diagnosed with acute promyelocytic leukemia (APL)(2, 65). During APL pathogenesis, the PLZF-RAR-α fusion erroneously recruits co-repressors like SMRT to RAR-α target genes that are important in DNA repair, apoptosis, and the cell cycle(2, 65). In a developmental context, it has been shown through the use of knock-out (KO) mice that PLZF is essential for correct patterning of the limbs and skeletal structure(2, 15, 65). Mice lacking PLZF have deformed limbs and display homeotic transformations where anterior skeletal elements are displaced to the posterior(2, 65). Another example of POZ-ZF transcription factors contributing to disease is BCL6, a transcriptional repressor normally involved in germinal-centre formation, but deregulated in patients with non-Hodgkin's B-cell lymphoma (B-NHL)(62). In B-NHL patients, chromosomal translocations place BCL-6 under control of a heterologous promoter, usually of the immunoglobulin (*Ig*) family(62). Although the exact role of BCL6 in germinal-centre formation and lymphomagenesis has not been realized, it was recently discovered that BCL6 can directly bind and repress expression of p53(66). Suppression of p53 by BCL6 contributes to lymphomagenesis since cells can bypass p53-dependendent

apoptotic pathways that would normally destroy cells that have undergone DNA damage(66). From these examples, it is clear that POZ-ZF proteins are essential for normal development but mutation or misregulation of POZ-ZF transcription factors contribute to disease pathogenesis.

1.10. The BTB/POZ-ZF Transcription Factor Kaiso

Kaiso is a BTB/POZ-ZF (hereafter POZ-ZF) transcription factor that is aberrantly expressed in breast and ovarian tumor tissues and is also linked to the canonical and non-canonical Wnt signaling pathway. Kaiso was initially identified in a yeast two-hybrid (Y2-H) screen, as a binding partner for the Src tyrosine kinase substrate, p120(17). Kaiso possesses an N-terminal POZ domain and a C-terminal DNA-binding zinc finger domain, typical of POZ-ZF transcription factors (Figure 5). Kaiso is a unique member of the POZ-ZF family; its DNA-binding zinc finger region can bind both methylated CpG dinucleotides as well as a consensus Kaiso binding sequence (KBS)(18). Surprisingly, a Y2-H interaction assay revealed that it was Kaiso's DNA-binding domain, rather than its protein-protein interaction POZ domain, that interacts specifically with the Armadillo repeat domain of p120(17). This led to the hypothesis that the role of p120's interaction with Kaiso was to inhibit Kaiso's DNA-binding abilities(17).

To gain insight into Kaiso's biological function, studies were performed using the *Xenopus* (African clawed frog) model. The *Xenopus* homolog of Kaiso, xKaiso, showed 66% similarity to its murine counterpart at the amino acid level and its interaction with p120 was evolutionarily conserved(41). RT-PCR analysis demonstrated that Kaiso is expressed at all stages of early *Xenopus* embryogenesis and *in situ* hybridization studies showed that Kaiso was expressed mainly in neural cell precursors and neural tissue(41). More recently, Kaiso has been shown to bind and repress transcription of a number of canonical and non-canonical Wnt target

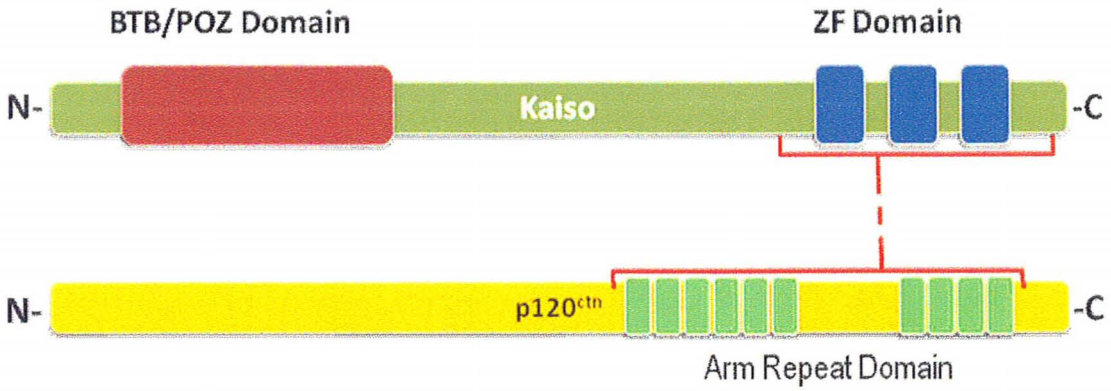

Figure 5 – Kaiso and p120 are Interaction Partners. Kaiso is a typical POZ-ZF transcription factor that contains an N-terminal POZ domain and three C-terminal zinc fingers. Kaiso interacts specifically with the Armadillo repeat domain of the Src substrate p120. Interestingly, the p120-binding site encompasses the Kaiso DNA-binding domain rather than its protein-protein interaction POZ domain.

genes (*Myc, mmp-7, cyclin-D1, Siamois,* and *Wnt11)(42, 64, 82).* Characterization of Kaiso in *Xenopus* provided the first experimental evidence of its link to the Wnt pathway(42, 64). Morpholino anti-sense oligonucleotides were used to deplete *Xenopus laevis* embryos of Kaiso and this resulted in severe gastrulation defects(42, 64). Specifically, xKaiso knockdown resulted in delayed blastopore closure that was due to a perturbation of convergent extension during gastrulation(42, 64). Loss of xKaiso also resulted in premature activation of genes necessary during the mid-blastula transition(64). A similar phenotype was noticed when the DNA methyltransferase *Dmnt1* was knocked down in these embryos(64). These abnormalities were rescued by injecting the embryos with an ectopic source of Kaiso(64). In the mammalian model system, however, Kaiso knockout mice showed no overt developmental defects at the organism or cellular levels(73). The accepted reasoning behind these conflicting results in different model systems is the fact that there are a number of Kaiso-related proteins in mammals that are absent in frogs(16, 73, 91). In mice, ZBTB4 and ZBTB38 share significant homology with Kaiso and could be functionally redundant, explaining the lack of obvious developmental disorders in Kaiso-null mice(16, 73, 91). The discrepancy between the amphibian and mammalian model system may be resolved by creating triple knockout mice that are null for Kaiso, ZBTB4, and ZBTB38. The expectation is that if ZBTB4 and ZBTB38 are redundant, a triple knockout (ZBTB4/Kaiso/ZBTB38) mouse would display a phenotype analogous to that of Kaiso-deficient frogs.

Further studies in the mouse and *Xenopus* model implicate Kaiso as a positive and negative regulator of Wnt signaling, respectively(64). When β-catenin is overexpressed in the animal pole of the developing *Xenopus* embryo, axis duplication results(24). However, Kaiso overexpression is able to suppress the overactive Wnt signaling and rescue this phenotype(64). In the mammalian $Apc^{Min/+}$ mouse model system, however, Kaiso has the opposite effect on Wnt signaling. When Kaiso null mice are crossed with $Apc^{Min/+}$ mice, there is a delay in tumor onset

and decreased tumor burden(73). These apparently contradictory roles for Kaiso in the Wnt signaling pathway suggest that Kaiso may have both oncogenic and tumor suppressor roles that are organism- or context-dependent.

1.11. Rationale for Experiments

Kaiso's role in development and the Wnt signaling pathway has been explored in two vertebrate systems, *Xenopus* and mouse, but conflicting results have been observed. In *Xenopus*, Kaiso depletion results in lethal embryonic defects but Kaiso null mice are viable and fertile. Additionally, in *Xenopus*, Kaiso acts as a negative regulator of constitutive Wnt signaling and counteracts the effects of overactive β-catenin. In the murine system, however, Kaiso null mice show a resistance to intestinal cancer caused by constitutive Wnt signaling. This suggests that Kaiso has a positive effect on Wnt signaling and intestinal tumor development. Hence, to resolve the discrepancy observed in these two model organisms and to clarify Kaiso's relevance to the Wnt signaling pathway, we generated an intestinal-specific Kaiso overexpression mouse. The long term goal of this project is to determine the role of Kaiso in a pathological context using the $Apc^{Min/+}$ mouse model of intestinal cancer.

<u>Hypothesis:</u> Kaiso is a component of a signaling network that contributes to constitutive Wnt/β-catenin signaling in the $Apc^{Min/+}$ mouse model of intestinal cancer.

Materials and Methods

2.1. Plasmids and Expression Vector Constructs

The murine 9 kb intestinal-specific villin promoter fragment was provided to us by Dr. Sylvie Robine (Institut Curie. Paris, France). The villin promoter is in the pBluescript II cloning vector upstream of a polyA tail derived from the SV40 virus. Myc-tagged murine Kaiso was amplified by PCR from the pCS2^{+}MT-mKaiso S11/38 vector (provided by Dr. Pierre McCrae) using the following primer pair: 5'-ATC GAT CGT ACG CCA CCA TGG AGC AAA AG-3' and 5'-ATC GAT ACG CGT TCA GTA AGA TTC TGG TAT-3'. After amplification, the PCR product was purified using the QIAquick PCR Purification Kit (Qiagen, Valencia, CA) according to the manufacturer's instructions. The purified PCR amplicon and the villin vector were digested with the restriction endonucleases BsiWI and MluI (New England Biolabs, Ipswich, MA) and purified once again using a QIAquick column. Picomolar amounts of insert and vector DNA were added in a 5:1 ratio and ligated using T4 DNA ligase (New England Biolabs) according to the manufacturer's instructions. The ligation products were transformed into DH5α competent cells (Invitrogen, Carlsbad, CA) according to manufacturer's instructions and transformants were selected by plating on LB-agar containing Carbenicillin (50 μg/ml) (Carbenicillin DIRECT, Dewsbury, UK). Antibiotic-resistant clones were screened by restriction enzyme digest using BsiWI and MluI and putative positive clones containing the Villin-mKaiso-MT gene were confirmed by sequencing (MOBIX Labs, McMaster University). Plasmids used in transfections were purified using the Quantum Prep Midi Prep Kit (Bio-Rad, Hercules, CA) and plasmids used for microinjection were purified using the QiaPrep Plasmid Maxi-Prep Kit (Qiagen).

2.2. Cell culture

Villin-positive rat IEC-6 cells were a gift from Dr. Kelly Meckling (Dept. Biology, Guelph University) and porcine LLC-PK1 cells were purchased from ATCC (ATCC, Manassas, VA). IEC-6 and LLC-PK1 cells were grown in Dulbecco's Modified Eagle Medium (Cellgro, Manassas, VA) and supplemented with 10% Fetal Bovine Serum (PAA, Pasching, Austria), 1% penicillin/streptomycin and 0.4% fungizone (Invitrogen). Villin-positive CaCO2 human colon carcinoma cells were a gift from Dr. Mary Purdue (Intestinal Disease Research Programme, McMaster University) and were cultured in MEM supplemented with 20% FBS, non-essential amino acids (Invitrogen), sodium pyruvate (Invitrogen), 1% penicillin/streptomycin, and 0.4% fungizone (Invitrogen). Cells were incubated at 37°C in a humidified atmosphere with 5% CO_2.

2.3. Transient Transfections and IP-Western Blot

Cells were transfected while in the logarithmic growth phase (~60-70% confluence) with 15 μg of plasmid DNA using ExGen 500 (Fermentas, Burlington, ON) or Lipofectamine 2000 (Invitrogen) according to the manufacturers' protocol. 24 hours after transfection, cells were rinsed with cold PBS and lysed in NP-40 lysis buffer (50 mM Tris-HCL; pH 7.4, 150 mM NaCl, and 0.5% NP-40 with a protease inhibitor cocktail (Roche, Indianapolis, IN)) on ice for 10 minutes. Lysates were scraped into a microcentrifuge tube and cell debris pelleted by centrifugation at 13,000 x *g* for 6 minutes. The supernatant was then transferred to a new tube and protein content was quantified by Bradford assay (Bio-Rad). 100 μg of total cell protein was used for western blot. For immunoprecipitation, 500 μg of whole cell lysate was incubated on a rotating platform with 4 μg of the antibody of interest for 1 hour at 4°C. After 1 hour, a 50% slurry of Protein A Sepharose beads (Amersham Biosciences, Piscataway, NJ), saturated with rabbit anti-mouse IgG (Jackson

Immunoresearch, West Grove, PA), was added to the cell lysate and the immunoprecipitation was continued with rotation at 4°C for an additional hour. The Sepharose beads were pelleted by centrifugation and washed 5 times with NP-40 lysis buffer without protease inhibitor cocktail to remove non-specifically bound protein. After washing, the beads were prepared for SDS-PAGE by boiling in Laemmli Sample Buffer (LSB) (100 mM Tris; pH 6.8, 2% SDS, 10% glycerol, 0.008% bromophenol blue, 0.24 M β-mercaptoethanol) for 5 minutes. Proteins were separated by SDS-PAGE on a 7% gel and subsequently transferred to a nitrocellulose membrane. The membrane was blocked using 3% non-fat milk in TBS for 10 minutes prior to incubation with the primary antibody overnight at 4°C with agitation. After overnight incubation, unbound primary antibody was removed by washing 5 times with TBS for 5 minutes each time. Horseradish peroxidase-conjugated secondary antibodies (Jackson Immunoresearch) were applied at a dilution of 1:40,000 and the membrane was incubated at room temperature for two hours with agitation. Unbound secondary antibody was washed with TBS and the membrane was then incubated with Western Lightning Enhanced ChemiLuminescence (ECL) substrate (Perkin Elmer, Waltham, MA) which allowed for detection using X-ray film (Kodak, Rochester, NY).

2.4. Transgenisis and Mouse Strains

Transgenic mice were generated by Dr. Sui-Pok Yee at the London Regional Cancer Center (www.lhsc.on.ca). Briefly, the Villin-mKaiso-MT vector was digested with SalI to separate the pBluescript backbone from the Villin-mKaiso-MT cDNA. This Villin-mKaiso cDNA fragment was then isolated using agarose gel electrophoresis, electroeluted from the agarose gel slice, and purified by ethanol precipitation. The Villin-mKaiso-MT DNA fragment was resuspended in an injection buffer and injected into 1-cell stage C57B6/CBA hybrid mouse embryos, which were then

implanted into pseudopregnant females. Transgenic pups were identified by PCR genotyping. C57/Black 6-Apc$^{Min/+}$ mice were purchased from Jackson Laboratories (Bar Harbor, ME) and wildtype C56/Black 6 mice were purchased from Taconic (Hudson, NY). All mice were housed in the Central Animal Facility (McMaster University) and fed a standard mouse diet.

2.5. Preparation of Mouse Genomic DNA and PCR Genotyping

Mouse tail snips (<0.5cm) were digested overnight at 55° C in 50 µl of digestion buffer containing 50 mM Tris-HCl; pH 8.0, 1 mM EDTA, 50 mM NaCl, 0.1% SDS and 1 mg/ml proteinase K. After overnight digestion, the proteinase K was inactivated by heating to 85°C for 10 minutes. Tissue debris was pelleted by centrifugation for 1 minute at 13,000 x *g* and 1 µl of the supernatant was used for PCR genotyping. PCR primers used to amplify the Kaiso transgene were 5'- ATC ATC AAA GCC GGG TGG GCA -3' and 5'- TTT TCT ACT CTC CAT TTC ATT CAA GTC CTC -3'. PCR conditions were as follows: 95°C for 5 minutes, followed by 30 cycles at 95°C for 30 sec, 55°C for 1 minute, 72°C for 1 minute followed by a final extension step at 72°C for 10 minutes. The primers produced a 400 bp amplicon which was resolved on a 1.5% agarose gel stained using ethidium bromide for visualization.

2.6. PCR Standards and Transgene Copy Number Determination

Transgene copy number was estimated using PCR by comparing transgenic mouse DNA from each strain to single and multiple copy number standards (previously described by University of Virginia Health System, Gene Targeting and Transgenic Facility; www.healthsystem.virgina.edu/internet/transgenic-mouse/copystandardspcr.cfm). This method makes the following three assumptions: (1) the haploid content of the mouse genome is 3 x 10^9 bp, (2) you are

using 100 ng DNA per PCR reaction, and (3) transgenic founder mice are hemizygous for the transgene. Standards were prepared by spiking wildtype mouse DNA with specific amounts of transgenic DNA, correlating to 1, 5, 10, 50, and 100 copies of the transgene per PCR reaction using primers described in Section 2.5. The mass of a single copy of transgenic DNA is equal to:

$$\frac{size\ of\ PCR\ band\ to\ be\ amplified\ (bp)}{haploid\ mouse\ genome\ (bp)} \times \frac{100\ ng\ gDNA\ per\ PCR\ reaction}{2\ (for\ hemizygous\ insertion)}$$

Since the PCR amplicon constitutes only a fraction of the Villin-mKaiso-MT vector the mass of plasmid vector added to 100 ng gDNA to attain a single copy is calculated according to the following equation:

$$\frac{size\ of\ entire\ plasmid\ (bp)}{size\ of\ PCR\ band\ to\ be\ amplified\ (bp)} \times \frac{mass\ of\ a\ single\ copy\ of\ transgenic\ DNA}{1}$$

100 ng standard DNA and tail DNA were used for each PCR reaction that was performed as described in section 2.5. PCR products were run on a 1.5% agarose gel, stained with ethidium bromide, and visualized under UV light.

2.7. Mouse Tissue Protein Harvest

All mice were sacrificed by CO_2 asphyxiation before tissue harvest. Mice were dissected and harvested tissue was rinsed in cold PBS, frozen in a liquid nitrogen-cooled container, and stored at -80°C until further processing. For protein purification, mouse tissue was thawed on ice and 250 mg of tissue was finely minced using a sterile scalpel blade. The minced tissue was then resuspended in cold RIPA buffer (50 mM Tris; pH 7.4, 1% NP-40, 0.25% sodium deoxycholate, 150 mM NaCl, 1 mM EDTA) and homogenized manually in a chilled tissue grinder

(Kontes #21 glass tissue grinder) (Kimble Chase, Vineland, NJ). Tissue lysate was transferred to a microcentrifuge tube and debris was pelleted by centrifugation at 13,000 x *g* for 10 minutes. Protein concentration was quantified by Bradford assay (Bio-Rad) and 100 μg was used for SDS-PAGE and western blot analysis.

2.8. Mouse Tissue RNA Purification

Mouse tissue was homogenized and total RNA purified using the RNeasy Kit (Qiagen). For homogenization, tissue was minced finely with a clean blade, suspended in 600 μl Qiagen Buffer RLT, and homogenized on ice in a glass tissue grinder. Total RNA was subsequently purified from the homogenized lyaste using the RNeasy kit according to manufacturer's instructions.

2.9. Semi-quantitative RT-PCR

Semi-quantitative reverse transcriptase-polymerase chain reaction (RT-PCR) analysis was performed using the Superscript II One-Step RT-PCR kit (Invitrogen). 50 ng total RNA was used for each reaction with primers specific to the villin-mKaiso-MT transcript, and transcription factor IID (TFIID) as a loading control. The primer pairs used in the RT-PCR reaction were as follows: villin-mKaiso-MT: 5'- CAA CTT CCT AAG ATC TCC CAG GT -3' and 5'- CAA GGA GTT CAG CAG ACT GG -3'; TFIID: 5'- CCA CGG ACA ACT GCG TTG AT -3' and 5'- GGC TCA TAG CTA CTG AAC TG -3'. The RT-PCR program included one round of cDNA synthesis for 30 minutes at 50°C, an initial denaturation at 95°C for 2 minutes and 30 cycles of 94°C for 15 sec (denaturation), 55°C for 30 sec (annealing), and 72°C for 30 sec (extension). A final extension step at 72°C for 10 minutes concluded the program. Samples were separated on a 1.5% agarose gel and visualized using ethidium bromide under ultraviolet light.

2.10. Immunohistochemistry

Intestinal tissue was harvested, cut open longitudinally, flattened on a piece of blotting paper, fixed in 10% neutral-buffered formalin for 48 hours, and then stored in 70% ethanol until further processing. Paraffin embedding and tissue sectioning was performed by the Core Histology Facility at the Center for Gene Therapeutics (McMaster University). For immunostaining, sections were first dewaxed in xylene with two 5 minute washes followed by hydration in an ethanol gradient. Antigen retrieval was accomplished by boiling tissue in a sodium citrate buffer (pH 6.0) for 13 minutes and allowing the slides to cool to RT for 30 minutes. Tissue was permeablized with TBS-T (Tris-buffered Saline, 0.05% Tween-20). Endogenous peroxidase activity was quenched with a 3% solution of hydrogen peroxide in TBS for 10 minutes followed by 1 hour incubation with normal donkey serum (Jackson Immunoresearch) and an avidin blocking solution (Vector Labs, Burlingame, CA) to prevent non-specific epitope and avidin binding. After blocking, the primary antibody was applied at a dilution of 1:2000 in the blocking solution and a biotin blocking solution (Vector Labs) was added to this mixture to block endogenous biotin sites. The primary antibody incubation occurred overnight in a humidified chamber at 4 ^{o}C. After overnight incubation, the primary antibody was washed with TBS-T and a biotin-conjugated donkey-anti-rabbit secondary was applied at a dilution of 1:1000 for 2 hours. The secondary antibody was washed using TBS-T and the Vectastain Elite ABC (avidin-biotin horseradish peroxidase complex) (Vector Labs) reagent was applied to the tissue for 30 minutes. After a brief wash in TBS, Vectastain DAB substrate (Vector Labs) was applied for 3 minutes and washed off with water for 5 minutes after satisfactory colour development. Tissue was then counterstained using Harris' modified hematoxylin (Sigma, St. Louis, MO), differentiated in acid ethanol, blued in Scott's tap water substitute, dehydrated in an ethanol series, cleared in xylene, and mounted using Polymount (Polysciences Inc,

Warrington, PA). Images were acquired using a Zeiss Axiovert 200 microscope and Adobe Photoshop was used to adjust the white balance and crop the images.

Results

3.1. Cloning and Transgenesis

As a first step toward understanding the role of Kaiso in the mammalian Wnt signaling pathway, we designed and engineered an intestinal-specific Kaiso overexpression mouse model. There are a number of gene promoters that can direct intestinal-specific gene expression but many are only activated in fully differentiated intestinal epithelial cells(20, 55, 74, 85). The villin promoter, however, is active in all villin-positive epithelial cells and is used as a tool to direct tissue-specific gene expression to the epithelial layer of the small and large intestines(69). Villin is a Ca^{2+}-dependent actin bundling protein localized to the brush border of polarized epithelial cells including the enterocytes lining the lumen of the intestines (Reviewed by Fath and Burgess, 1995)(21). The human villin promoter was first characterized in 1993 and was shown to activate transcription of heterologous genes not only in terminally differentiated villin positive cell lines like CaCO2, HepG2, and LLC-PK1 but also in differentiating HT29 cells(74). In 1999, however, the same group cloned and characterized a 9-kb fragment of the murine villin promoter capable of directing heterologous gene expression in both immature and differentiated epithelial cells of the small and large intestine(69). This villin promoter was therefore used in the creation of the intestinal-specific Kaiso overexpression mouse model.

The Kaiso overexpression construct was designed using an N-terminal myc-tagged copy of murine Kaiso that was cloned downstream of the villin promoter (Figure 6). The promoter construct DNA was injected into the pronucleus of C57B6/CBA F1 hybrid mouse embryos that were then implanted into pseudopregnant females (cloning and transgenesis are described above in the *Materials and Methods* section). Litters borne from implanted embryos were screened by PCR using primers specific for the transgene and four founders were initially identified. Breeding colonies were established by mating each of the four

Figure 6 – The Villin-Kaiso Transgene. To create an intestinal-specific Kaiso overexpression model, murine Kaiso was cloned downstream of the intestinal-specific villin promoter. The transgene was also tagged with a myc epitope in order to facilitate differentiation between endogenous Kaiso and that expressed by the transgene.

founders with wildtype C57B6 mice. PCR genotyping of the resultant litters revealed that founders "A," "B," and "C" were able to transmit the transgene to both male and female progeny whereas founder "D" was unable to do so (Figure 7). Additionally, founders "A," "B," and "C" transmitted the gene to their progeny at rates of 15%, 32%, and 57%, respectively (comparing transgenic vs. non-transgenic littermates from each founder). These values are quite different from the expected Mendelian ratios but could indicate that Kaiso overexpression is toxic during mouse development and some animals die *in utero* or that the transgene has integrated into a locus where it interferes with normal embryonic gene expression and causes embryonic death.

3.2. Transgene Copy Number

Villin-Kaiso transgenic mice were created via DNA pronuclear injection which results in random genome integration, it is therefore important to determine transgene copy number of the founders. In this type of transgenesis, it is possible for transgene concatemers to integrate head-to-tail into the recipient genome. Thus, techniques like Southern Blotting or PCR are used to estimate gene copy number (described in Materials and Methods). PCR genotyping using standardized amounts of tail DNA spiked with known quantities of purified plasmid transgene DNA allow for an estimation of Villin-Kaiso transgene copy number in each transgenic line used in this study (Figure 8). Using this approach, it is estimated that transgenic line A contains between 50-100 copies of the transgene while transgenic lines, B, and C contain approximately 10 and 50 copies, respectively.

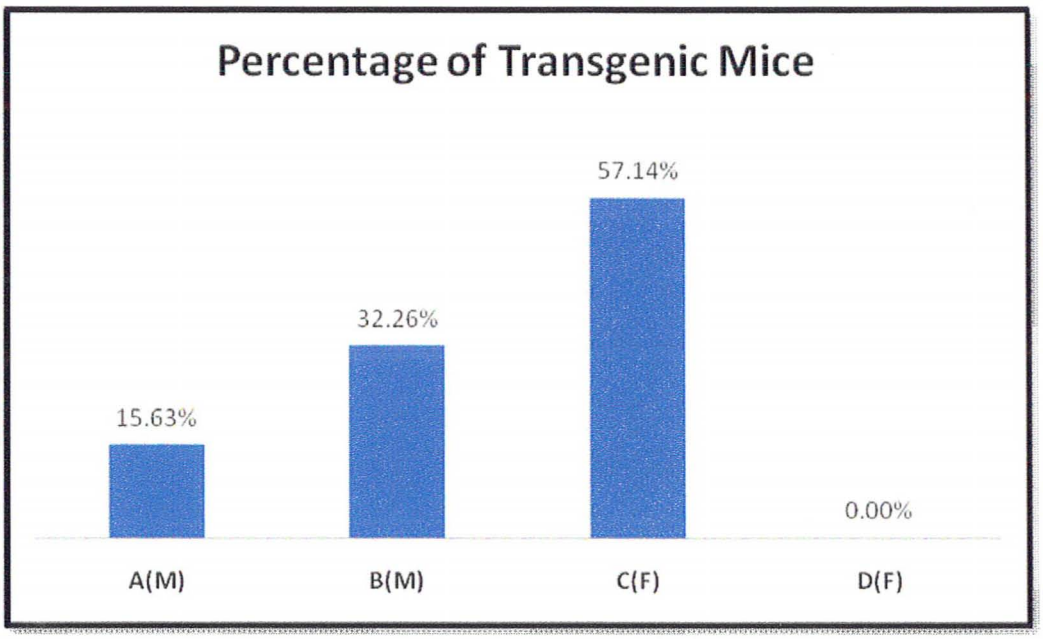

Figure 7 – Kaiso-Tg Mice Breeding Colony Statistics. Genotyping of villin-Kaiso transgenic mice show that the transgene is transmitted at different rates by the four founder animals. "A," "B," "C," and "D" represent the four founder lines and they transmit the villin-Kaiso gene to their offspring at a frequency of 15.65%, 32.26%, 57.14%, and 0%, respectively. "M" and "F" represent the gender of the transgenic founder used to initiate each breeding colony.

3.3. Kaiso Overexpression in Transgenic Mice

In vivo expression of the transgene was confirmed by western blot analysis of intestinal tissue. Unfortunately, several attempts to purify small intestine protein failed due to contamination by protein present in the mouse diet. Hence, western blot analysis was only performed on large intestine tissue. Kaiso overexpression was observed in the large intestines of transgenic mice from each founder line; overexpression from transgenic lines A, B, and C, were strong, moderate, and mild, respectively (Figure 9). In each line, however, Kaiso was being expressed in the transgenic animals at higher levels compared to their non-transgenic littermates. To differentiate between endogenous Kaiso and Kaiso overexpressed due to the villin promoter, large intestine lysates were probed with an α-myc antibody since the Kaiso transgene was myc-tagged. The α-myc antibody detects a band at the correct molecular weight only in tissue derived from transgenic animals, indicating that the Kaiso overexpression was indeed a result of the transgene (Figure 9). Furthermore, when probed with the α-myc antibody, the same pattern of strong, moderate, and mild Kaiso overexpression was observed in the respective transgenic lines.

Since small intestine tissue could not be used for western blotting analysis, semi-quantitative RT-PCR was used to confirm Kaiso overexpression in both the small and large intestine. PCR primers were designed to specifically amplify mRNA encoded by the transgene while excluding endogenous Kaiso mRNA, Kaiso genomic DNA, and transgenic DNA. RT-PCR analysis of intestinal tissue from each transgenic line and a control littermate shows that both the small and large intestines express transgenic mRNA while this product is not present in non-transgenic littermates; amplification of TFIID transcripts were used as a control to indicate equal mRNA loading (Figure 10, 11, 12). Additionally, to confirm the specificity of the promoter and that Kaiso overexpression was limited only to tissue in which villin is normally

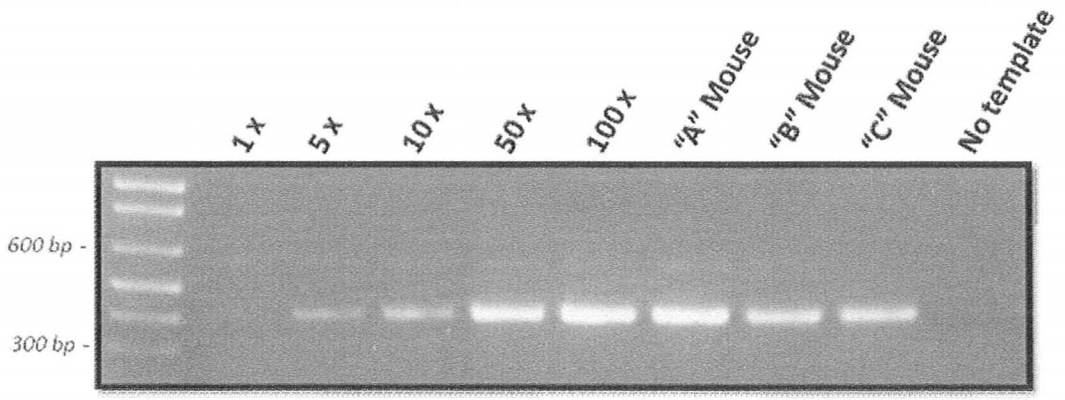

Figure 8 – Villin-Kaiso Transgnene Copy Number Determination. PCR was used to compare the transgene copy number in each transgenic line. Standards were prepared by spiking wildtype tail DNA with specific amounts of purified transgenic DNA. A standard PCR reaction was performed using standard DNA and transgenic DNA from each founder line. The intensity of the band amplified in each of the transgenic animals is compared to that of the standards in order to estimate transgene copy number.

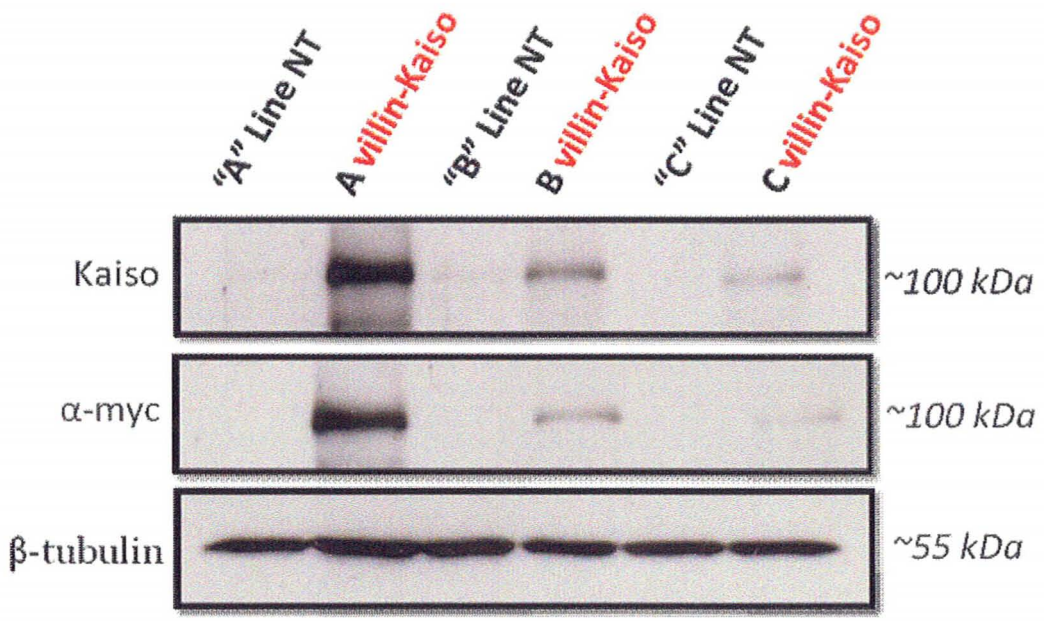

Figure 9 - Kaiso Overexpression in the Large Intestines. Western blot of large intestine tissue from A, B, and C line transgenic and wildtype littermates indicates that Kaiso is expressed at low levels in a wildtype background but at higher levels in the transgenic animals. Each transgenic line expresses Kaiso at varying levels with lines A, B, and C exhibiting strong, moderate, and weak levels of overexpression.

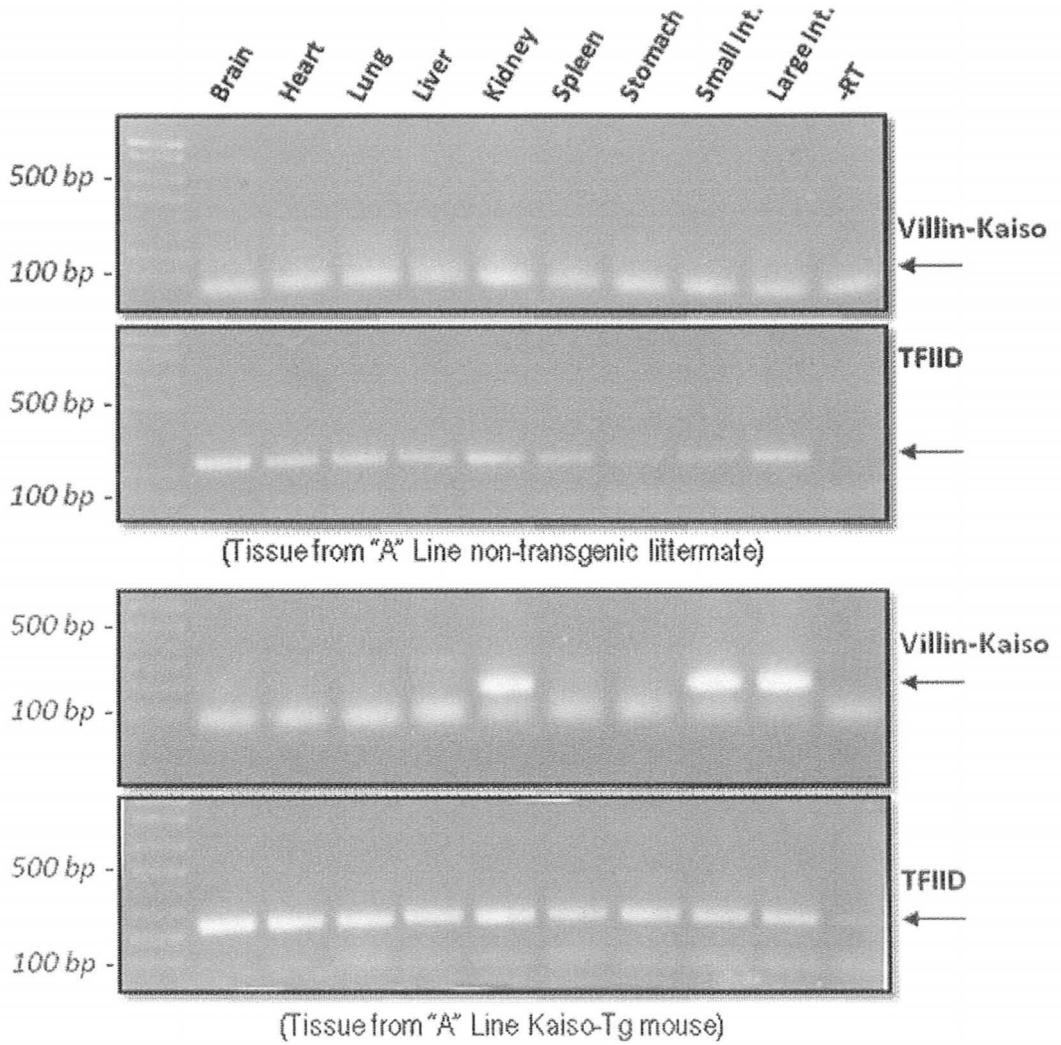

Figure 10 – Tissue RT-PCR from "A" Line Kaiso-Tg and non-transgenic mice. RT-PCR analysis was used to detect transgene expression in the small intestines; TFIID was used as a loading control. This technique was also used to confirm that transgenic gene expression was confined only to villin-positive tissues like the kidney, small intestines, and colon. RT-PCR results show that the transgene is being expressed in the small intestines, large intestines, and kidney of only the transgenic animal while these products are not detected in tissue from its non-transgenic littermate.

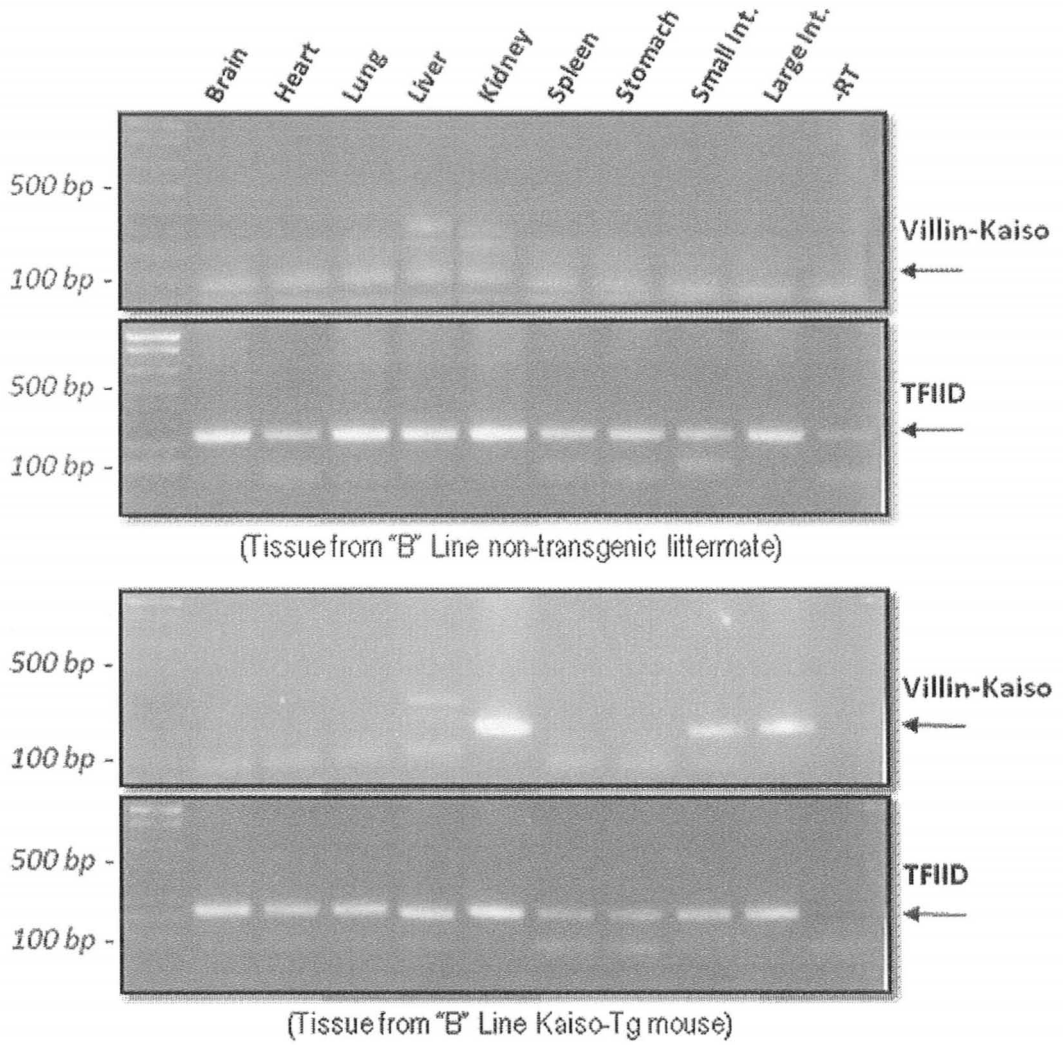

Figure 11 – Tissue RT-PCR from "B" Line Kaiso-Tg and non-transgenic mice. RT-PCR analysis was used to detect transgene expression in the small intestines; TFIID was used as a loading control. This technique was also used to confirm that transgenic gene expression was confined only to villin-positive tissues like the kidney, small intestines, and colon. RT-PCR results show that the transgene is being expressed in the small intestines, large intestines, and kidney of only the transgenic animal while these products are not detected in tissue from its non-transgenic littermate.

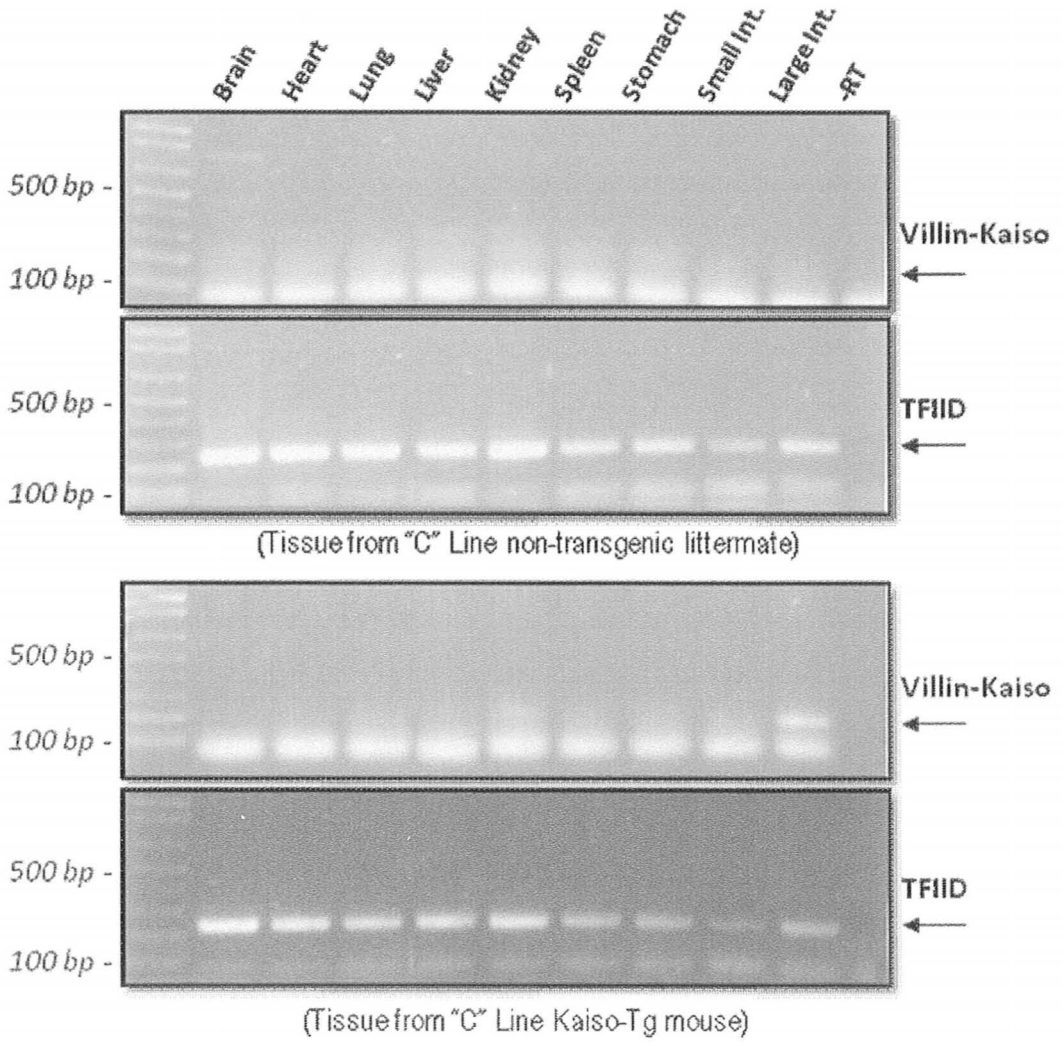

Figure 12 – Tissue RT-PCR from "C" Line Kaiso-Tg and non-transgenic mice. RT-PCR analysis was used to detect transgene expression in the small intestines; TFIID was used as a loading control. This technique was also used to confirm that transgenic gene expression was confined only to villin-positive tissues like the kidney, small intestines, and colon. RT-PCR results show that the transgene is being expressed mainly in the large intestines of only the transgenic animal while these products are not detected in tissue from its non-transgenic littermate. The lower expression levels are likely attributed to the fact that there are fewer copies of the transgene in "C" line transgenic mice compared to the transgene copy number in "A" and "B" line transgenic mice.

expressed; RT-PCR analysis was performed using a variety of tissues from the mouse. RT-PCR results indicate that the transgene is expressed only in villin-positive tissues such as the kidneys, small, and large intestines but not in any other tissues of "A" and "B" line mice. In "C" line transgenic mice, however, transgenic mRNA levels are low in the kidney and almost absent in the small intestine. It is likely that the low levels of transgenic transcript are due to the fact that "C" line mice have far fewer copies of the transgene than mice from the "A" and "B" lines.

While molecular analyses confirmed that the transgene is being expressed, it was necessary to determine the subcellular localization and expression levels of the Kaiso protein. Immunohistochemistry was used to determine whether the transgenic Kaiso exhibits the same diffuse nuclear localization as its endogenous counterpart. Small and large intestinal segments from Kaiso-Tg and non-transgenic littermates were stained using an α-Kaiso antibody to observe its tissue-specific localization and to confirm its nuclear localization. In normal small intestine tissue, Kaiso is expressed along the length of the villus and in all cells lining the crypts, including the Paneth cells found at the base of the crypt (Figure 13, 14, 15). Kaiso exhibits mainly strong diffuse nuclear expression in these cells, with very weak cytoplasmic expression. This pattern is similar to the Kaiso localization observed in cultured epithelial cells. In the large intestine, diffuse nuclear expression and weak cytoplasmic expression is observed in all of the cells lining the intestinal crypt (Figure 16, 17, 18). In both the small and large intestine, Kaiso expression is noticeably absent in the lamina propria, lacteal, and underlying muscularis mucosa. When the intestines from Kaiso-Tg mice from each of the "A," "B," and "C" lines were examined, they displayed a similar expression pattern compared to wildtype littermates. That is, epithelial cells of both the small and large intestine in A, B, and C line transgenic mice exhibit strong, diffuse nuclear Kaiso, and weak cytoplasmic staining. Consistent with the expression pattern in wildtype littermates, Kaiso-Tg mice had no Kaiso expression in the lacteal, muscularis musosa, and lamina propria.

3.4. Kaiso Overexpression in the Mouse Intestines

Kaiso and other POZ-ZF proteins have important roles in the normal development of a number of organisms including mice and frogs. Intestinal-specific Kaiso overexpression has no obvious effects on mouse phenotype and development since transgenic mice were healthy, showed no signs of distress such as ruffled fur, hunched posture, or severe weight loss (Table I and Figure 19, 20, 21). In 3 out of 5 gender- and age-matched pairs of mice used in this study, the Kaiso-Tg mice weighed less than their non-transgenic littermates (Table A-I). In order to confirm whether Kaiso overexpression contributes changes in body mass, a larger sample size would be necessary. To determine whether Kaiso overexpression had an effect on normal intestinal development histological analysis of transgenic intestinal tissue was performed. Large and small intestine tissue were prepared for visualization by formalin fixation and paraffin embedding followed by staining with hematoxylin and eosin (H&E) after sectioning. Tissue from each transgenic line, "A," "B," and "C," was visualized after both H&E and immunostaining. Small and large intestines were divided into proximal (anterior) and distal (posterior) portions and two images were taken for each segment of the intestine to gain insight into overall intestinal morphology.

The small and large intestines are functionally and histologically distinct, the former having villi that extend into the lumen and both having intestinal crypts. The lack of intact villi in small intestinal preparations is presumably an artifact of the tissue handling experienced during the embedding process and is not a result of Kaiso overexpression. There are two reasons why this conclusion has been drawn: (1) the villi are present after the fixation but before embedding (as observed through a dissecting microscope) and (2) villi are also missing or destroyed in the non-transgenic littermates, ruling out Kaiso overexpression as a mechanism. This situation prevents an analysis of Kaiso overexpression on villus length and morphology but the crypts of both the small and large intestines remained intact

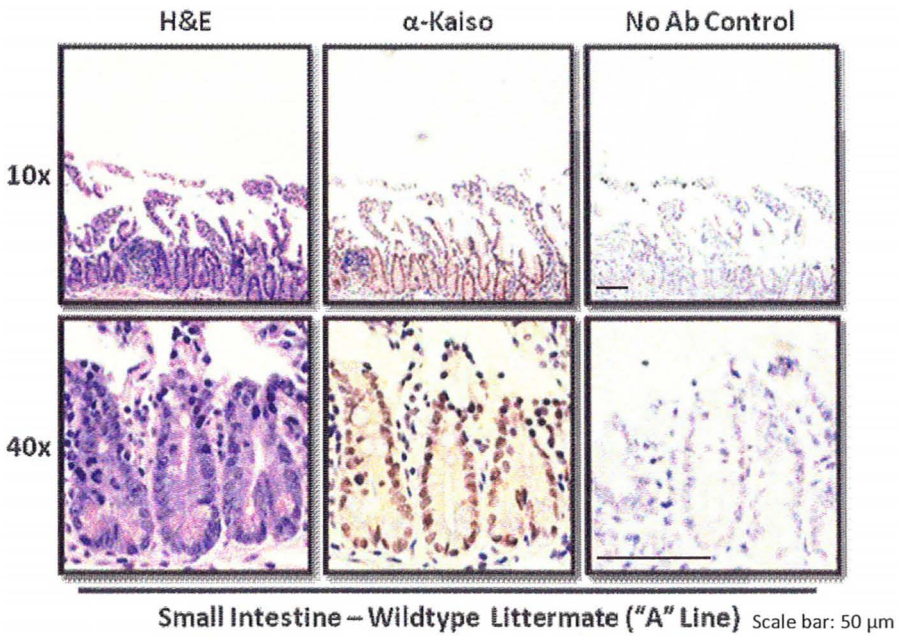

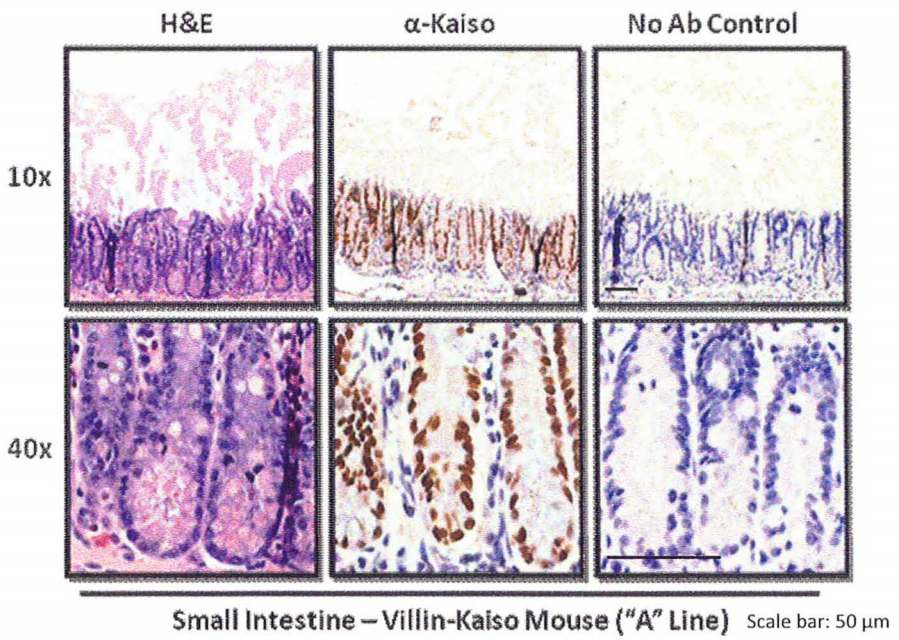

Figure 13 – Kaiso Localization in the Small Intestines ("A" Line mice).
Immunostaining with Kaiso antibodies shows that Kaiso localization is restricted to cells along the intestinal crypt and in brush border cells of the villi (where present). The lacteal and underlying mucosa lack Kaiso expression. Kaiso expression is also strongly nuclear in both wildtype and the villin-Kaiso transgenic intestines with very weak cytoplasmic staining.

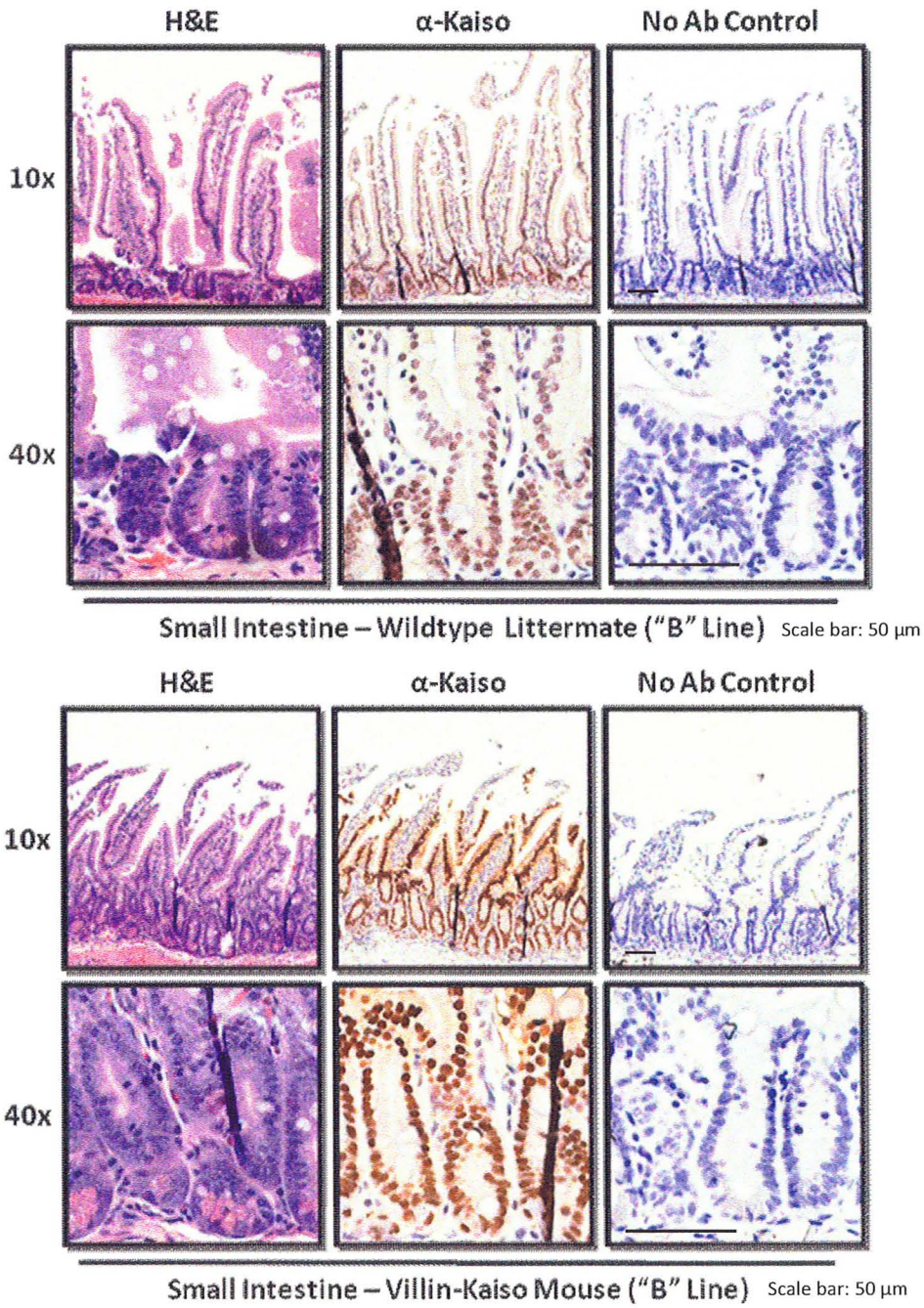

Figure 14 – Kaiso Localization in the Small Intestines ("B" Line mice). Immunostaining with Kaiso antibodies shows that Kaiso localization is restricted to cells along the intestinal crypt and in brush border cells of the villi (where present). The lacteal and underlying mucosa lack Kaiso expression. Kaiso expression is also strongly nuclear in both wildtype and the villin-Kaiso transgenic intestines with very weak cytoplasmic staining.

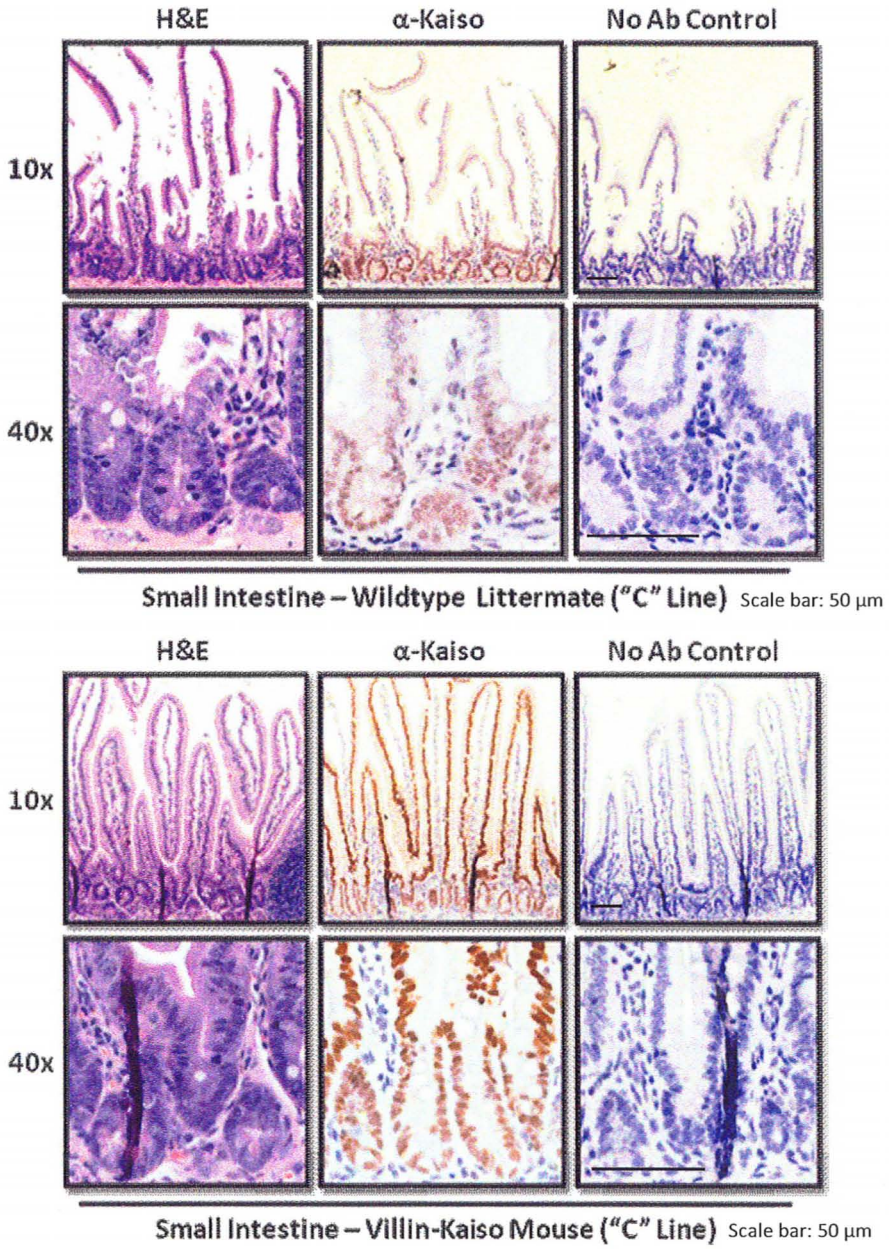

Figure 15 – Kaiso Localization in the Small Intestines ("C" Line mice). Immunostaining with Kaiso antibodies shows that Kaiso localization is restricted to cells along the intestinal crypt and in brush border cells of the villi (where present). The lacteal and underlying mucosa lack Kaiso expression. Kaiso expression is also strongly nuclear in both wildtype and the villin-Kaiso transgenic intestines with very weak cytoplasmic staining.

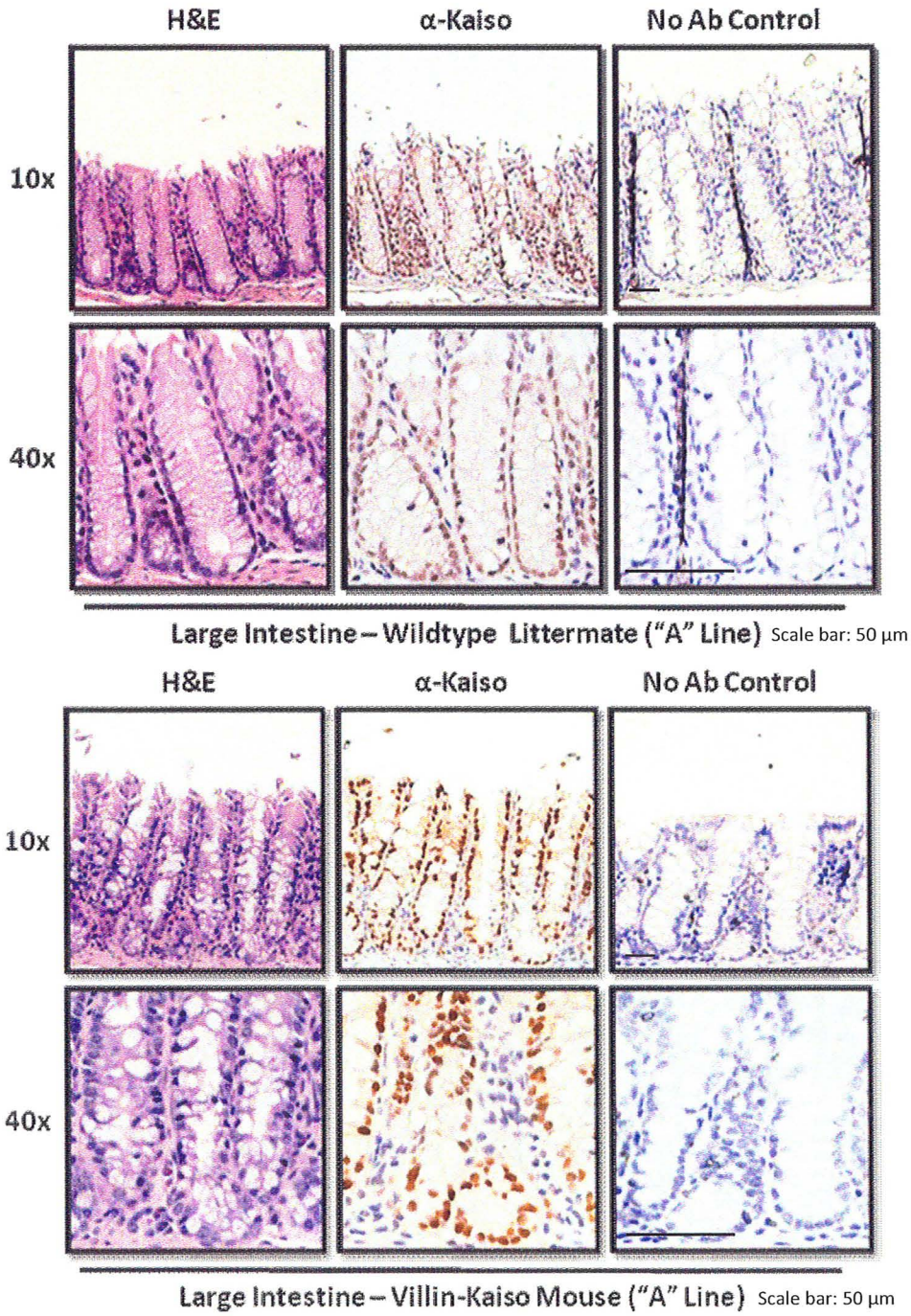

Figure 16 – Kaiso Localization in the Large Intestine ("A" Line mice). Immunostaining with Kaiso antibodies shows that Kaiso localization is restricted to cells along the intestinal crypt. The lamina propria and underlying mucosa lack Kaiso expression. Kaiso expression is also strongly nuclear in both wildtype and the villin-Kaiso transgenic intestines with very weak cytoplasmic staining.

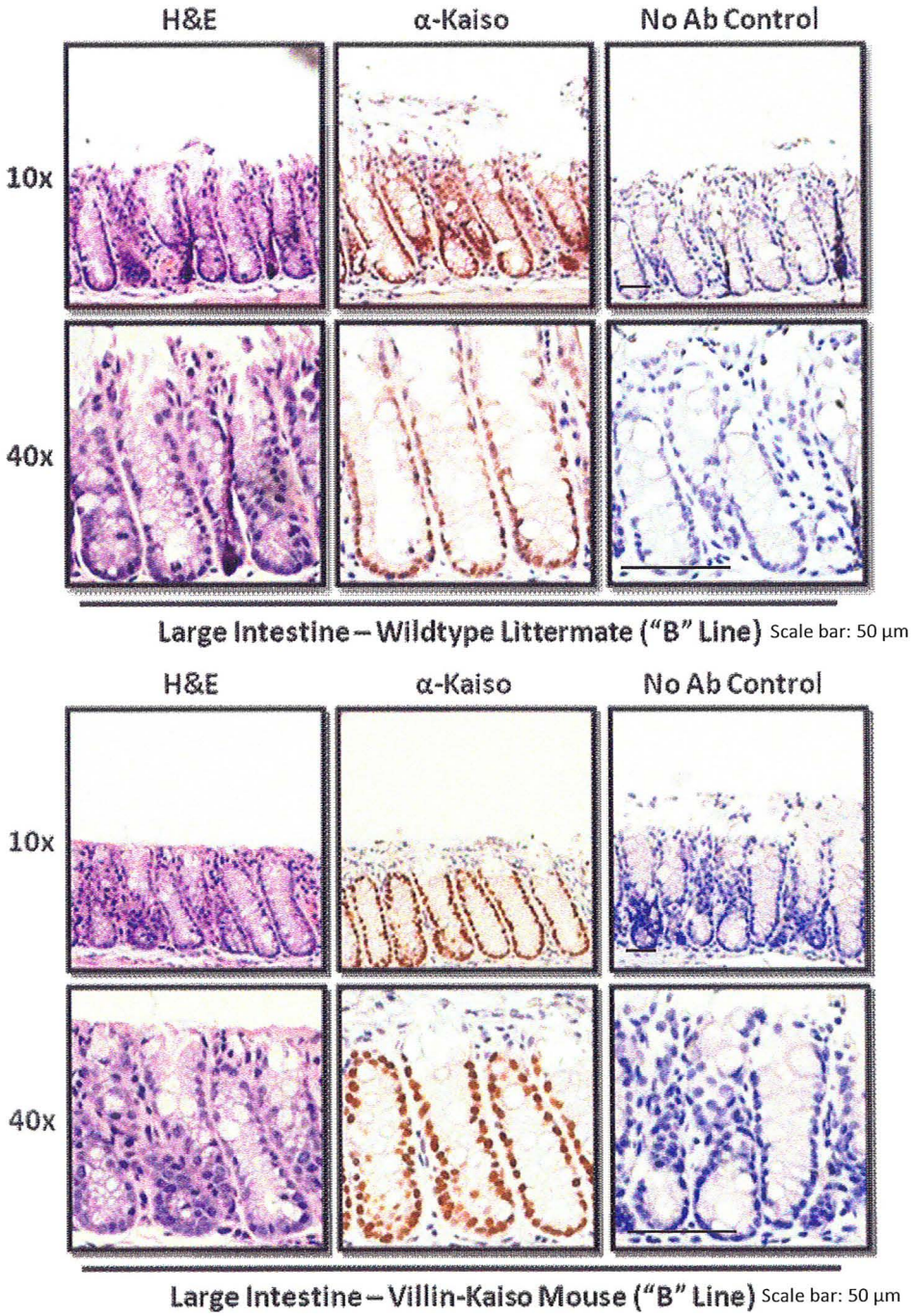

Figure 17 – Kaiso Localization in the Large Intestines ("B" Line mice). Immunostaining with Kaiso antibodies shows that Kaiso localization is restricted to cells along the intestinal crypt. The lamina propria and underlying mucosa lack Kaiso expression. Kaiso expression is also strongly nuclear in both wildtype and the villin-Kaiso transgenic intestines with very weak cytoplasmic staining.

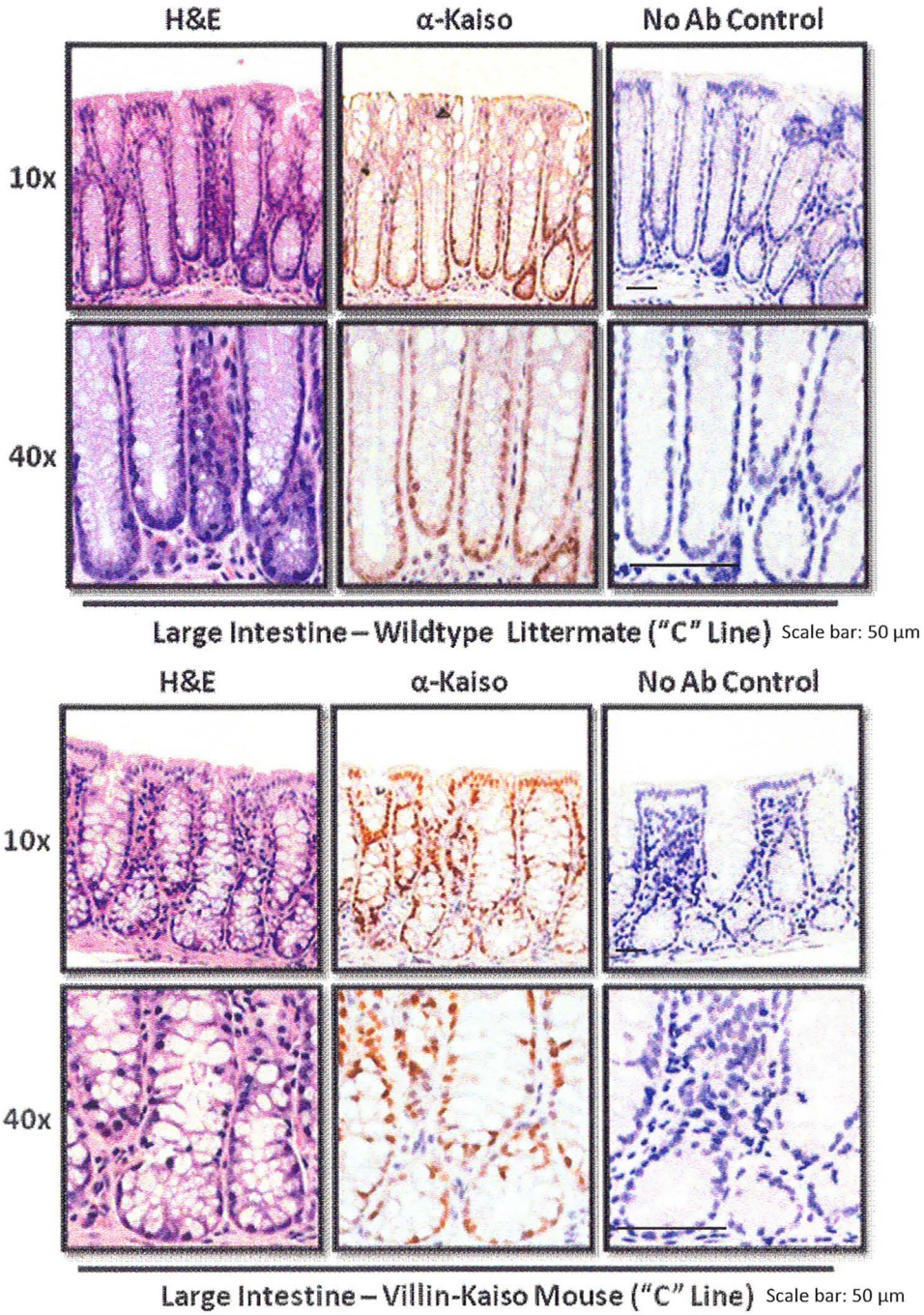

Figure 18 – Kaiso Localization in the Large Intestines ("C" Line mice). Immunostaining with Kaiso antibodies shows that Kaiso localization is restricted to cells along the intestinal crypt. The lamina propria and underlying mucosa lack Kaiso expression. Kaiso expression is also strongly nuclear in both wildtype and the villin-Kaiso transgenic intestines with very weak cytoplasmic staining.

Table I – Mouse Vital Statistics Table includes vital statistics regarding age, gender, and weight of mice under study. The table indicates that Kaiso-Tg and their age- and gender-matched littermates were of comparable weights.

Animal ID	Genotype	Sex	Age (mts)	Weight (g)
10A2F	C57/CBA-Kaiso-Tg ("A" Line)	F	7	26.61
10A1F	C57/CBA WT ("A" Line)	F	7	30.53
13B1M	C57/CBA-Kaiso-Tg ("B" Line)	M	7	38.19
13B1M	C57/CBA WT ("B" Line)	M	7	35.15
11C1M	C57/CBA-Kaiso-Tg ("C" Line)	M	7	43.65
11C1M	C57/CBA WT ("C" Line)	M	7	51.16

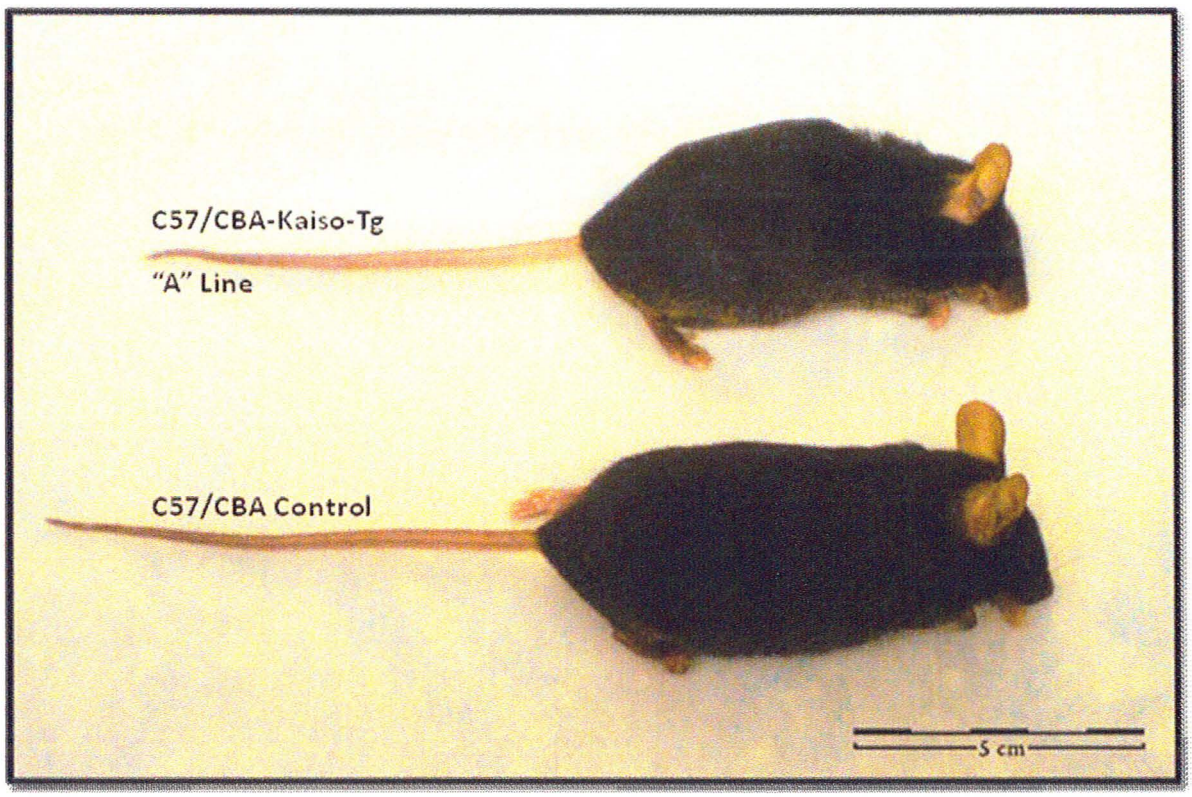

Figure 19 – Kaiso Transgenic and Non-transgenic Litermate ("A" Line). Image shows Kaiso overexpression mouse (above) in comparison to non-trasngenic littermate (below). Kaiso overexpression mice are phenotypically normal as they appear to be of a healthy size and weight.

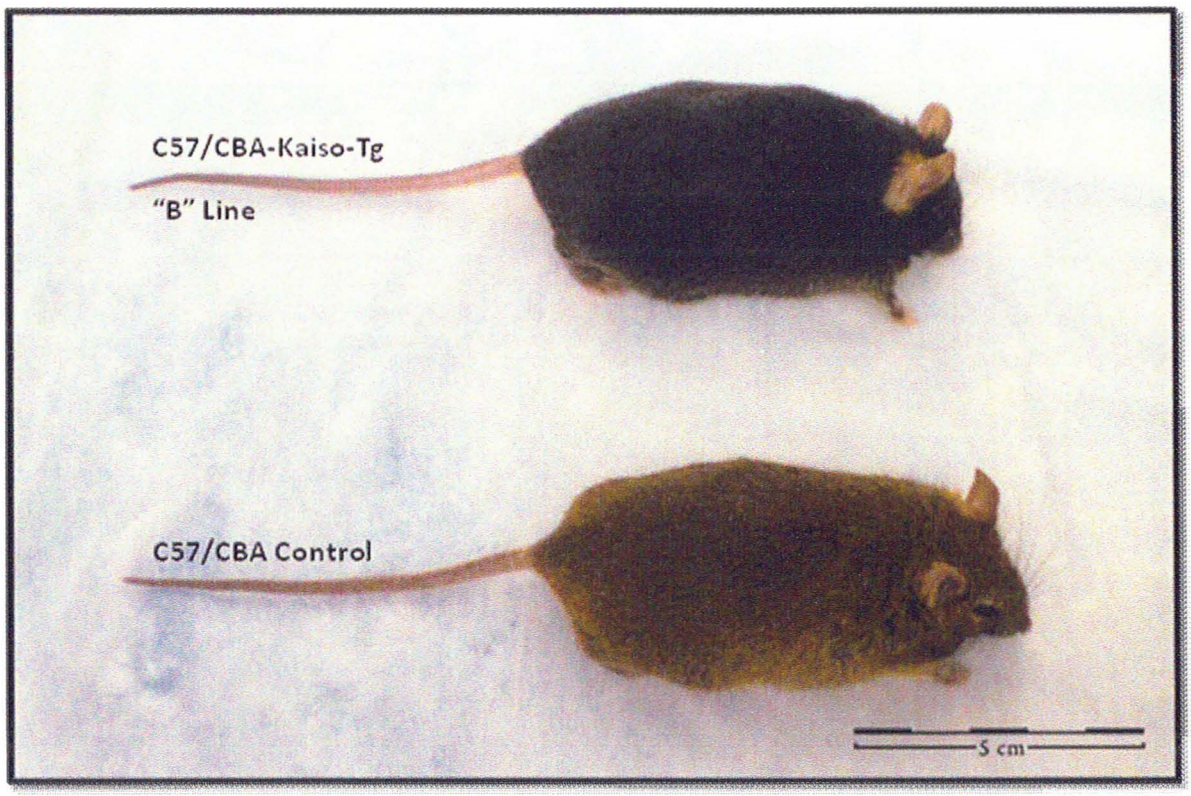

Figure 20 – Kaiso Transgenic and Non-transgenic Litermate ("B" Line). Image shows Kaiso overexpression mouse (above) in comparison to non-trasngenic littermate (below). Kaiso overexpression mice are phenotypically normal as they appear to be of a healthy size and weight.

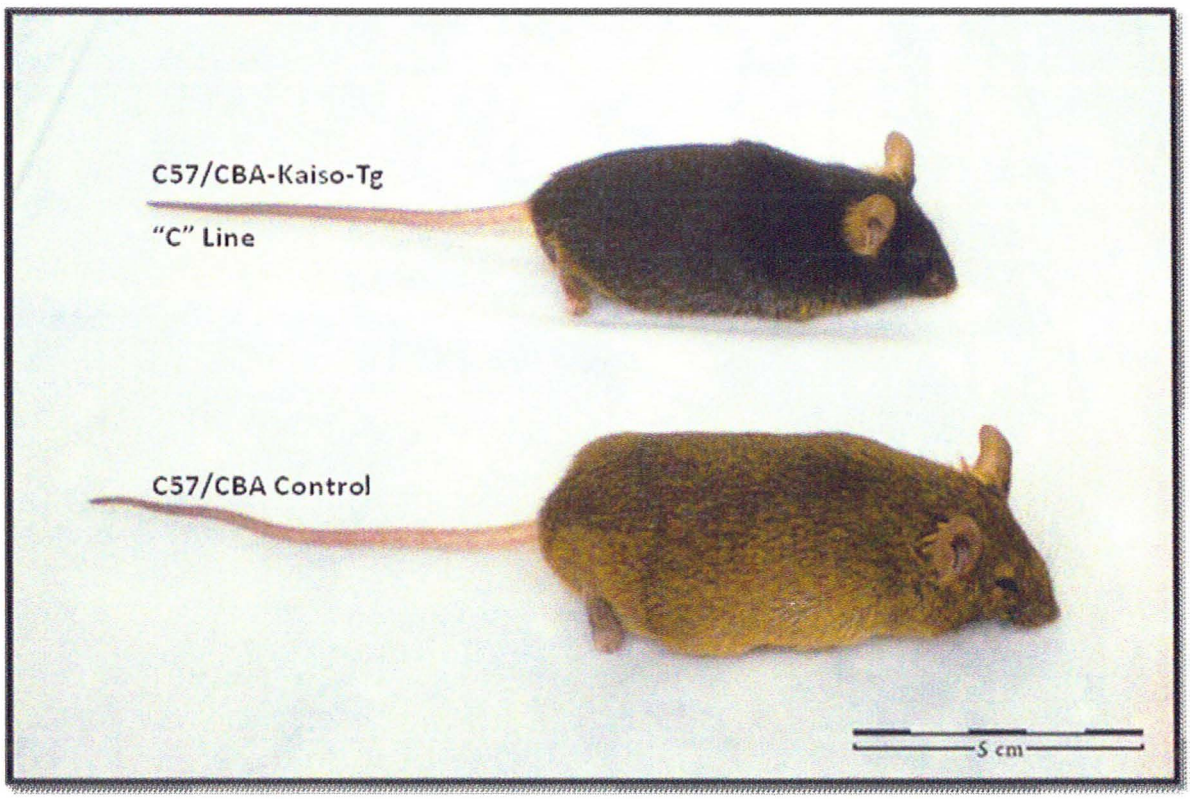

Figure 21 – Kaiso Transgenic and Non-transgenic Litermate ("C" Line). Image shows Kaiso overexpression mouse (above) in comparison to non-trasngenic littermate (below). Kaiso overexpression mice are phenotypically normal as they appear to be of a healthy size and weight.

and available for study. H&E staining indicates that the proximal segment of the small (Figure 22, 23, 24) and large (Figure 25, 26, 27) intestines appear normal in the Kaiso overexpression mouse when compared to its non-transgenic littermate. There is no obvious neoplasia or dysplastic growth and all of the expected crypt cell lineages are present, including Paneth and goblet cells. There is, however, a small difference in crypt depth in Kaiso transgenic mice at the distal segment compared to their wildtype littermates. Crypts of the distal segment appear shallower and more disorganized in the transgenic small and large intestine when compared to its wildtype counterpart. This effect is observed in A, B, and C line transgenic mice when compared to their respective age and sex-matched littermates. It is likely that Kaiso overexpression in the intestine is having an effect on the cellular mechanisms that control crypt depth and morphology at the distal end of the intestines but more mice will need to be analyzed to confirm this.

3.5. Kaiso Localization in $Apc^{Min/+}$ Mouse Intestines

Before investigating the effects of intestinal-specific Kaiso overexpression on the $Apc^{Min/+}$ phenotype, it is important to assess Kaiso expression in the $Apc^{Min/+}$ background. Kaiso is expressed in epithelial and crypt cells in normal segments of both the small and large intestines of the $Apc^{Min/+}$ mice. As in wildtype and Kaiso overexpression mice, the lamina propria, lacteal, and muscularis musoca of the small intestine do not stain positive for Kaiso (Figure 28). The large intestines of the $Apc^{Min/+}$ mice also show a similar pattern of Kaiso expression compared to wildtype and Kaiso-Tg mice (Figure 29). In $Apc^{Min/+}$ intestinal tumors, Kaiso is expressed homogenously throughout the tumors (Figure 30 and 31). Kaiso remains mainly nuclear and weakly cytoplasmic throughout the majority of the tumor. This pattern of Kaiso expression in Min tumors is surprising as it was reported by Soubry *et al.*, 2005 that Kaiso expression and localization is dictated by the tumor

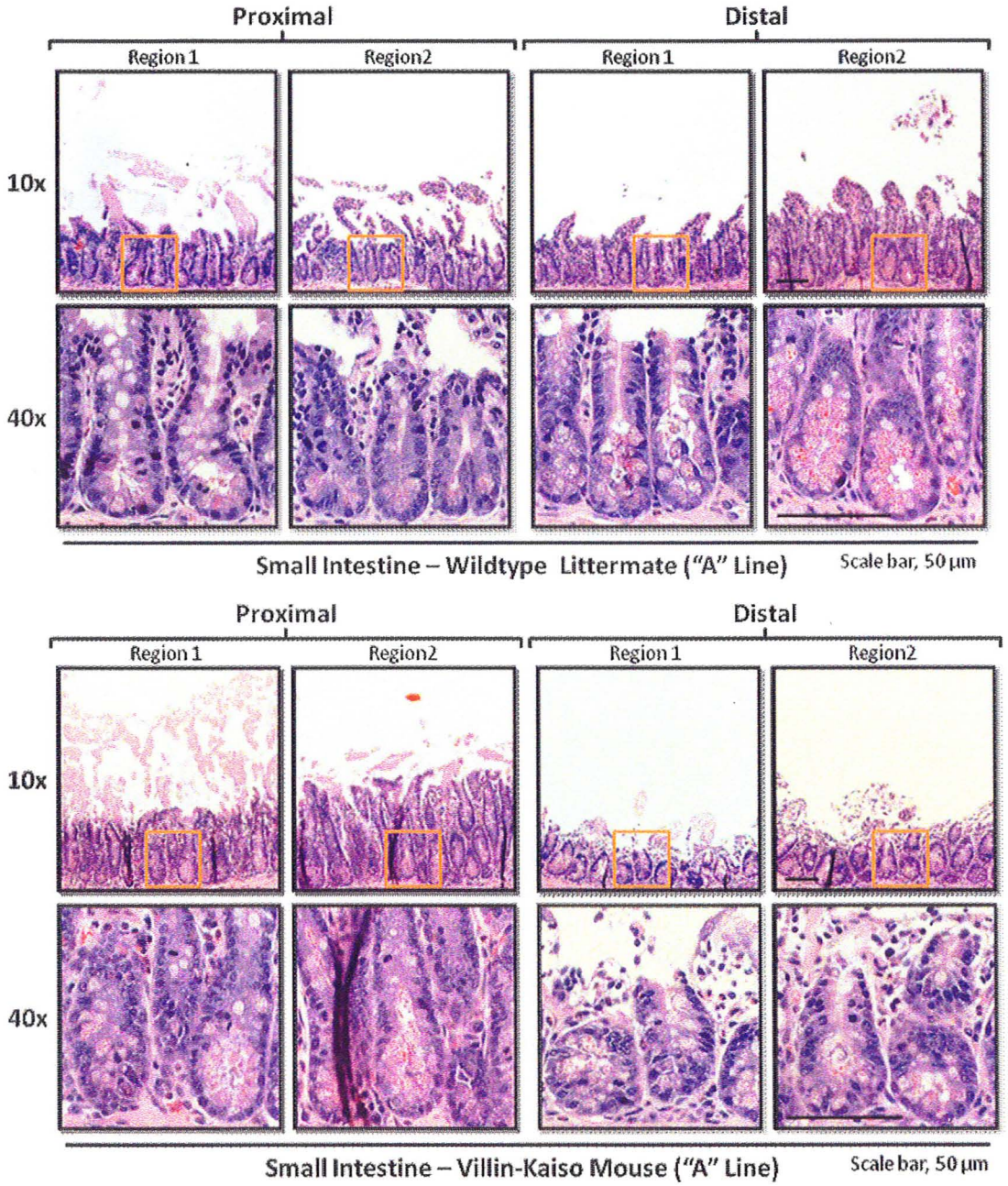

Figure 22 – Effect of Kaiso Overexpression on the Small Intestines ("A" Line). Semi-thin sections of Kaiso-Tg and non-transgenic mouse small intestines were stained using hematoxylin and eosin (H&E). Microscopic analysis shows that there is no detectable neoplastic intestinal growth or dysplasia in Kaiso overexpression mice compared to their non-transgenic littermates.

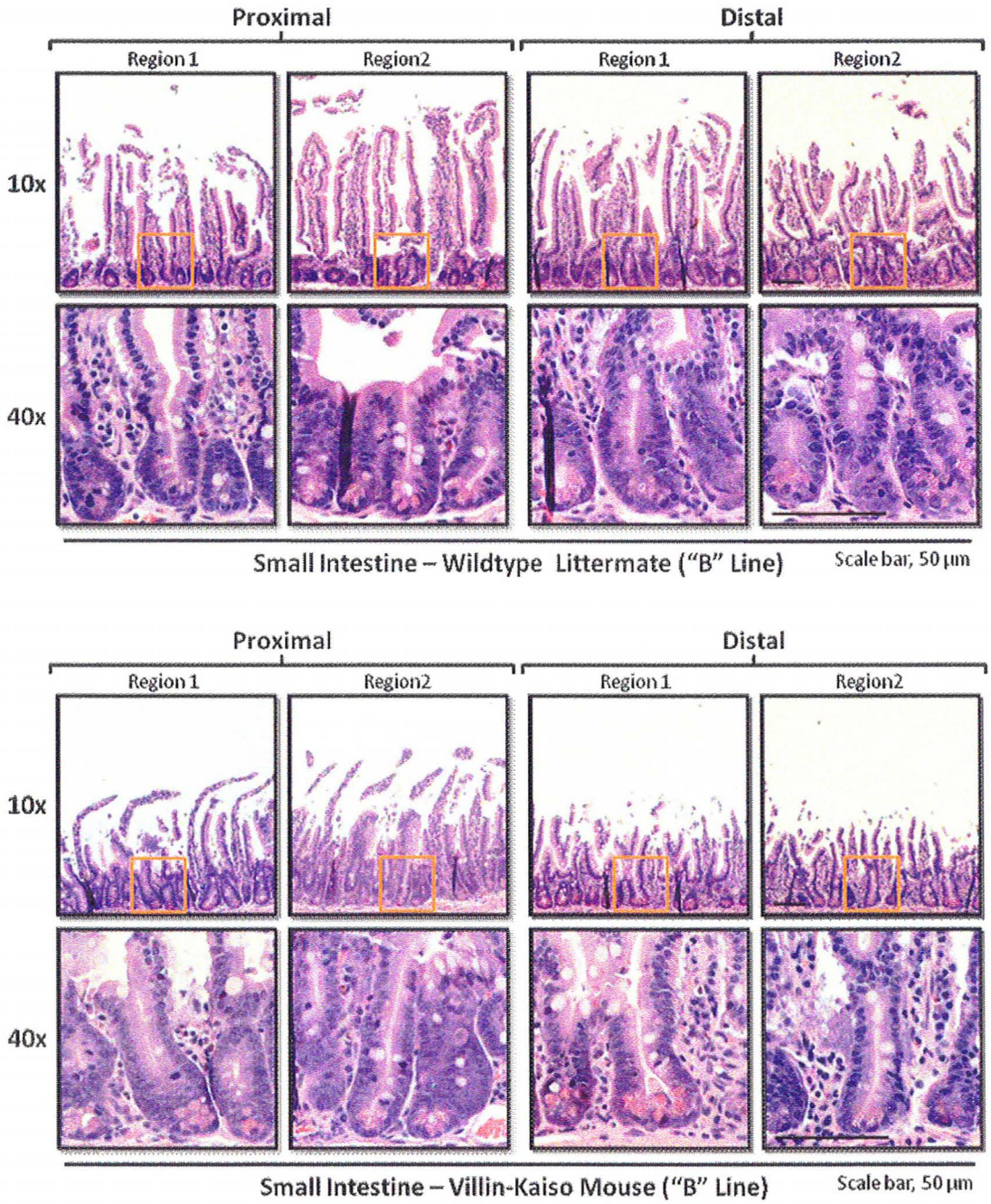

Figure 23 – Effect of Kaiso Overexpression on the Small Intestines ("B" Line). Semi-thin sections of Kaiso-Tg and non-transgenic mouse small intestines were stained using hematoxylin and eosin (H&E). Microscopic analysis shows that there is no detectable neoplastic intestinal growth or dysplasia in Kaiso overexpression mice compared to their non-transgenic littermates.

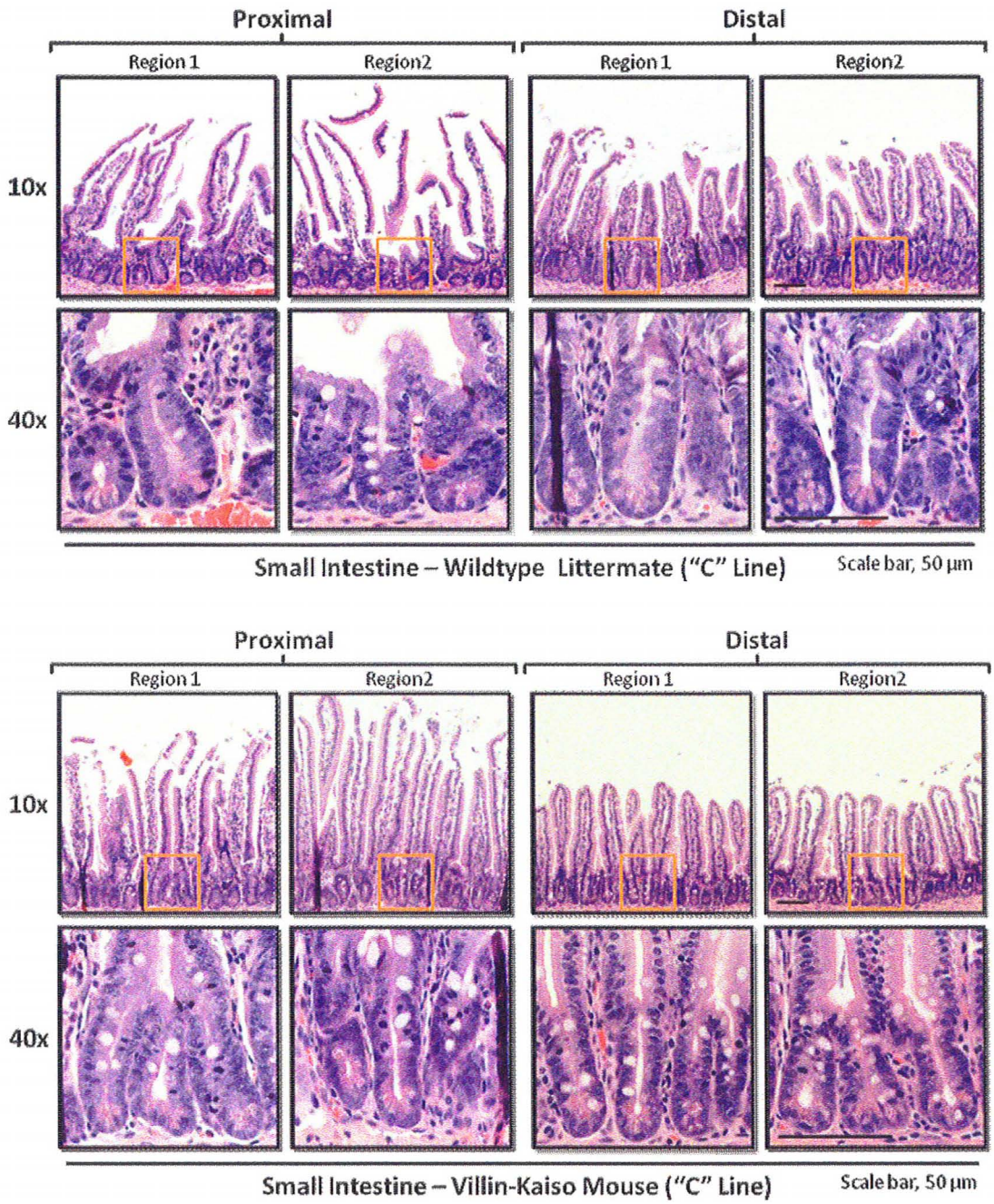

Figure 24 – Effect of Kaiso Overexpression on the Small Intestines ("C" Line). Semi-thin sections of Kaiso-Tg and non-transgenic mouse small intestines were stained using hematoxylin and eosin (H&E). Microscopic analysis shows that there is no detectable neoplastic intestinal growth or dysplasia in Kaiso overexpression mice compared to their non-transgenic littermates.

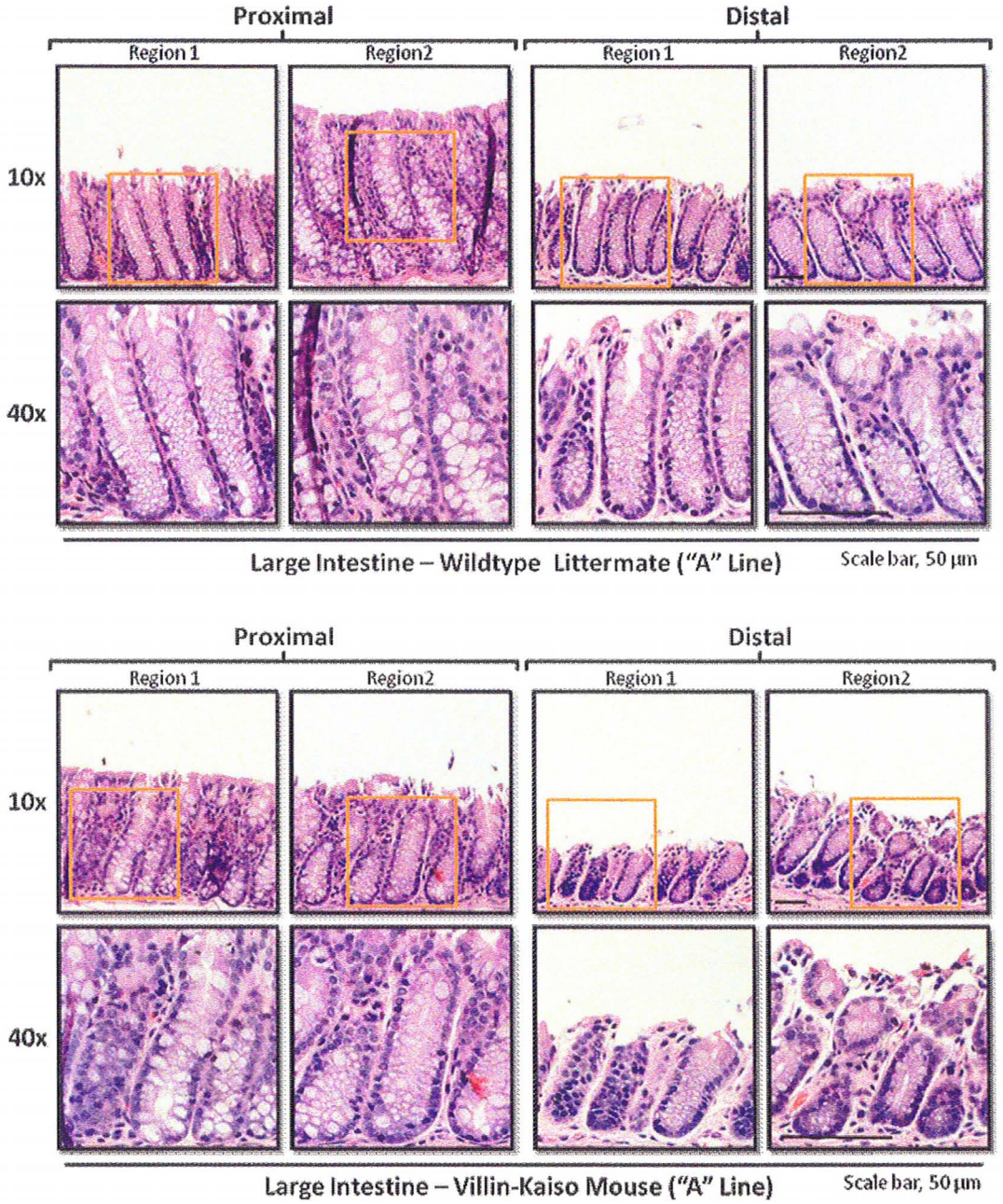

Figure 25 – Effect of Kaiso Overexpression on the Large Intestines ("A" Line). Semi-thin sections of Kaiso-Tg and non-transgenic mouse large intestines were stained using hematoxylin and eosin (H&E). Microscopic analysis shows that there is no detectable neoplastic intestinal growth or dysplasia in Kaiso overexpression mice compared to their non-transgenic littermates.

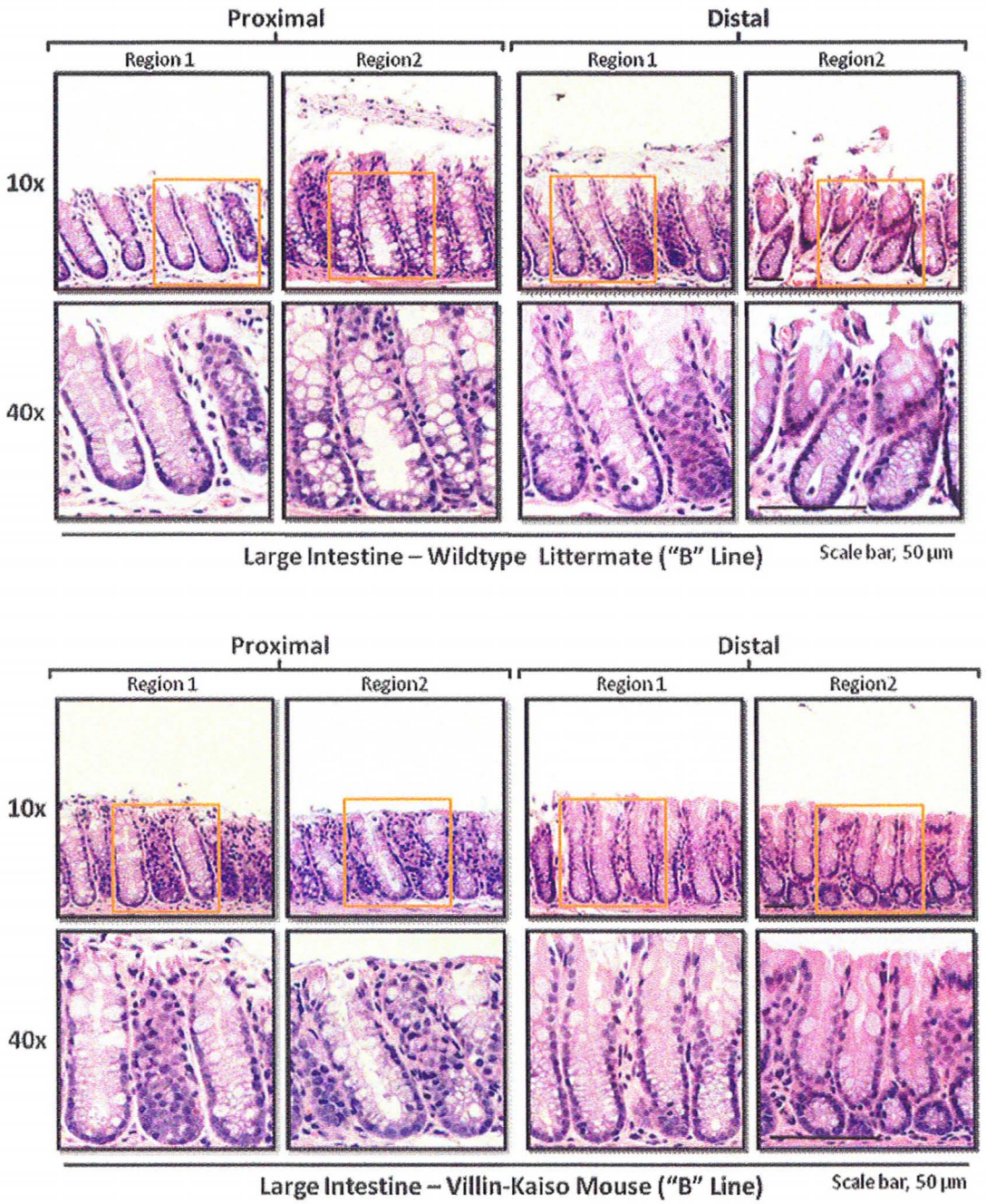

Figure 26 – Effect of Kaiso Overexpression on the Large Intestines ("B" Line). Semi-thin sections of Kaiso-Tg and non-transgenic mouse large intestines were stained using hematoxylin and eosin (H&E). Microscopic analysis shows that there is no detectable neoplastic intestinal growth or dysplasia in Kaiso overexpression mice compared to their non-transgenic littermates.

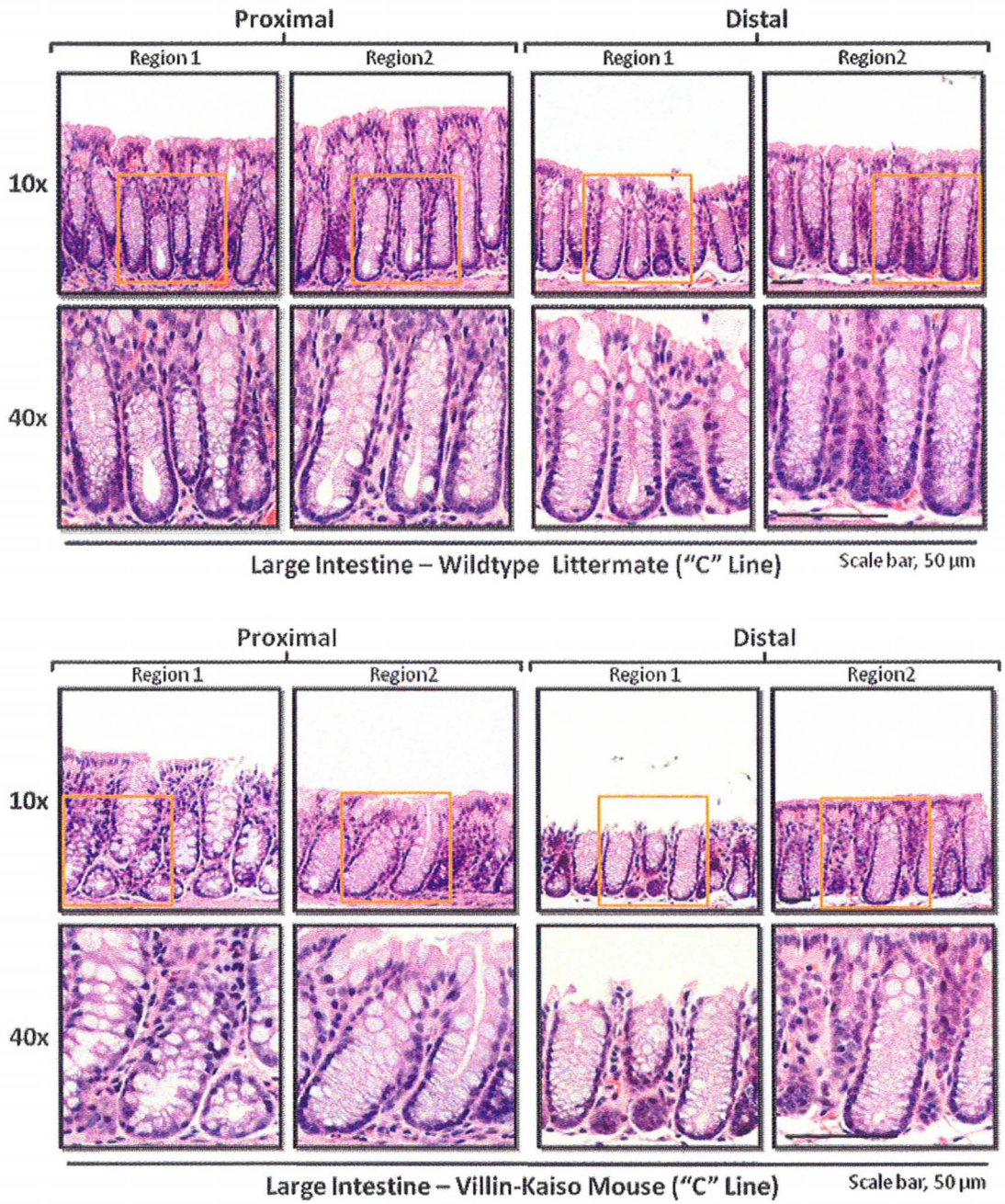

Figure 27 – Effect of Kaiso Overexpression on the Large Intestines ("C" Line). Semi-thin sections of Kaiso-Tg and non-transgenic mouse large intestines were stained using hematoxylin and eosin (H&E). Microscopic analysis shows that there is no detectable neoplastic intestinal growth or dysplasia in Kaiso overexpression mice compared to their non-transgenic littermates.

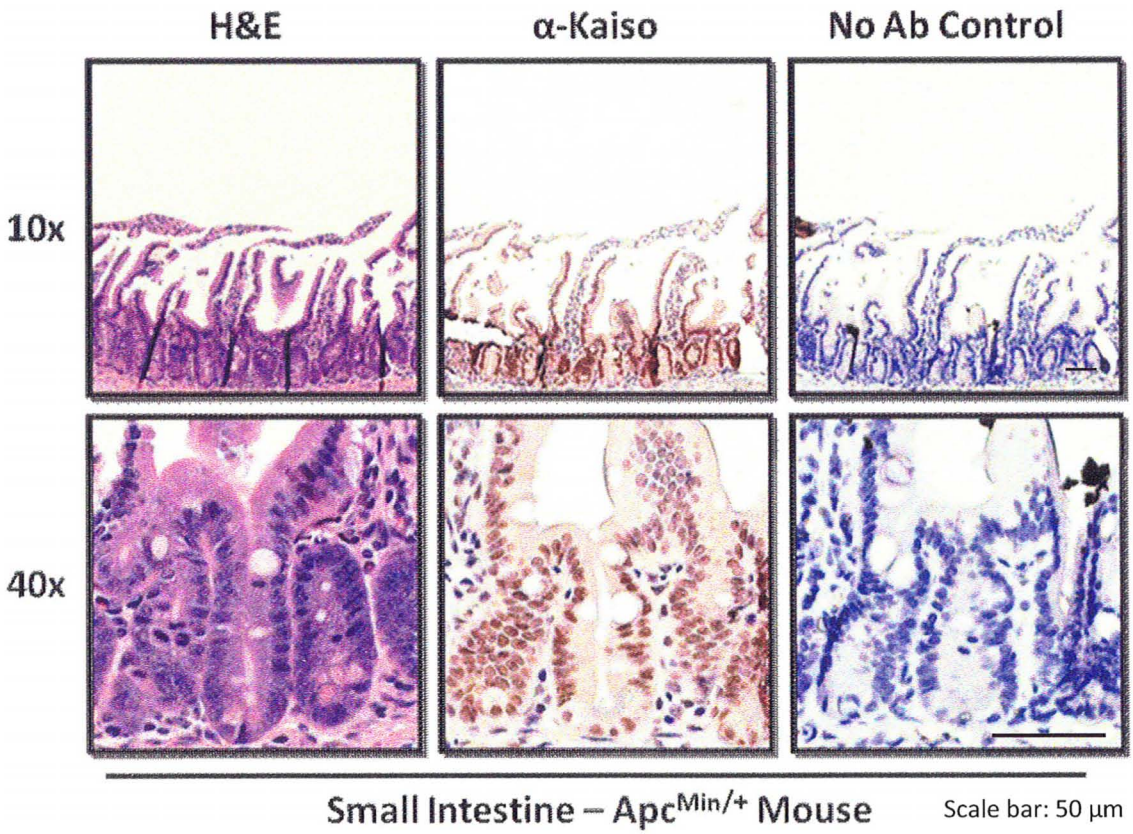

Figure 28 – Kaiso Localization in the $Apc^{Min/+}$ Small Intestine. Kaiso is localized in the $Apc^{Min/+}$ small intestine similarly to its localization in both the Kaiso-Tg and wildtype small intestines. Kaiso maintains its strong diffuse nuclear staining with weak cytoplasmic staining. Kaiso expression is variable throughout the crypt and is absent in the lacteal, lamina propria, and underlying muscularis mucosa of the small intestine tissue.

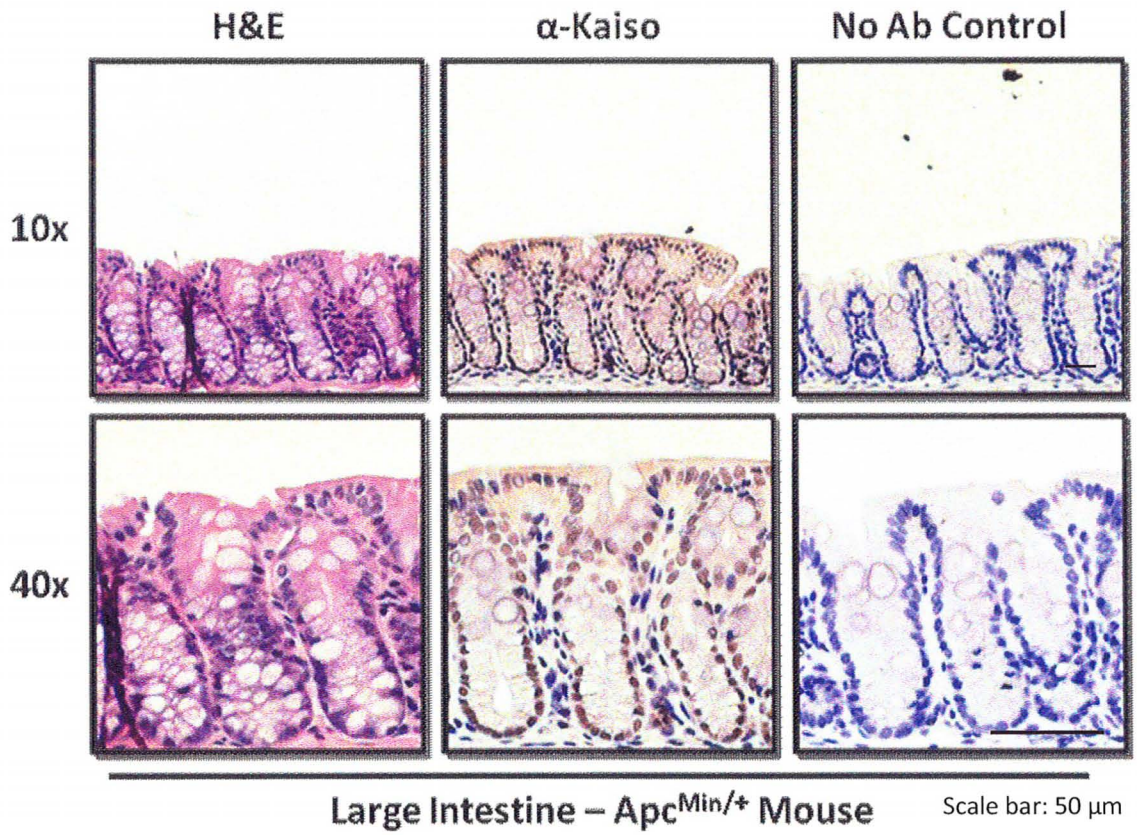

Figure 29 – Kaiso Localization in Apc$^{Min/+}$ Large Intestines. Kaiso is localized similarly in Apc$^{Min/+}$ large intestines as it is in Kaiso-Tg and wildtype intestines. Kaiso maintains its strong diffuse nuclear staining with weak cytoplasmic staining. Kaiso expression is variable throughout the crypt and is absent in the lamina propria and underlying muscularis mucosa.

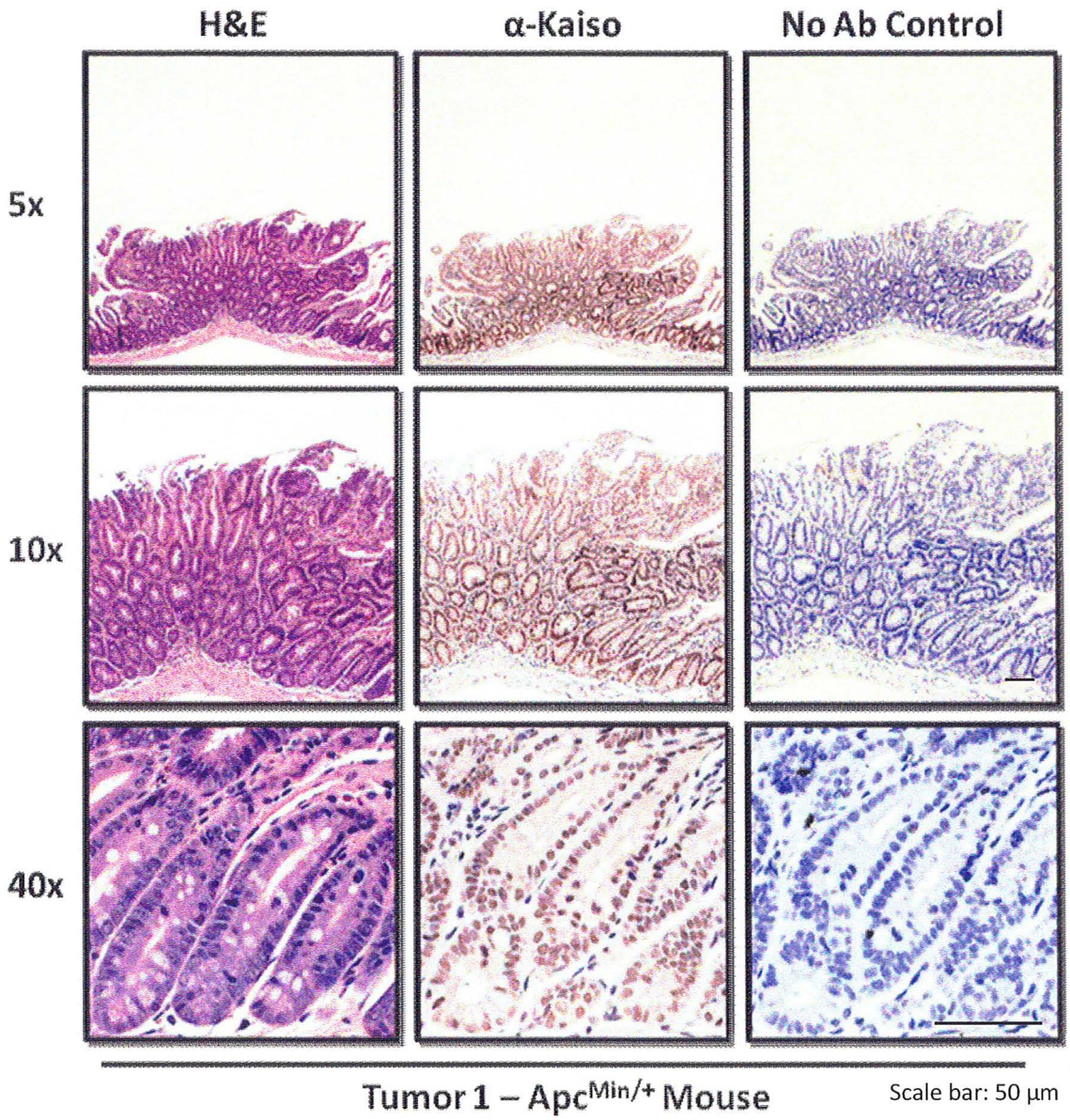

Figure 30 – Kaiso localization in $Apc^{Min/+}$ Tumors (Tumor 1). Kaiso is expressed throughout the tumor in the $Apc^{Min/+}$ small intestine. Kaiso expression is mainly nuclear and appears to be stronger at the base of the tumor compared to the apical surface. Kaiso expression also appears to be weakly cytoplasmic in some cells of the tumor. Even though Kaiso is expressed throughout the tumor, its expression varies from cell-to-cell within the tumor.

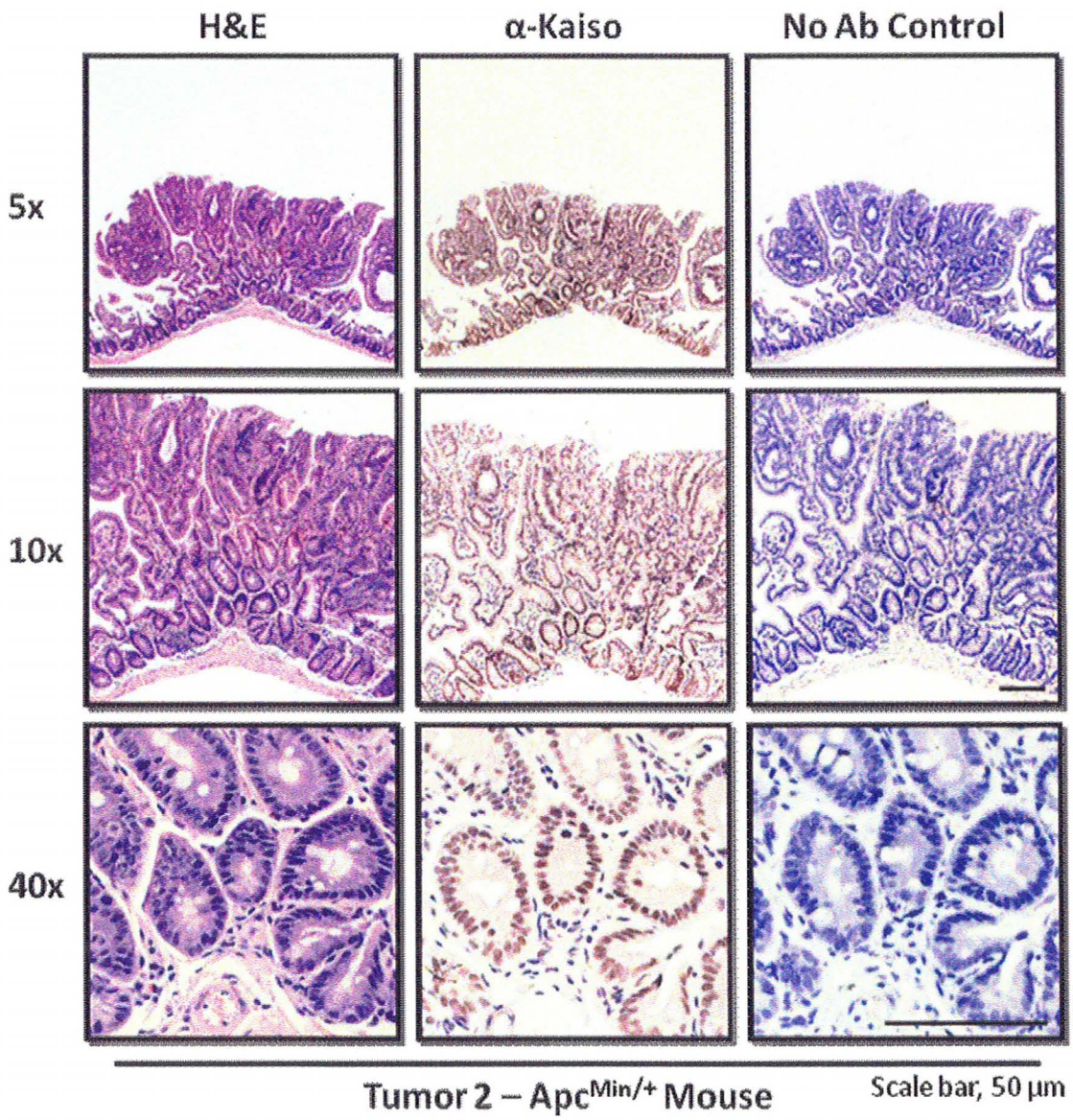

Figure 31 – Kaiso Localization in Apc$^{Min/+}$ Tumors (Tumor 2). Kaiso is expressed throughout the tumor in the Apc$^{Min/+}$ small intestine. Kaiso expression is mainly nuclear and expression appears to be slightly stronger at the base of the tumor compared to the apical surface.

microenvironment(81). Specifically, it was demonstrated that Kaiso expression in tumor xenografts either shifts from the nucleus to become predominantly cytoplasmic or is lost completely(81). It was proposed that this was in response to hypoxic stress in regions of the tumor that were not adequately innervated(81). The homogenous Kaiso expression observed in $Apc^{Min/+}$ tumors suggest that they are not undergoing hypoxic stress; this hypothesis could be confirmed by immunostaining for a marker such as carbonic anhydrase since this gene product is present in areas of localized hypoxia of the tumor. Even though Kaiso is expressed throughout the tumor, its expression varies from cell-to-cell within the tumor.

3.6. Effects of Kaiso on Polyp Formation in $Apc^{Min/+}$ Mouse

To test the effects of intestinal Kaiso overexpression in the $Apc^{Min/+}$ background, Kaiso overexpressing females were crossed with $Apc^{Min/+}$ males. A segment of the small intestine and the entire large intestine were examined for adenoma development in the progeny. The second quarter of the small intestine and the entire large intestine of double mutant progeny were removed, opened longitudinally, and adenomas scored. Non-transgenic $Apc^{Min/+}$ mice had an average of 13 tumors whereas a Kaiso overexpression mice had 130 and 12 adenomas in the small intestine of "A" and "B" mice, respectively. Tumor diameter was also measured and $Apc^{Min/+}$;Kaiso-Tg mice had smaller tumors compared to $Apc^{Min/+}$ mice (Table II). On average, $Apc^{Min/+}$:Kaiso-Tg mice from the "A" and "B" line had small intestine tumor diameters of 1.13 and 0.92 mm, respectively. These are smaller in size compared to tumors of the $Apc^{Min/+}$ mice, which were an average of 1.90 mm in diameter. Due to the small sample size, these results can only be considered preliminary but they hint at an important role for Kaiso in adenoma formation in the $Apc^{Min/+}$ background.

Table II - Average size of intestinal tumors. Small intestine tumors were measured under the dissecting microscope for each genotype; their average diameters were calculated and displayed below. When crossed with the $Apc^{Min/+}$ mouse, both Kaiso overexpressing lines, "A" and "B," show decreased polyp size in comparison to the $Apc^{Min/+}$ single mutant. It is important to note that this should be classified as "preliminary data" due to the small sample size of individual mice (3 $Apc^{Min/+}$ mice, 2 $Apc^{Min/+}$;Kaiso-Tg from the "B" line and only one $Apc^{Min/+}$;Kaiso-Tg mouse from the "A" line).

Genotype	**Number of Tumors**	**Average Tumor Size (Ave. ± SEM, n=10 tumors)**
C57/Black6 - $Apc^{Min/+}$	13 (n=3 mice)	1.90 ± 0.19 mm
C57/CBA-Kaiso-Tg ("A" Line)	130 (n=1 mouse)	1.13 ± 0.09 mm
C57/CBA-Kaiso-Tg ("B" Line)	12 (n=2 mice)	0.92 ± 0.10 mm

3.7. Kaiso expression in $Apc^{Min/+}$;Kaiso-Tg Tumors

To determine whether Kaiso localization might be having an effect on tumor growth in the $Apc^{Min/+}$;Kaiso-Tg mice, IHC was performed on intestinal tumors. In $Apc^{Min/+}$ tumors, Kaiso is expressed throughout the tumor. In contrast, distribution of Kaiso-expressing cells in $Apc^{Min/+}$:KaisoTg is drastically different. Kaiso displays a more heterogeneous expression pattern when compared to the pattern of expression observed in $Apc^{Min/+}$ tumors (Figure 32, 33, and 34). Kaiso expression remains strong on the basal surface of the tumor but is greatly reduced in the center and towards the apical surface of the tumor. It is possible that the villin promoter is not active in the center of these tumors, resulting in a downregulation of transgenic Kaiso. Immunostaining using α-villin antibodies would indicate whether villin is expressed in this tissue and we would be able to compare the pattern of villin expression with Kaiso's expression pattern. It is also not clear whether there is a specific decrease in Kaiso expression from the transgene or whether endogenous Kaiso is lost (or both). In order to determine this, immunostaining with an α-myc antibody would be necessary.

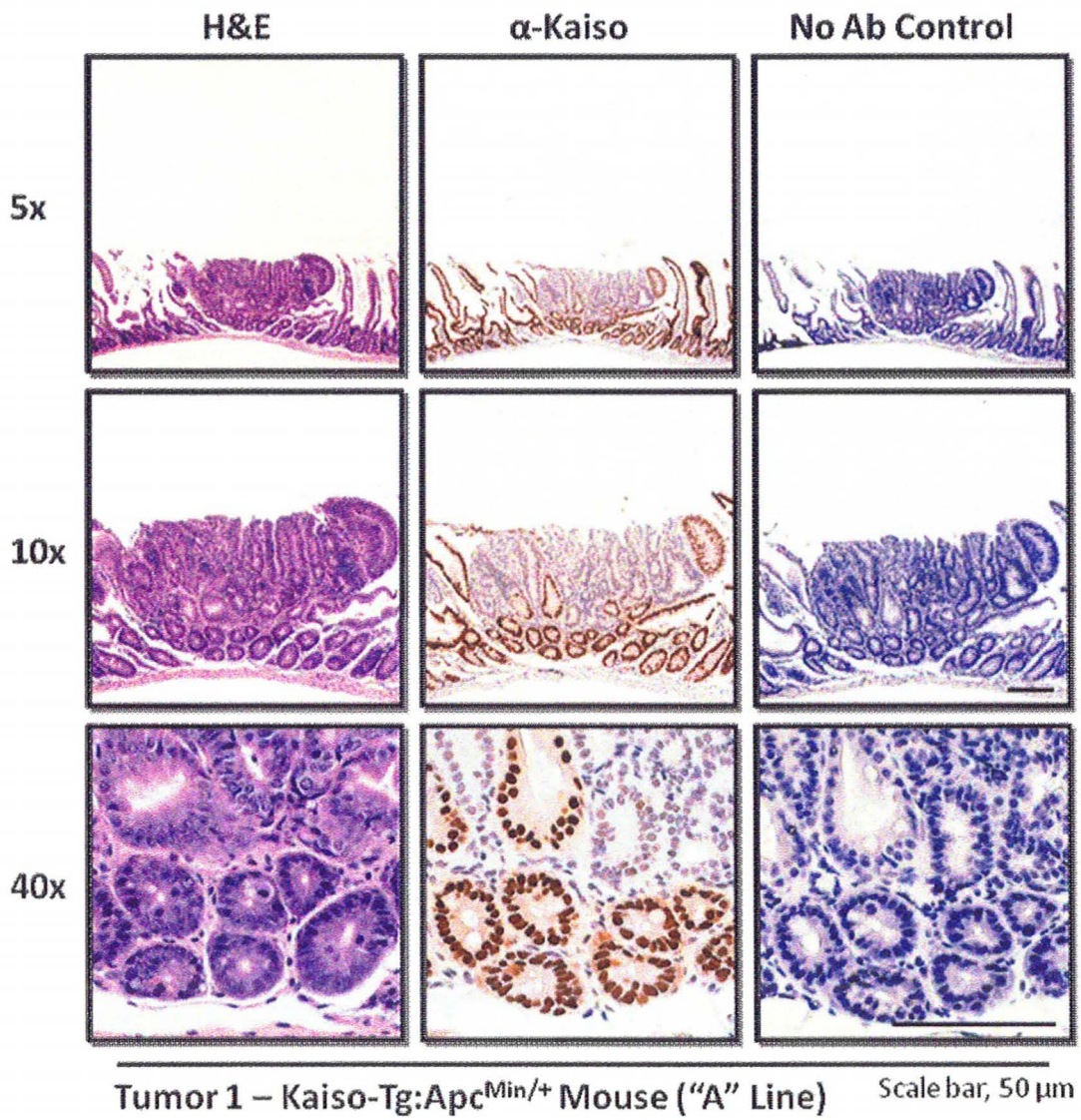

Figure 32 – Kaiso Localization in ApcMin/+;Kaiso-Tg ("A" Line) Tumors (Tumor 1). Kaiso localization pattern is dramatically different in Apc$^{Min/+}$;Kaiso-Tg tumors. Kaiso is no longer homogenously expressed throughout the entire tumor but is instead lost in the majority of the tumor and concentrated only in localized areas within the tumor, particularly near the crypts.

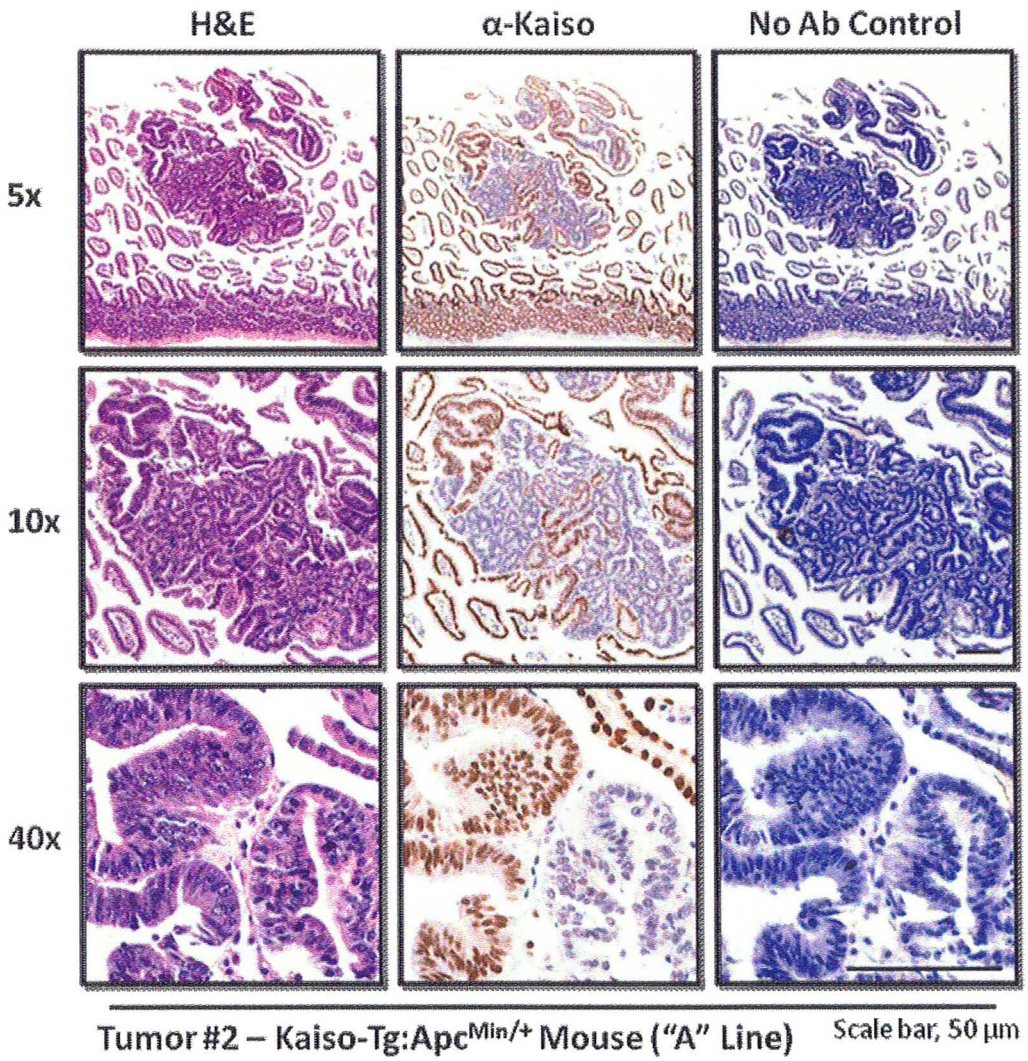

Figure 33 – Kaiso Localization in $Apc^{Min/+}$;Kaiso-Tg ("A" Line) Tumors (Tumor 2). Kaiso localization pattern is dramatically different in $Apc^{Min/+}$;Kaiso-Tg tumors. Kaiso is no longer homogenously expressed throughout the entire tumor but is instead lost in the majority of the tumor and concentrated only in localized areas within the tumor, particularly near the crypts.

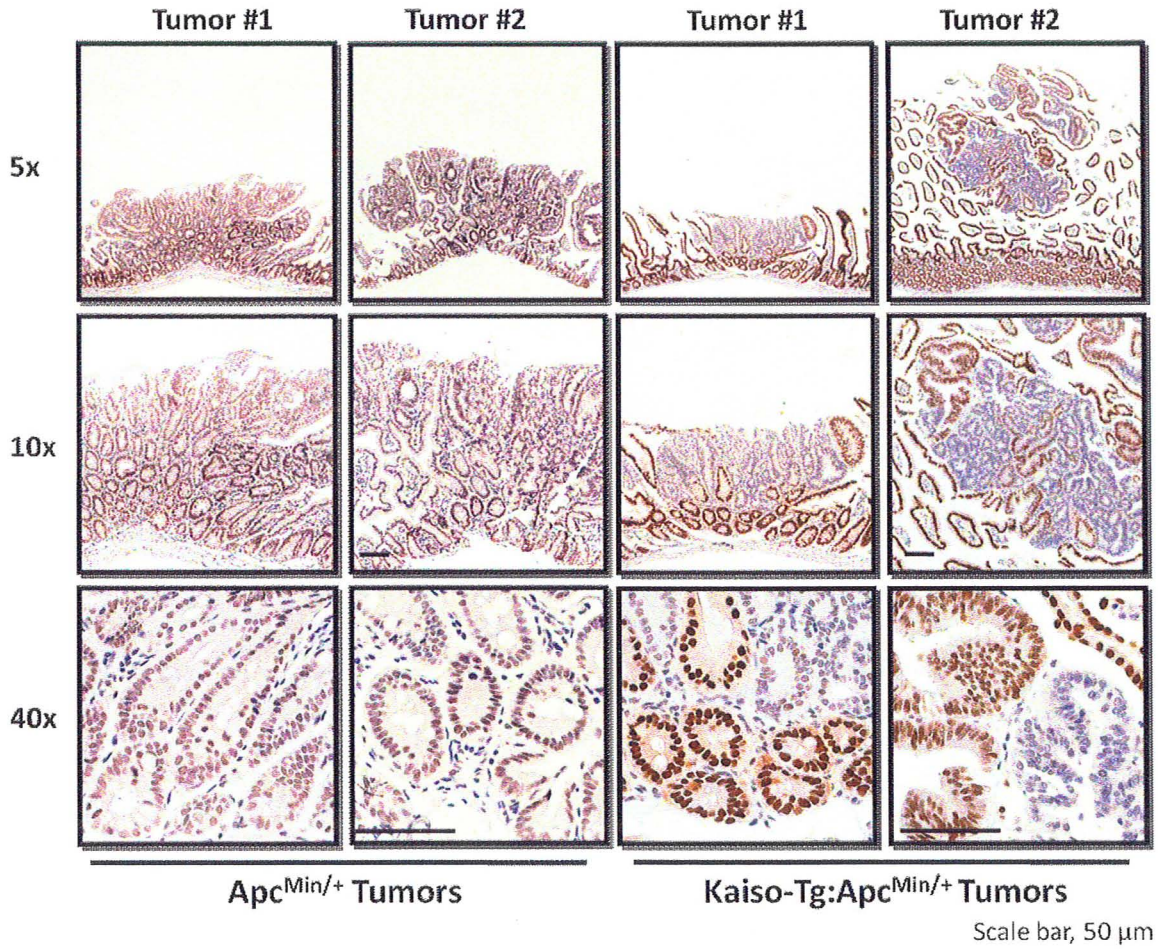

Figure 34 – Comparison of Kaiso Localization in $Apc^{Min/+}$ and $Apc^{Min/+}$;Kaiso-Tg Tumors of the Small Intestine. $Apc^{Min/+}$ tumors show uniform Kaiso staining throughout the entire tumor. $Apc^{Min/+}$;Kaiso-Tg mice show patchy Kaiso staining within the tumor. In both $Apc^{Min/+}$ and $Apc^{Min/+}$;Kaiso-Tg mice, however, Kaiso subcellular localization still remains mostly nuclear.

Discussion

Several lines of evidence from independent studies demonstrate the importance of Kaiso in a developmental context and implicate Kaiso in the Wnt signaling system. Kaiso was shown to be essential for normal development in the *Xenopus* model system and it was also shown to be a negative regulator of canonical and non-canonical Wnt signaling(42, 64). The role of Kaiso in the mouse model system, however, is completely different. First, Kaiso null mice show no developmental defects, and this is likely attributed to the Kaiso-like proteins ZBTB4 and ZBTB48(73). Second, the role of Kaiso in Wnt signaling was examined using the $Apc^{Min/+}$ mouse model and it was found that Kaiso acts as a positive regulator Wnt signaling. In this study, a Kaiso overexpression mouse model was developed to confirm whether Kaiso acts as a positive or negative regulator of mammalian Wnt signaling.

4.1. A Mouse Model for Intestinal-Specific Kaiso Overexpression

To determine the effect of Kaiso on the Wnt signaling pathway, we developed a Kaiso overexpression mouse model where Kaiso is under control of the intestinal-specific villin promoter (Figure 6). The promoter is able to efficiently drive heterologous gene expression in villin-positive tissues like the proximal tubules of the kidney, the small intestines, and the colon(69). The transgene contained a myc-tagged copy of murine Kaiso downstream of the villin promoter. The myc tag allows us to differentiate transgenic Kaiso from its endogenous counterpart. The transgenesis was achieved by pronuclear injection and PCR genotyping identified four founder lines, A-D, that were established. Each founder was viable and fertile and was used to establish breeding colonies. Genotyping by PCR revealed that each founder line was able to transmit the transgene to its offspring with the exception of founder "D." It is likely that founder "D" was unable to transmit the villin-Kaiso

transgene to its progeny because the transgene was incorporated into somatic, rather than germ cells, of founder "D" during embryogenesis. Since the transgenic mice was not made with a targeted approach, it was necessary to determine the number of integrations of the transgene. PCR copy number analysis was used to determine the number of transgene integrations from each of the founder lines. Founder "A" possessed between 50-100 copies of the transgene while founders "B" and "C" possessed only 50 and 10 copies in their respective genomes (Figure 8).

Although PCR genotyping was useful to determine whether the founders harboured the transgene it was necessary to perform western blot and RT-PCR analysis to determine whether the gene was being expressed in the intestines. Unfortunately, we were unable to obtain pure protein from mouse small intestines as these preparations were contaminated with protein from their diets. It is hypothesized that residual food was trapped in the numerous folds and villi of the small intestine and this contaminated the final protein preparation used for western blotting. Conversely, the large intestines do not display the same degree of folding nor do they have villi that project into the lumen and were therefore more compatible with the protein extraction protocol. Western blotting using large intestine tissue showed that Kaiso is overxpressed in the large intestines of each of the three Kaiso overexpression lines tested. Each of the founder lines expressed the transgene to variable degrees but they all expressed Kaiso more strongly than their non-transgenic counterparts. It was determined by western blot that founders A, B, and C displayed strong, moderate, and mild levels of Kaiso overexpression, respectively (Figure 9). To confirm that Kaiso overexpression was under control of the villin promter, the lysates were probed with an α-myc antibody that differentiates between endogenous and myc-tagged transgenic Kaiso. The α-myc antibody detected bands corresponding to the expected molecular weight of the transgenic Kaiso and the pattern of strong, moderate, and mild overexpression was maintained in each transgenic line (Figure 9). Western blotting results with both

the α-Kaiso and α-myc antibody parallel the relative transgene copy number as determined by PCR. Since the "A" line had between 50-100 copies of the transgene, Kaiso overexpression was more pronounced when compared to the "B" and "C" lines, which contained fewer copies of the transgene.

All western blot data was gathered from large intestine tissue but it was also necessary to demonstrate the expression of the transgene in the small intestines. Since there were problems with small intestine protein isolation, semi-quantitative reverse transcriptase PCR (RT-PCR) was used to demonstrate Kaiso transgene expression. RT-PCR primers were used to amplify regions of Kaiso transgenic mRNA and transcription factor IID (TFIID) mRNA was amplified as a loading control. Kaiso RT-PCR primers were designed such that they specifically amplified the transgenic Kaiso mRNA but not any endogenous Kaiso mRNA or genomic DNA. In each of the transgenic lines, RT-PCR data shows that Kaiso is expressed in all villin positive tissues including the small intestines, large intestines, and kidney (Figure 10, 11, 12). Hence, western blot and RT-PCR data indicate that each transgenic line is capable of expressing Kaiso under control of the villin promoter as expected.

To examine the tissue distribution and subcellular localization of Kaiso under normal conditions, small and large intestines of wildtype mice were immunostained with α-Kaiso antibodies and the sections were viewed under a microscope. IHC data revealed that Kaiso is expressed in all cells lining the crypt of the small and large intestine and also in epithelial cells along the entire length of the villus (where present) (Figures 13-18). The majority of Kaiso positive cells showed diffuse nuclear localization with weak cytoplasmic staining. Kaiso was, however, absent in the lacteal, lamina propria, and underlying mucosa. This pattern of expression was also observed in Kaiso-Tg small and large intestines. The villin promoter directed Kaiso expression in the cells lining the intestinal crypt as well as in cells along the villus. Like endogenous Kaiso, transgenic Kaiso protein remains mainly nuclear

with weak cytoplasmic staining. Examination of the intestinal crypts in both wildtype and Kaiso-Tg mice shows that Kaiso exhibits differential expression levels depending on its location in the crypt compartment. Since there are numerous biological processes, including migration, proliferation, and differentiation, that happen in the intestinal crypts, it is possible that differential regulation of Kaiso target genes are necessary for these processes to occur. In order to confirm whether Kaiso or its target genes are involved in controlling intestinal crypt migration, proliferation, or differentiation, double labeling with Kaiso and cell-type specific antibodies would be necessary to determine whether high or low Kaiso levels is associated with certain cell phenotypes. Alternatively, Kaiso expression could be varied throughout the cell cycle. To explore this possibility, double labeling with proliferative markers like proliferating cell nuclear antigen (PCNA), p53, cyclins, or Ki-67 could be used to correlate Kaiso levels with various cell cycle stages.

4.2. Effects of Kaiso Overexpression on Normal Intestinal Development

Histological analysis of the small and large intestines was used to determine whether Kaiso overexpression had an effect on normal intestinal development in each of the founder lines, A, B, and C. H&E staining was used to give an overview of the different cell types that comprised the small intestines. Numerous cell types, including the granule-containing Paneth cells of the small intestine as well as the absorptive enterocytes and mucus-secreting goblet cells were visible under H&E staining. Micrographs from various positions along the length of the small (Figure 22, 23, 24) and large intestines (25, 26, 27) show that there is no difference in the shape, size, or location of each of the different cell types in Kaiso-Tg mice when compared to wildtype littermates. While Kaiso-Tg intestines are essentially comparable in morphology to their non-transgenic counterparts, there is a slight

difference observed in crypt depth of some segments. Crypts in the proximal segment of both the small and large intestines are of comparable depth in wildtype and transgenic animals. In the distal segment, however, the intestinal crypts of transgenic mice appear to be shallower and more disorganized than its wildtype counterpart. These results implicate Kaiso as a regulator of developmental patterning of the mouse intestine. There are a number of genes, including Cdx1 and Cdx2, which are differentially expressed along the length of the intestine(79). Cdx1 is expressed in the distal portion of the mouse small intestine while Cdx2 is limited to the proximal portion(79). These genes each have roles in regulating proliferation and differentiation along the crypt-villus axis as well as maintaining the intestinal phenotype(79). Additionally, a bioinformatic analysis of the Cdx1 promoter revealed the presence of six Kaiso binding sites within a region 2000 nucleotides upstream of the start codon; the Cdx2 promoter contained only one partial Kaiso binding site. It is possible that Kaiso overexpression could repress Cdx1 expression in the distal region of the small intestine and this could produce the shallow crypts observed. To determine whether Cdx1/2 are direct targets of Kaiso, ChIP could be performed using α-Kaiso antibodies and primers specific to the promter of the Cdx genes. Luciferase reporter analysis could be performed in cultured cells to determine whether Kaiso acts as a positive or negative regulator of Cdx1/2 transcription. Although these are several possible biological scenarios, it important to note that these results are gathered from only a single matched pair of mice from each of the transgenic lines. In order to confirm whether this is a *bona fide* phenomenon, the same effect would need to be observed in multiple animals from each founder line.

If intestinal crypts of Kaiso-Tg mice are genuinely shallower and more disorganized, the effect could also indicate that Kaiso overexpression is affecting Wnt target genes involved in regulating intestinal development and maintaining intestinal homeostasis. For instance, overexpression of Kaiso may cause aberrant

downregulation of the Wnt and Kaiso target gene Cyclin-D1, which promotes cell proliferation. This change in gene expression could affect the rate at which stem cells of the crypt divide and could result in a change in crypt depth. Another possible mechanism by which Kaiso overexpression could affect crypt depth is through the action of MMP-7. Kaiso has been shown to bind and repress transcription from the MMP-7 promoter *in vivo* through ChIP and luciferase reporter analysis(82). MMP-7 facilitates the breakdown of the surrounding extracellular matrix and allows cells to migrate within a specific tissue. With Kaiso-mediated repression of MMP-7 in Kaiso-Tg mice, this process may be inhibited, resulting in decreased cell migration and thus decreased crypt depth. To determine if these possibilities actually exist, RT-PCR or immunostaining for Cyclin-D1 or MMP-7 in both Kaiso-Tg and normal intestinal tissue should be performed. RT-PCR would indicate whether Cyclin-D1 or MMP-7 transcript levels are varied between Kaiso-Tg and non-transgenic intestinal tissue. Quantitative immunohistochemistry (Q-IHC) techniques could then be used to compare the relative protein expression of these genes in Kaiso-Tg tissue. These experiments would give some insight into the function of Kaiso in the intestine and explain its role, if any, in determining intestinal crypt depth.

4.3. Kaiso Expression and Localization in the $Apc^{Min/+}$ Intestines

Before observing the effects of Kaiso overexpression in the $Apc^{Min/+}$ background, it was necessary to observe the pattern of Kaiso expression in normal $Apc^{Min/+}$ intestines and in $Apc^{Min/+}$ tumors. Immunostaining using α-Kaiso antibodies in the $Apc^{Min/+}$ large and small intestines show a similar distribution of Kaiso positive cells throughout the tissue as compared to wildtype intestines (Figure 28 and 29). All cells along the intestinal crypts of both the large and small intestines stain positively for Kaiso. As in the wildtype intestines, Kaiso is mainly

nuclear with weak cytoplasmic staining and varying levels of Kaiso expression are seen throughout the intestinal crypt. In $Apc^{Min/+}$ small intestine tumors, Kaiso is expressed through the entire tumor with a high level of expression near the crypts and lower expression at the apical surface of the tumor (Figure 30 and 31). It is important to note, however, that Kaiso maintains its diffuse nuclear expression throughout the tumor. Within the tumor, as in the normal intestinal crypts, the cells express variable levels of Kaiso. It was reported that Kaiso expression and localization is affected by the tumor microenvironment and this could explain the differential Kaiso expression observed in these intestinal tumors(81). In the study by Soubry and colleagues, they determined that Kaiso localization may be affected by hypoxia (low oxygen levels). To determine if Kaiso levels or subcellular localization are altered by hypoxia, dual immunostaining for Kaiso and a hypoxic marker like carbonic anhydrase would indicate whether this is the reason for the observed effect.

4.4. Kaiso overexpression in the $Apc^{Min/+}$ background

One of the main goals of this study was to determine whether Kaiso is a positive or negative regulator of mammalian Wnt signaling and the $Apc^{Min/+}$ mouse is an ideal tool to help answer this question. Previous studies have addressed the role of Kaiso in murine Wnt signaling through the use of the $Apc^{Min/+}$ model and Kaiso null mice(73). That study revealed that Kaiso deficient $Apc^{Min/+}$ mice showed a resistance to intestinal tumorigenesis, suggesting that Kaiso was a positive regulator of Wnt signaling(73). Preliminary data from our study now confirms the study by Prokhortchouk. After engineering an intestinal-specific Kaiso overexpression mouse, these mice were bred with $Apc^{Min/+}$ mice and their intestinal tumor burden was analyzed. In the most striking situation, one $Apc^{Min/+}$;Kaiso-Tg mouse had tumor numbers 10-fold higher than that of the $Apc^{Min/+}$ mouse, with 130

versus 13 tumors. This experimental finding agrees with established data by Prokhortchouk and colleagues; Kaiso overexpression has a positive effect on Wnt signaling and tumorigenesis in the $Apc^{Min/+}$ intestine(73). Although polyp numbers increased as expected, there was an unexpected decrease in average tumor size in $Apc^{Min/+}$;Kaiso-Tg mice when compared to non-transgenic $Apc^{Min/+}$ mice. The average tumor diameter in $Apc^{Min/+}$ mice was 1.90 ± 0.19 mm while $Apc^{Min/+}$;Kaiso-Tg ("A" line) small intestine tumors were 1.13 ± 0.09 mm in diameter and $Apc^{Min/+}$;Kaiso-Tg ("B" line) tumors had even smaller average diameters of 0.92 ± 0.10 mm (Table II). There are two scenarios that could be occurring to result in smaller tumor diameter: (1) Kaiso overexpression may cause a delay in tumor onset or (2) Kaiso overexpression could affect the rate of cellular proliferation within the tumors, causing an overall decrease in tumor growth rate or increased apoptosis. To investigate the first possibility, a time-course of intestinal tumor development in $Apc^{Min/+}$ and $Apc^{Min/+}$;Kaiso-Tg would help to determine whether Kaiso overexpressing mice experience a delay in tumor onset in comparison to non-transgenic $Apc^{Min/+}$ mice. To examine the second possibility, RT-PCR analysis of intestinal polyps or Q-IHC could be used to assay for changes in cell cycle, and proliferative markers like Cyclin-D1, p53, Ki-62, and PCNA.

Further study of Kaiso expression and localization in $Apc^{Min/+}$ intestinal tumors show that there is strong Kaiso expression near the crypts at the basal surface of the tumors and this expression decreases towards the apical surface. Past evidence indicates that Kaiso expression and localization is regulated by the tumor microenvironment and it is possible that extracellular signals from nearby tumor cells or a hypoxic environment are responsible for the change in Kaiso expression that is observed in these tumors. In $Apc^{Min/+}$:Kaiso-Tg double mutants, however, Kaiso localization in the tumor is drastically different. Kaiso is still expressed strongly at the basal surface of the tumor but is essentially lost throughout the center and at the tumor's apical surface (Figure 32, 33, and 34). It is possible that

the transgenic villin promoter used to drive Kaiso expression is inactive in those regions of the tumor or that there is the majority of tumor cells experience a loss-of-heterozygosity with regards to the transgene. In order to determine whether the villin promoter is inactivated, future experiments should stain for endogenous villin expression in the tumor. To ensure that cells of the tumor have not lost the villin-Kaiso transgene, *in situ* hybridization within the tumor should be used to detect whether the villin-Kaiso transgene is still a part of the $Apc^{Min/+}$ genome.

4.5. Conclusions and Significance

In this study, we generated a Kaiso overexpression mouse model for studying the effects of Kaiso overexpression on overeactive Wnt signaling in the $Apc^{Min/+}$ mouse intestine. This study demonstrates that intestinal-specific Kaiso overexpression does not contribute to any overt developmental defect in a wildtype background. This was also the first study to investigate the tissue and subcellular localization of Kaiso in the mouse intestines using IHC. We found that Kaiso is mainly nuclear and is expressed in the epithelial cells of the intestinal crypts and villi but not in the surrounding tissue. In order to confirm IHC data regarding Kaiso localization in Kaiso-Tg mice, it is necessary to immunostain using an α-myc antibody as this would aid in the differentiation of endogenous and transgenic Kaiso protein. In an $Apc^{Min/+}$ background, we have found that high levels of Kaiso overexpression greatly exacerbates the phenotype seen in $Apc^{Min/+}$ small intestines and increases the number of intestinal polyps. Further investigation of Kaiso spatio-temporal expression in the mouse intestine could give insight into its roles in normal intestinal homeostasis and in intestinal tumorigenesis. The Kaiso overxpression mouse is an excellent tool for studying intestinal development and the effect of Kaiso on other intestinal malignancies. For example, Kaiso overexpression mice could be crossed with p120 overexpression or knockout mice to observe the effect

either component has on intestinal development and homeostasis. Additionally, the role of Kaiso in a number of other intestinal diseases like Crohn's disease, intestinal fibrosis, and ulcerative colitis, could be explored by crossing Kaiso overexpression mice with established mouse models that closely mimic those diseases.

Appendix A

Data presented in Appendix A represents control experiments that were performed to test the efficacy of the Villin-Kaiso-MT construct before its use in transgenesis.

Materials and Methods

A.1.1. Cell culture and Transient Transfections

Villin-positive rat IEC-6 cells were a gift from Dr. Kelly Meckling (Guelph University) and porcine LLC-PK1 cells were purchased from ATCC. IEC-6 and LLC-PK1 cells were grown in Dulbecco's Modified Eagle Medium (Mediatech, CA) and supplemented with 10% Fetal Bovine Serum (PAA), 1% penicillin/streptomycin and 0.4% fungizone (Gibco). Villin-positive CaCO2 human colon carcinoma cells were a gift from Dr. Mary Purdue (McMaster University) and were cultured in MEM supplemented with 20% FBS, non-essential amino acids (Gibco), sodium pyruvate (Gibco), 1% penicillin/streptomycin, and 0.4% fungizone (Gibco). Cells were incubated at 37°C in a humidified atmosphere with 5% CO_2. Cells were transfected while in the logarithmic phase of growth (~60-70% confluence) with 15 μg of plasmid DNA using ExGen 500 or Lipofectamine according to the manufacturers' protocol.

A.1.2. Immunoprecipitation (IP) and Western Blot

To prepare whole-cell lysates, cells were rinsed with cold PBS and lysed in NP-40 lysis buffer (50 mM Tris-HCL; pH 7.4, 150 mM NaCl, and 0.5% NP-40 with a protease inhibitor cocktail (Roche)) on ice for 10 minutes. Lysates were scraped into a microcentrifuge tube and cell debris pelleted by centrifugation at 13,000 x *g* for 6 minutes. Supernatant was transferred to a new tube and protein was quantified by Bradford assay. 100 μg of total cell protein was used for western blot. For immunoprecipitation, 500 μg of whole cell lysate was incubated on a rotating platform with 4 μg of the antibody of interest for 1 hour at 4°C. After 1 hour, a 50% slurry of Protein A Sepharose beads (Amersham Biosciences), saturated with rabbit anti-mouse IgG (Jackson Immunoresearch), was added and the

immunoprecipitation continued with rotation at 4°C for an additional hour. Sepharose beads were pelleted by centrifugation and washed 5 times with NP-40 lysis buffer without protease inhibitor cocktail to remove non-specifically bound protein. Beads were then prepared for SDS-PAGE by boiling in Laemmli Sample Buffer (LSB) (100 mM Tris; pH 6.8, 2% SDS, 10% glycerol, 0.008% bromophenol blue, 0.24 M β-mercaptoethanol) for 5 minutes. Proteins were separated by SDS-PAGE on a 7% gel and subsequently transferred to a nitrocellulose membrane. The membrane was blocked using 3% non-fat milk in TBS for 10 minutes prior to incubation with the primary antibody overnight at 4°C with agitation. After overnight incubation, unbound primary antibody was removed by washing 5 times with TBS for 5 minutes each time. Horseradish peroxidase-conjugated secondary antibodies (Jackson Immunoresearch) were applied at a dilution of 1:40,000 and the membrane was incubated at room temperature for two hours with agitation. Unbound secondary antibody was washed with TBS and the membrane was incubated with Western Lightning Enhanced ChemiLuminescence substrate (Perkin Elmer) was used for detection.

Results and Discussion

A.2. The Villin-Kaiso-MT Vector Lacks Functionality in Tissue Culture Cells

Before transgenesis, it was recommended that we test the *in vivo* functionality of our expression vector to ensure that there were no cloning artifacts since small amounts of bacterial-derived DNA could affect the efficiency of transgenic expression. To test the functionality of the transgene, it is necessary to transfect the plasmid into villin-positive cells and assay for transgene expression by western blot. Initially, the villin-positive IEC-6, derived from adult rat intestinal crypts, was used to test the efficacy of the promter. Cells were transfected using Lipofectamine 2000 reagent and varying amounts of Villin-Kaiso DNA. IP followed by western blotting was used to determine whether the gene of interest was being expressed in the cells (Figure A-1). Western blot data indicates that Kaiso is not being overexpressed in comparison the levels observed in untreated cells. Furthermore, it appears that the simple addition of Lipofectamine 2000 to the cells affected Kaiso expression in this cell line. It was therefore necessary to try a different villin-positive cell line.

CaCO2 cells are human colon carcinoma cells that express the villin protein. These cells were also used to test the effectiveness of the villin-Kaiso transgene by transient transfection. These cells were transfected with villin-Kaiso and control plasmids (pCS2+MT-hKaiso and eGFP-mKaiso) using the Exgen 500 transfection reagent. Western blot analysis shows that the control plasmids are being expressed at their appropriate molecular weight but expression of the transgene is absent. In a final effort to test the *in vivo* functionality of the trasngene, LLC-PK1 cells were transfected with the villin-Kaiso construct. LLC-PK1 cells are villin-positive cells derived from the pig kidney proximal tubules. Since the villin promter used to drive expression of the Kaiso transgene was derived from a murine source, we only expected low levels of transgene expression. Instead, there was no overexpression

observed while control vectors were active in these cells. Having attempted on multiple occasions, with different cell lines, and under different occasions and failed to show the *in vivo* functionality of the transgene, we were still instructed by the London Regional Cancer Center to use the gene in the transgenesis.

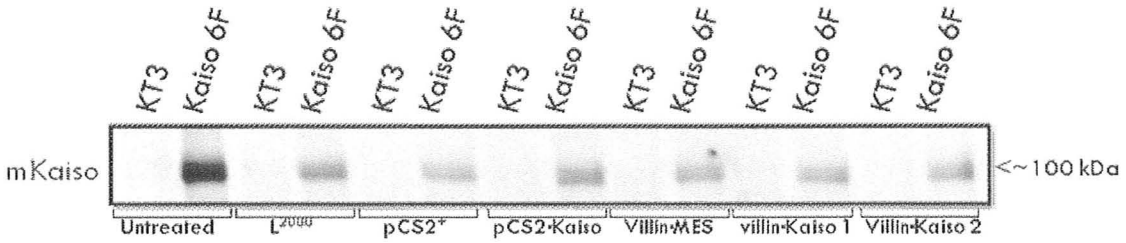

Figure A-1. Villin-Kaiso Overexpression in IEC-6 Cells. IEC-6 cells were transfected with between 10-15 μg villin-Kaiso plasmid DNA and assayed for transgene expression by western blot. pCS2^{+}-Kaiso was included as a positive control as this plasmid was shown to promote strong Kaiso overexpression in a variety of cell lines (Daniel Lab unpublished data). Western blot analysis shows that the transgene is not being overexpressed in these cells. Furthermore, it appears that simple treatment with Lipofectamine 2000 reduces Kaiso expression level compared to wildtype.

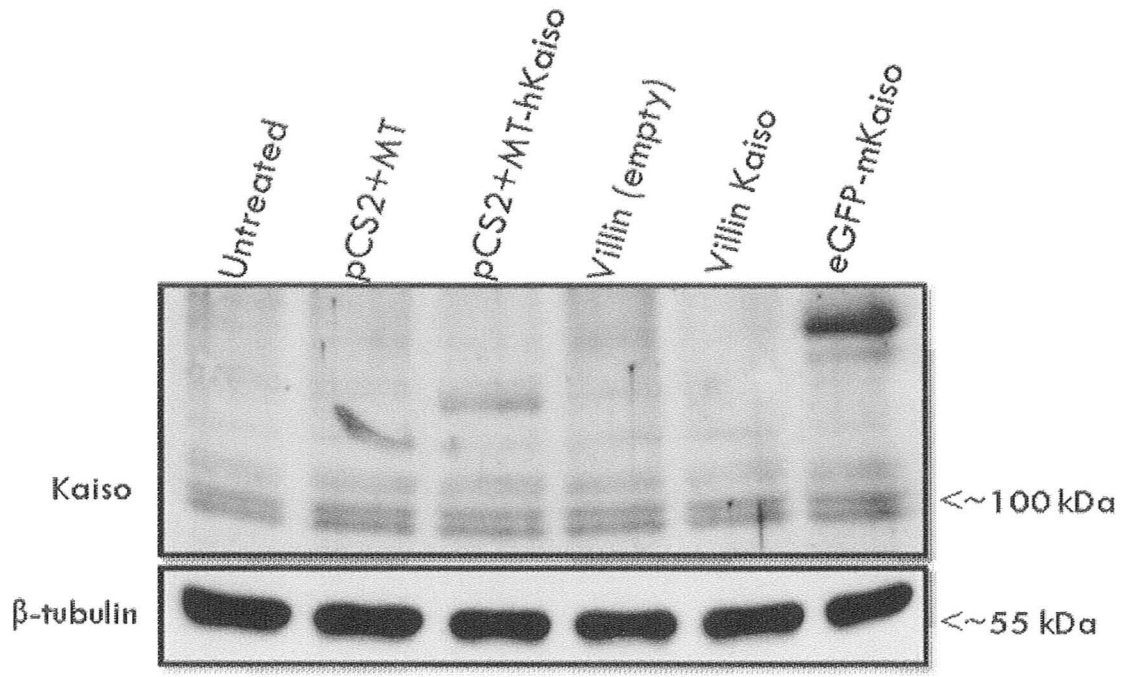

Figure A-2. Villin-Kaiso Overexpression in CaCO2 Cells. 15 μg of Villin-Kaiso and control plasmids was transfected into villin-positive CaCO2 cells using Exgen 500. Western blot analysis shows that the control vectors, pCS2+MT-hKaiso and eGFP-mKaiso, are being expressed but there is no expression from the Villin-Kaiso construct.

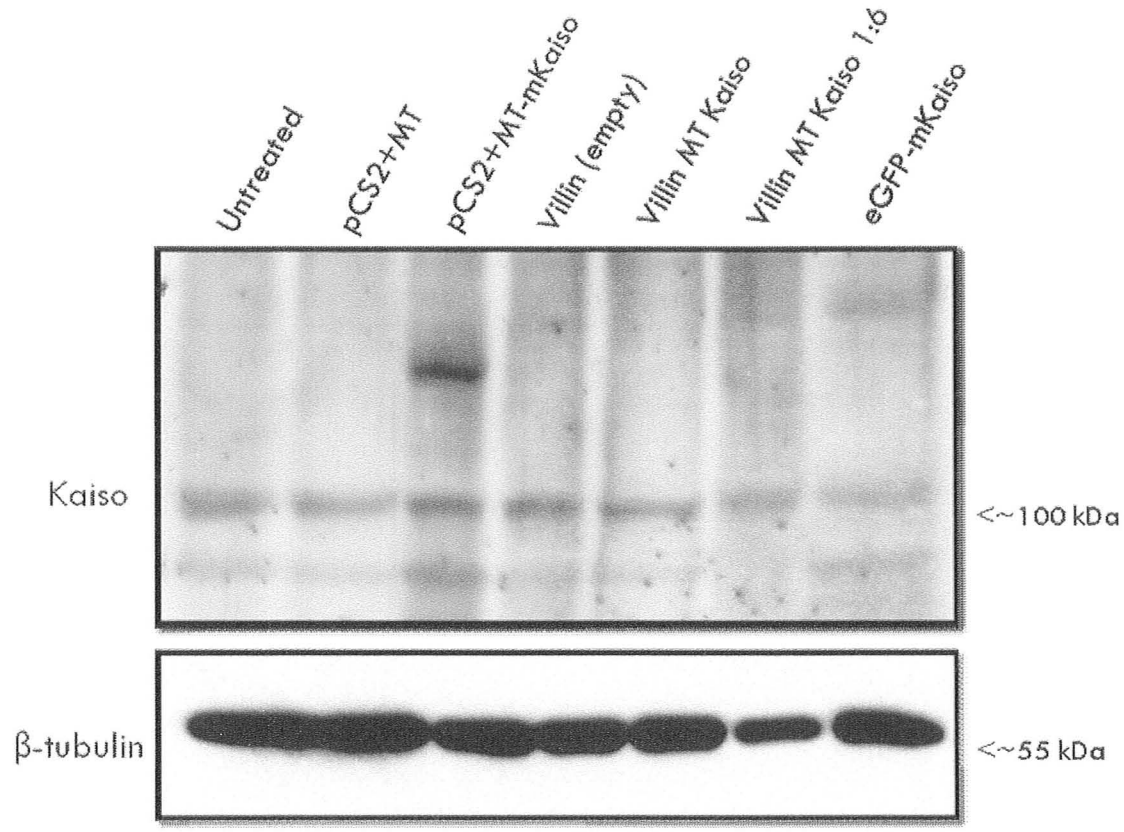

Figure A-3. Villin-Kaiso Overexpression in LLC-PK1 Cells. Villin-Kaiso and control plasmids were transfected into villin-positive LLC-PK1 cells using Exgen 500 and exogenous gene expression was assayed by western blot. As in the CaCO2 cells, expression from control vectors, pCS2+MT-hKaiso and eGFP-mKaiso is observed but villin-Kaiso overexpression is absent even at two different concentrations of plasmid.

Table A-I – Mouse Identification and Information. Table includes vital statistics regarding age, sex, and weight of mice used in each experiment. Figures can be cross-referenced with this table to determine the vital statistics of the animals used in any particular experiment.

Animal ID	Genotype	Sex	Age (mts)	Weight (g)
15A2M	C57/CBA-Kaiso-Tg ("A" Line)	M	4	36.62
15A3M	C57/CBA WT ("A" Line)	M	4	31.63
18A3F	C57/CBA-Kaiso-Tg ("A" Line)	F	3.5	31.77
18A1F	C57/CBA WT ("A" Line)	F	3.5	32.16
29C1M	C57/CBA-Kaiso-Tg ("C" Line)	M	3.5	34.67
30C1F	C57/CBA WT ("C" Line)	F	3.5	26.03
10A2F	C57/CBA-Kaiso-Tg ("A" Line)	F	7	26.61
10A1F	C57/CBA WT ("A" Line)	F	7	30.53
13B1M	C57/CBA-Kaiso-Tg ("B" Line)	M	7	38.19
13B1M	C57/CBA WT ("B" Line)	M	7	35.15
11C1M	C57/CBA-Kaiso-Tg ("C" Line)	M	7	43.65
11C1M	C57/CBA WT ("C" Line)	M	7	51.16
26B1M	C57/CBA-Kaiso-Tg ("B" Line)	M	5.5	28.25
28B1M	C57/CBA WT ("B" Line)	M	5	35.40
5A/APC3M	C57/B6-$Apc^{Min/+}$;Kaiso-Tg ("A" Line)	M	3	14.92
7B/APC2M	C57/B6-$Apc^{Min/+}$;Kaiso-Tg ("B" Line)	M	3	27.58
8B/APC1M	C57/B6-$Apc^{Min/+}$;Kaiso-Tg ("B" Line)	M	3	19.05
6APC1F	C57/B6-$Apc^{Min/+}$	F	3	19.55
3APC4F	C57/B6-$Apc^{Min/+}$	F	3	19.38
4APC1M	C57/B6-$Apc^{Min/+}$	M	3	27.29

References

1. **Angst, B. D., C. Marcozzi, and A. I. Magee.** 2001. The cadherin superfamily: diversity in form and function. J Cell Sci **114:**629-41.
2. **Barna, M., N. Hawe, L. Niswander, and P. P. Pandolfi.** 2000. Plzf regulates limb and axial skeletal patterning. Nat Genet **25:**166-72.
3. **Baum, B., J. Settleman, and M. P. Quinlan.** 2008. Transitions between epithelial and mesenchymal states in development and disease. Semin Cell Dev Biol **19:**294-308.
4. **Behrens, J., J. P. von Kries, M. Kuhl, L. Bruhn, D. Wedlich, R. Grosschedl, and W. Birchmeier.** 1996. Functional interaction of beta-catenin with the transcription factor LEF-1. Nature **382:**638-42.
5. **Bhanot, P., M. Brink, C. H. Samos, J. C. Hsieh, Y. Wang, J. P. Macke, D. Andrew, J. Nathans, and R. Nusse.** 1996. A new member of the frizzled family from Drosophila functions as a Wingless receptor. Nature **382:**225-30.
6. **Boyden, L. M., J. Mao, J. Belsky, L. Mitzner, A. Farhi, M. A. Mitnick, D. Wu, K. Insogna, and R. P. Lifton.** 2002. High bone density due to a mutation in LDL-receptor-related protein 5. N Engl J Med **346:**1513-21.
7. **Brembeck, F. H., M. Rosario, and W. Birchmeier.** 2006. Balancing cell adhesion and Wnt signaling, the key role of beta-catenin. Curr Opin Genet Dev **16:**51-9.
8. **Cadigan, K. M., and R. Nusse.** 1997. Wnt signaling: a common theme in animal development. Genes Dev **11:**3286-305.
9. **Castells, A., S. Castellvi-Bel, and F. Balaguer.** 2009. Concepts in familial colorectal cancer: where do we stand and what is the future? Gastroenterology **137:**404-9.
10. **Cavallaro, U., and G. Christofori.** 2004. Cell adhesion and signalling by cadherins and Ig-CAMs in cancer. Nat Rev Cancer **4:**118-32.
11. **Chen, W., D. ten Berge, J. Brown, S. Ahn, L. A. Hu, W. E. Miller, M. G. Caron, L. S. Barak, R. Nusse, and R. J. Lefkowitz.** 2003. Dishevelled 2 recruits beta-arrestin 2 to mediate Wnt5A-stimulated endocytosis of Frizzled 4. Science **301:**1391-4.
12. **Chuai, M., and C. J. Weijer.** 2008. The mechanisms underlying primitive streak formation in the chick embryo. Curr Top Dev Biol **81:**135-56.
13. **Clarke, A. R.** 2007. Cancer genetics: mouse models of intestinal cancer. Biochem Soc Trans **35:**1338-41.
14. **Clevers, H.** 2006. Wnt/beta-catenin signaling in development and disease. Cell **127:**469-80.
15. **Costoya, J. A.** 2007. Functional analysis of the role of POK transcriptional repressors. Brief Funct Genomic Proteomic **6:**8-18.
16. **Daniel, J. M.** 2007. Dancing in and out of the nucleus: p120(ctn) and the transcription factor Kaiso. Biochim Biophys Acta **1773:**59-68.
17. **Daniel, J. M., and A. B. Reynolds.** 1999. The catenin p120(ctn) interacts with Kaiso, a novel BTB/POZ domain zinc finger transcription factor. Mol Cell Biol **19:**3614-23.
18. **Daniel, J. M., C. M. Spring, H. C. Crawford, A. B. Reynolds, and A. Baig.** 2002. The p120(ctn)-binding partner Kaiso is a bi-modal DNA-binding protein that recognizes both

a sequence-specific consensus and methylated CpG dinucleotides. Nucleic Acids Res **30:**2911-9.

19. **Dann, C. E., J. C. Hsieh, A. Rattner, D. Sharma, J. Nathans, and D. J. Leahy.** 2001. Insights into Wnt binding and signalling from the structures of two Frizzled cysteine-rich domains. Nature **412:**86-90.
20. **Elshourbagy, N. A., D. W. Walker, Y. K. Paik, M. S. Boguski, M. Freeman, J. I. Gordon, and J. M. Taylor.** 1987. Structure and expression of the human apolipoprotein A-IV gene. J Biol Chem **262:**7973-81.
21. **Fath, K. R., and D. R. Burgess.** 1995. Microvillus assembly. Not actin alone. Curr Biol **5:**591-3.
22. **Fearon, E. R., and B. Vogelstein.** 1990. A genetic model for colorectal tumorigenesis. Cell **61:**759-67.
23. **Frixen, U. H., J. Behrens, M. Sachs, G. Eberle, B. Voss, A. Warda, D. Lochner, and W. Birchmeier.** 1991. E-cadherin-mediated cell-cell adhesion prevents invasiveness of human carcinoma cells. J Cell Biol **113:**173-85.
24. **Funayama, N., F. Fagotto, P. McCrea, and B. M. Gumbiner.** 1995. Embryonic axis induction by the armadillo repeat domain of beta-catenin: evidence for intracellular signaling. J Cell Biol **128:**959-68.
25. **Gabbert, H., R. Wagner, R. Moll, and C. D. Gerharz.** 1985. Tumor dedifferentiation: an important step in tumor invasion. Clin Exp Metastasis **3:**257-79.
26. **Gavert, N., and A. Ben-Ze'ev.** 2007. beta-Catenin signaling in biological control and cancer. J Cell Biochem **102:**820-8.
27. **Gong, Y., R. B. Slee, N. Fukai, G. Rawadi, S. Roman-Roman, A. M. Reginato, H. Wang, T. Cundy, F. H. Glorieux, D. Lev, M. Zacharin, K. Oexle, J. Marcelino, W. Suwairi, S. Heeger, G. Sabatakos, S. Apte, W. N. Adkins, J. Allgrove, M. Arslan-Kirchner, J. A. Batch, P. Beighton, G. C. Black, R. G. Boles, L. M. Boon, C. Borrone, H. G. Brunner, G. F. Carle, B. Dallapiccola, A. De Paepe, B. Floege, M. L. Halfhide, B. Hall, R. C. Hennekam, T. Hirose, A. Jans, H. Juppner, C. A. Kim, K. Keppler-Noreuil, A. Kohlschuetter, D. LaCombe, M. Lambert, E. Lemyre, T. Letteboer, L. Peltonen, R. S. Ramesar, M. Romanengo, H. Somer, E. Steichen-Gersdorf, B. Steinmann, B. Sullivan, A. Superti-Furga, W. Swoboda, M. J. van den Boogaard, W. Van Hul, M. Vikkula, M. Votruba, B. Zabel, T. Garcia, R. Baron, B. R. Olsen, and M. L. Warman.** 2001. LDL receptor-related protein 5 (LRP5) affects bone accrual and eye development. Cell **107:**513-23.
28. **Gregorieff, A., and H. Clevers.** 2005. Wnt signaling in the intestinal epithelium: from endoderm to cancer. Genes Dev **19:**877-90.
29. **Gregorieff, A., R. Grosschedl, and H. Clevers.** 2004. Hindgut defects and transformation of the gastro-intestinal tract in Tcf4(-/-)/Tcf1(-/-) embryos. Embo J **23:**1825-33.
30. **Groden, J., A. Thliveris, W. Samowitz, M. Carlson, L. Gelbert, H. Albertsen, G. Joslyn, J. Stevens, L. Spirio, M. Robertson, and et al.** 1991. Identification and characterization of the familial adenomatous polyposis coli gene. Cell **66:**589-600.
31. **Hall, P. A., P. J. Coates, B. Ansari, and D. Hopwood.** 1994. Regulation of cell number in the mammalian gastrointestinal tract: the importance of apoptosis. J Cell Sci **107 (Pt 12):**3569-77.
32. **Hatzfeld, M.** 1999. The armadillo family of structural proteins. Int Rev Cytol **186:**179-224.

33. **Ichii, S., A. Horii, S. Nakatsuru, J. Furuyama, J. Utsunomiya, and Y. Nakamura.** 1992. Inactivation of both APC alleles in an early stage of colon adenomas in a patient with familial adenomatous polyposis (FAP). Hum Mol Genet **1:**387-90.
34. **Imai, K., N. Takada, N. Satoh, and Y. Satou.** 2000. (beta)-catenin mediates the specification of endoderm cells in ascidian embryos. Development **127:**3009-20.
35. **Ireland, H., R. Kemp, C. Houghton, L. Howard, A. R. Clarke, O. J. Sansom, and D. J. Winton.** 2004. Inducible Cre-mediated control of gene expression in the murine gastrointestinal tract: effect of loss of beta-catenin. Gastroenterology **126:**1236-46.
36. **Ishikawa, T. O., Y. Tamai, Q. Li, M. Oshima, and M. M. Taketo.** 2003. Requirement for tumor suppressor Apc in the morphogenesis of anterior and ventral mouse embryo. Dev Biol **253:**230-46.
37. **Jemal, A., R. Siegel, E. Ward, Y. Hao, J. Xu, T. Murray, and M. J. Thun.** 2008. Cancer statistics, 2008. CA Cancer J Clin **58:**71-96.
38. **Jones, C., and P. Chen.** 2007. Planar cell polarity signaling in vertebrates. Bioessays **29:**120-32.
39. **Kelly, K. F., and J. M. Daniel.** 2006. POZ for effect--POZ-ZF transcription factors in cancer and development. Trends Cell Biol **16:**578-87.
40. **Kelly, K. F., C. M. Spring, A. A. Otchere, and J. M. Daniel.** 2004. NLS-dependent nuclear localization of p120ctn is necessary to relieve Kaiso-mediated transcriptional repression. J Cell Sci **117:**2675-86.
41. **Kim, S. W., X. Fang, H. Ji, A. F. Paulson, J. M. Daniel, M. Ciesiolka, F. van Roy, and P. D. McCrea.** 2002. Isolation and characterization of XKaiso, a transcriptional repressor that associates with the catenin Xp120(ctn) in Xenopus laevis. J Biol Chem **277:**8202-8.
42. **Kim, S. W., J. I. Park, C. M. Spring, A. K. Sater, H. Ji, A. A. Otchere, J. M. Daniel, and P. D. McCrea.** 2004. Non-canonical Wnt signals are modulated by the Kaiso transcriptional repressor and p120-catenin. Nat Cell Biol **6:**1212-20.
43. **Kinzler, K. W., M. C. Nilbert, L. K. Su, B. Vogelstein, T. M. Bryan, D. B. Levy, K. J. Smith, A. C. Preisinger, P. Hedge, D. McKechnie, and et al.** 1991. Identification of FAP locus genes from chromosome 5q21. Science **253:**661-5.
44. **Knudson, A. G., Jr.** 1971. Mutation and cancer: statistical study of retinoblastoma. Proc Natl Acad Sci U S A **68:**820-3.
45. **Korinek, V., N. Barker, P. Moerer, E. van Donselaar, G. Huls, P. J. Peters, and H. Clevers.** 1998. Depletion of epithelial stem-cell compartments in the small intestine of mice lacking Tcf-4. Nat Genet **19:**379-83.
46. **Lammi, L., S. Arte, M. Somer, H. Jarvinen, P. Lahermo, I. Thesleff, S. Pirinen, and P. Nieminen.** 2004. Mutations in AXIN2 cause familial tooth agenesis and predispose to colorectal cancer. Am J Hum Genet **74:**1043-50.
47. **Lickert, H., S. Kutsch, B. Kanzler, Y. Tamai, M. M. Taketo, and R. Kemler.** 2002. Formation of multiple hearts in mice following deletion of beta-catenin in the embryonic endoderm. Dev Cell **3:**171-81.
48. **Liu, P., M. Wakamiya, M. J. Shea, U. Albrecht, R. R. Behringer, and A. Bradley.** 1999. Requirement for Wnt3 in vertebrate axis formation. Nat Genet **22:**361-5.
49. **Liu, W., X. Dong, M. Mai, R. S. Seelan, K. Taniguchi, K. K. Krishnadath, K. C. Halling, J. M. Cunningham, L. A. Boardman, C. Qian, E. Christensen, S. S. Schmidt, P. C. Roche, D. I. Smith, and S. N. Thibodeau.** 2000. Mutations in AXIN2 cause colorectal cancer with

defective mismatch repair by activating beta-catenin/TCF signalling. Nat Genet **26:**146-7.

50. **Logan, C. Y., and R. Nusse.** 2004. The Wnt signaling pathway in development and disease. Annu Rev Cell Dev Biol **20:**781-810.
51. **Luongo, C., A. R. Moser, S. Gledhill, and W. F. Dove.** 1994. Loss of Apc+ in intestinal adenomas from Min mice. Cancer Res **54:**5947-52.
52. **Marshman, E., C. Booth, and C. S. Potten.** 2002. The intestinal epithelial stem cell. Bioessays **24:**91-8.
53. **McMahon, A. P., and A. Bradley.** 1990. The Wnt-1 (int-1) proto-oncogene is required for development of a large region of the mouse brain. Cell **62:**1073-85.
54. **Merriam, J. M., A. B. Rubenstein, and M. W. Klymkowsky.** 1997. Cytoplasmically anchored plakoglobin induces a WNT-like phenotype in Xenopus. Dev Biol **185:**67-81.
55. **Millan, J. L.** 1987. Promoter structure of the human intestinal alkaline phosphatase gene. Nucleic Acids Res **15:**10599.
56. **Moser, A. R., H. C. Pitot, and W. F. Dove.** 1990. A dominant mutation that predisposes to multiple intestinal neoplasia in the mouse. Science **247:**322-4.
57. **Mosimann, C., G. Hausmann, and K. Basler.** 2009. Beta-catenin hits chromatin: regulation of Wnt target gene activation. Nat Rev Mol Cell Biol **10:**276-86.
58. **Nagase, H., and Y. Nakamura.** 1993. Mutations of the APC (adenomatous polyposis coli) gene. Hum Mutat **2:**425-34.
59. **Nakaya, Y., and G. Sheng.** 2008. Epithelial to mesenchymal transition during gastrulation: an embryological view. Dev Growth Differ **50:**755-66.
60. **Nelson, W. J., and R. Nusse.** 2004. Convergence of Wnt, beta-catenin, and cadherin pathways. Science **303:**1483-7.
61. **Nishisho, I., Y. Nakamura, Y. Miyoshi, Y. Miki, H. Ando, A. Horii, K. Koyama, J. Utsunomiya, S. Baba, and P. Hedge.** 1991. Mutations of chromosome 5q21 genes in FAP and colorectal cancer patients. Science **253:**665-9.
62. **Ohno, H.** 2006. Pathogenetic and clinical implications of non-immunoglobulin ; BCL6 translocations in B-cell non-Hodgkin's lymphoma. J Clin Exp Hematop **46:**43-53.
63. **Oshima, M., H. Oshima, K. Kitagawa, M. Kobayashi, C. Itakura, and M. Taketo.** 1995. Loss of Apc heterozygosity and abnormal tissue building in nascent intestinal polyps in mice carrying a truncated Apc gene. Proc Natl Acad Sci U S A **92:**4482-6.
64. **Park, J. I., S. W. Kim, J. P. Lyons, H. Ji, T. T. Nguyen, K. Cho, M. C. Barton, T. Deroo, K. Vleminckx, R. T. Moon, and P. D. McCrea.** 2005. Kaiso/p120-catenin and TCF/beta-catenin complexes coordinately regulate canonical Wnt gene targets. Dev Cell **8:**843-54.
65. **Perez-Torrado, R., D. Yamada, and P. A. Defossez.** 2006. Born to bind: the BTB protein-protein interaction domain. Bioessays **28:**1194-202.
66. **Phan, R. T., and R. Dalla-Favera.** 2004. The BCL6 proto-oncogene suppresses p53 expression in germinal-centre B cells. Nature **432:**635-9.
67. **Pinto, D., and H. Clevers.** 2005. Wnt, stem cells and cancer in the intestine. Biol Cell **97:**185-96.
68. **Pinto, D., A. Gregorieff, H. Begthel, and H. Clevers.** 2003. Canonical Wnt signals are essential for homeostasis of the intestinal epithelium. Genes Dev **17:**1709-13.
69. **Pinto, D., S. Robine, F. Jaisser, F. E. El Marjou, and D. Louvard.** 1999. Regulatory sequences of the mouse villin gene that efficiently drive transgenic expression in

immature and differentiated epithelial cells of small and large intestines. J Biol Chem **274:**6476-82.

70. **Potten, C. S., J. H. Hendry, and J. V. Moore.** 1987. Estimates of the number of clonogenic cells in crypts of murine small intestine. Virchows Arch B Cell Pathol Incl Mol Pathol **53:**227-34.
71. **Potten, C. S., and M. Loeffler.** 1990. Stem cells: attributes, cycles, spirals, pitfalls and uncertainties. Lessons for and from the crypt. Development **110:**1001-20.
72. **Powell, S. M., N. Zilz, Y. Beazer-Barclay, T. M. Bryan, S. R. Hamilton, S. N. Thibodeau, B. Vogelstein, and K. W. Kinzler.** 1992. APC mutations occur early during colorectal tumorigenesis. Nature **359:**235-7.
73. **Prokhortchouk, A., O. Sansom, J. Selfridge, I. M. Caballero, S. Salozhin, D. Aithozhina, L. Cerchietti, F. G. Meng, L. H. Augenlicht, J. M. Mariadason, B. Hendrich, A. Melnick, E. Prokhortchouk, A. Clarke, and A. Bird.** 2006. Kaiso-deficient mice show resistance to intestinal cancer. Mol Cell Biol **26:**199-208.
74. **Robine, S., C. Sahuquillo-Merino, D. Louvard, and E. Pringault.** 1993. Regulatory sequences on the human villin gene trigger the expression of a reporter gene in a differentiating HT29 intestinal cell line. J Biol Chem **268:**11426-34.
75. **Roczniak-Ferguson, A., and A. B. Reynolds.** 2003. Regulation of p120-catenin nucleocytoplasmic shuttling activity. J Cell Sci **116:**4201-12.
76. **Rudini, N., and E. Dejana.** 2008. Adherens junctions. Curr Biol **18:**R1080-2.
77. **Sansom, O. J., K. R. Reed, A. J. Hayes, H. Ireland, H. Brinkmann, I. P. Newton, E. Batlle, P. Simon-Assmann, H. Clevers, I. S. Nathke, A. R. Clarke, and D. J. Winton.** 2004. Loss of Apc in vivo immediately perturbs Wnt signaling, differentiation, and migration. Genes Dev **18:**1385-90.
78. **Shoemaker, A. R., K. A. Gould, C. Luongo, A. R. Moser, and W. F. Dove.** 1997. Studies of neoplasia in the Min mouse. Biochim Biophys Acta **1332:**F25-48.
79. **Silberg, D. G., G. P. Swain, E. R. Suh, and P. G. Traber.** 2000. Cdx1 and cdx2 expression during intestinal development. Gastroenterology **119:**961-71.
80. **Smith, K. J., K. A. Johnson, T. M. Bryan, D. E. Hill, S. Markowitz, J. K. Willson, C. Paraskeva, G. M. Petersen, S. R. Hamilton, B. Vogelstein, and et al.** 1993. The APC gene product in normal and tumor cells. Proc Natl Acad Sci U S A **90:**2846-50.
81. **Soubry, A., J. van Hengel, E. Parthoens, C. Colpaert, E. Van Marck, D. Waltregny, A. B. Reynolds, and F. van Roy.** 2005. Expression and nuclear location of the transcriptional repressor Kaiso is regulated by the tumor microenvironment. Cancer Res **65:**2224-33.
82. **Spring, C. M., K. F. Kelly, I. O'Kelly, M. Graham, H. C. Crawford, and J. M. Daniel.** 2005. The catenin p120ctn inhibits Kaiso-mediated transcriptional repression of the beta-catenin/TCF target gene matrilysin. Exp Cell Res **305:**253-65.
83. **Steeg, P. S.** 2006. Tumor metastasis: mechanistic insights and clinical challenges. Nat Med **12:**895-904.
84. **Su, L. K., K. W. Kinzler, B. Vogelstein, A. C. Preisinger, A. R. Moser, C. Luongo, K. A. Gould, and W. F. Dove.** 1992. Multiple intestinal neoplasia caused by a mutation in the murine homolog of the APC gene. Science **256:**668-70.
85. **Sweetser, D. A., E. H. Birkenmeier, I. J. Klisak, S. Zollman, R. S. Sparkes, T. Mohandas, A. J. Lusis, and J. I. Gordon.** 1987. The human and rodent intestinal fatty acid binding

protein genes. A comparative analysis of their structure, expression, and linkage relationships. J Biol Chem **262:**16060-71.

86. **Thiery, J. P.** 2002. Epithelial-mesenchymal transitions in tumour progression. Nat Rev Cancer **2:**442-54.
87. **Thomas, K. R., and M. R. Capecchi.** 1990. Targeted disruption of the murine int-1 proto-oncogene resulting in severe abnormalities in midbrain and cerebellar development. Nature **346:**847-50.
88. **van de Wetering, M., R. Cavallo, D. Dooijes, M. van Beest, J. van Es, J. Loureiro, A. Ypma, D. Hursh, T. Jones, A. Bejsovec, M. Peifer, M. Mortin, and H. Clevers.** 1997. Armadillo coactivates transcription driven by the product of the Drosophila segment polarity gene dTCF. Cell **88:**789-99.
89. **van de Wetering, M., E. Sancho, C. Verweij, W. de Lau, I. Oving, A. Hurlstone, K. van der Horn, E. Batlle, D. Coudreuse, A. P. Haramis, M. Tjon-Pon-Fong, P. Moerer, M. van den Born, G. Soete, S. Pals, M. Eilers, R. Medema, and H. Clevers.** 2002. The beta-catenin/TCF-4 complex imposes a crypt progenitor phenotype on colorectal cancer cells. Cell **111:**241-50.
90. **van Roy, F., and G. Berx.** 2008. The cell-cell adhesion molecule E-cadherin. Cell Mol Life Sci **65:**3756-88.
91. **van Roy, F. M., and P. D. McCrea.** 2005. A role for Kaiso-p120ctn complexes in cancer? Nat Rev Cancer **5:**956-64.
92. **Wehrli, M., S. T. Dougan, K. Caldwell, L. O'Keefe, S. Schwartz, D. Vaizel-Ohayon, E. Schejter, A. Tomlinson, and S. DiNardo.** 2000. arrow encodes an LDL-receptor-related protein essential for Wingless signalling. Nature **407:**527-30.
93. **Widelitz, R.** 2005. Wnt signaling through canonical and non-canonical pathways: recent progress. Growth Factors **23:**111-6.
94. **Wikramanayake, A. H., M. Hong, P. N. Lee, K. Pang, C. A. Byrum, J. M. Bince, R. Xu, and M. Q. Martindale.** 2003. An ancient role for nuclear beta-catenin in the evolution of axial polarity and germ layer segregation. Nature **426:**446-50.
95. **Willert, K., J. D. Brown, E. Danenberg, A. W. Duncan, I. L. Weissman, T. Reya, J. R. Yates, 3rd, and R. Nusse.** 2003. Wnt proteins are lipid-modified and can act as stem cell growth factors. Nature **423:**448-52.
96. **Wong, H. C., A. Bourdelas, A. Krauss, H. J. Lee, Y. Shao, D. Wu, M. Mlodzik, D. L. Shi, and J. Zheng.** 2003. Direct binding of the PDZ domain of Dishevelled to a conserved internal sequence in the C-terminal region of Frizzled. Mol Cell **12:**1251-60.
97. **Yamada, Y., and H. Mori.** 2007. Multistep carcinogenesis of the colon in Apc(Min/+) mouse. Cancer Sci **98:**6-10.
98. **Yamanaka, H., T. Moriguchi, N. Masuyama, M. Kusakabe, H. Hanafusa, R. Takada, S. Takada, and E. Nishida.** 2002. JNK functions in the non-canonical Wnt pathway to regulate convergent extension movements in vertebrates. EMBO Rep **3:**69-75.
99. **Yang, J., and R. A. Weinberg.** 2008. Epithelial-mesenchymal transition: at the crossroads of development and tumor metastasis. Dev Cell **14:**818-29.
100. **Zallen, J. A.** 2007. Planar polarity and tissue morphogenesis. Cell **129:**1051-63.